

Elucidating the Transcriptional Regulatory Roles of STAT3 and FOXA1 Transcription Factors in Genetically Engineered Mouse Models of Human Breast Cancer

By

Linjia Ji

A thesis submitted to McGill University in partial fulfillment of the requirements of the degree
of Master of Science in Experimental Medicine

©Linjia Ji 2024
Department of Medicine, Division of Experimental Medicine
McGill University
April 2024

Table of Contents

ABSTRACT	5
RÉSUMÉ	7
ACKNOWLEDGEMENTS	9
CONTRIBUTION OF AUTHORS.....	11
LIST OF FIGURES AND TABLES.....	13
LIST of ABBREVIATIONS	15
Chapter 1: Literature Review.....	19
1.1. Mammary Gland and Breast Cancer.....	19
1.1.1. Breast Cancer Epidemiology.....	19
1.1.2. Mammary Gland Anatomy and Basic Structure.....	19
1.1.3. Breast Cancer Development.....	21
1.1.4. Histological and Molecular Subtypes of Breast Cancer	22
1.1.5. Genetically Engineered Mouse Models (GEMM) of Breast Cancer	23
1.2. HER2-Positive Breast Cancer.....	25
1.2.1. Mechanism of HER2-Positive Breast Cancer	25
1.2.2. Metastasis of HER2-Positive Breast Cancer	26
1.2.3. Therapeutics of HER2-Positive Breast Cancer.....	28
1.2.4. Mouse Models of HER2-Positive Breast Cancer.....	29
1.3. ER-Positive Breast Cancer.....	30
1.3.1. Mechanism of ER Signaling in Mammary Gland	30
1.3.2. Therapeutics of ER-Positive Breast Cancer	32
1.3.3. Mouse Models of ER-Positive Breast Cancer	35
1.3.4. A novel ESR1 point mutation mouse model that drives male mouse feminization	39
1.4. Transcription Factors in Breast Cancer	39
1.4.1. Overview of Transcription Factors in Breast Cancer	39
1.4.2. Signal Transducer and Activator of Transcription 3 (Stat3)	41
1.4.2.1. Canonical and Non-canonical Stat3 Signaling	42
1.4.2.2. Stat3 in Breast Cancer Initiation and Progression.....	44
1.4.2.3. Stat3 in Breast Cancer Metastasis.....	45
1.4.2.4. Stat3 target gene Lgals3	46
1.4.2.4.1. Biology and Signaling of Galectin-3	46
1.4.2.4.2. Galectin-3 in Cancer.....	48
1.4.2.5. Experimental rationale	49
1.4.3. Forkhead Box A1 (FOXA1)	49
1.4.3.1. FOXA1 in mammary gland development	50
1.4.3.2. FOXA1 and ER-Positive Breast Cancer	51
1.4.3.3. Experimental Rationale	53
Chapter 2: Results.....	54
2.1. Stat3 promotes metastasis in HER2-Positive Breast Cancer through the regulation of Lgals3 ...	54
2.1.1. Stat3 deficiency results in a significant decrease in metastasis in MMTV-Neu-Ires-Cre (NIC) mouse models	54
2.1.1.1. Stat3 deficiency increases apoptosis in NIC mouse model	55
2.1.1.2. Stat3-deficiency leads to elevated focal adhesion level	57

2.1.1.3. Transcriptomic and bioinformatic analysis.....	59
2.1.1.4. Lgals3 is the most significantly down-regulated gene in the Stat3-deficient lesions	61
2.1.1.5. Knockdown of Lgals3 decreases migration and invasion	64
2.1.1.6. Pharmacological inhibition of Gal-3 decreases migration and invasion	67
2.1.1.7. Knockdown of Lgals3 increases focal adhesion markers.....	68
2.1.2. Stat3 deficiency results in a significant delay in tumor onset and a decrease in metastasis in TetO- ErbB2-Ires-Cre (EIC) mouse models.....	69
2.1.2.1. Stat3 deficiency results in a delay in tumor onset and decreased tumor burden	70
2.1.2.2. Stat3 deficiency results in decreased metastasis	71
2.1.2.3. Stat3 deficiency results in a trend of decreased proliferation	73
2.1.2.4. Transcriptomic and bioinformatic analysis.....	74
2.1.2.5. Lgals3 is significantly down-regulated in the Stat3-deficient lesions.....	76
2.2. Creating a novel ER-Positive Breast Cancer Mouse Model: TetO-FOXA1-Ires-Cre (FIC)	78
2.2.1. FIC/MTB mouse model.....	78
2.2.1.1. Validation of FOXA1 expression and comparisons of founder lines	79
2.2.1.2. <i>In vitro</i> study of mammary gland-derived organoids showed abnormal filled sphere structure upon doxycycline induction	82
2.2.1.3. <i>In vivo</i> 4-week induction.....	86
2.2.1.4. <i>In vivo</i> 12-week induction.....	87
2.2.1.5. <i>In vivo</i> 20-week induction.....	89
2.2.2. FIC/MTB/ESR1 mouse model	90
2.2.2.1. Excision PCR	91
2.2.2.2. 20-week induced FIC2/MTB/ESR1 mouse mammary glands	92
Chapter 3: Discussion and Concluding Statements	94
3.1. Summary.....	94
3.2. Discussion	97
3.3. Future Directions.....	103
Chapter 4. Materials and Methods.....	104
4.1. Animal Work.....	104
4.1.1. Animal maintenance	104
4.1.2. Tumor monitoring	104
4.1.3. Necropsy and tissue collection.....	104
4.1.4. Wholmount of mammary glands	105
4.2. DNA Analysis	105
4.2.1. DNA extraction and genotyping	105
4.2.2. DNA extraction and excision PCR	106
4.3. RNA Analysis.....	107
4.3.1. RNA extraction	107
4.3.2. Quantitative Reverse Transcriptase PCR (qRT-PCR).....	107
4.4. Cell Culture	108
4.4.1. Cell lines and maintenance	108
4.4.2. 3D mammary gland-derived organoids.....	109
4.4.3. <i>In vitro</i> migration and invasion assay.....	109
4.4.4. shRNA knockdown stable cell lines	110
4.4.5. <i>In vitro</i> proliferation assay.....	110
4.5. Protein Analysis	110

4.5.1.	Protein extraction and immunoblotting	110
4.5.2.	Fluorescent immunohistochemistry	111
4.5.3.	Immunofluorescence	112
4.5.4.	List of antibodies for immunoblotting, immunohistofluorescence, immunofluorescence.....	112
4.6.	Statistics	113
Chapter 5: References		114

ABSTRACT

Breast cancer is the predominant cancer type among Canadian women, with a striking incidence rate of one in eight women during their lifetime. Transcription factors play pivotal roles in breast cancer initiation and progression. Signal transducer and activator of transcription 3 (Stat3) is a transcription factor that mediates the expression of a variety of genes in response to cytokines and growth factors. The activation of Stat3 plays key roles in cell growth, survival and apoptosis, cell migration and invasion, and inflammation. Using the conditional Stat3 knockout mouse model, our lab previously demonstrated that Stat3 deficiency can impede the metastasis of ErbB2-positive breast cancer. However, the mechanism remains unclear. By doing transcriptomic analysis of Stat3-null and wildtype ErbB2 positive breast cancer cells dissociated from mouse tumors, Lgals3 turned out to be a target of Stat3 that could have mediated the metastatic phenotype. Upon shRNA knockdown of Lgals3, ErbB2 positive breast cancer cells demonstrated dramatically reduced migration and invasion. They also formed elevated levels of focal adhesions that may lead to reduced migration and metastasis. Furthermore, the pharmacological inhibition of Gal-3 leads to decreased cell migration and invasion. This reveals the therapeutic potential of Lgals3 inhibition in ErbB2-Positive breast cancer metastasis prevention.

Estrogen receptor (ER) positive breast cancer accounts for about 70% of total breast cancer and metastatic ER-Positive breast cancer accounts for the majority of breast cancer mortality. Although ER-Positive breast cancer is the most common subtype of breast cancer, there is a lack of mouse models that faithfully recapitulate ER-driven breast cancer. Published research from our lab has shown that knock-in mutation of ESR1^{Y541S} results in constitutive activation of ER, abnormal mammary gland development, male mouse feminization, and

decreased survival, but no tumor growth is associated with this mouse model. Forkhead box protein A1 (FOXA1) is a transcription factor that facilitates ER-chromatin association, and promotes tumorigenesis through a variety of mechanisms. By overexpressing FOXA1 in the doxycycline-inducible mouse model named FIC/MTB and crossing it to ESR1 mouse model (FIC/MTB/ESR1), we may be able to create a novel ER-Positive breast cancer mouse model. We demonstrated that FIC/MTB mouse mammary gland-derived organoids developed a filled sphere structure upon doxycycline induction, mimicking human mammary gland hyperplasia. Moreover, the FIC/MTB/ESR1 mice developed significant hyperplasia after 20-week induction. Although *in vivo* tumor kinetics study is ongoing, our current findings suggest that the novel mouse model FIC/MTB/ESR1 has the potential to develop mammary tumors.

RÉSUMÉ

Le cancer du sein est le type de cancer prédominant chez les femmes canadiennes, avec un taux d'incidence d'une femme sur huit au cours de leur vie. Les facteurs de transcription jouent des rôles pivots dans l'initiation et la progression du cancer du sein. Le transducteur de signal et activateur de transcription 3 (Stat3) est un facteur de transcription qui médie l'expression d'une variété de gènes en réponse aux cytokines et aux facteurs de croissance. L'activation de Stat3 joue des rôles clés dans la croissance cellulaire, la survie et l'apoptose, la migration et l'invasion cellulaires, ainsi que l'inflammation. En utilisant le modèle de souris avec une inactivation conditionnelle de Stat3, notre laboratoire a précédemment démontré que la déficience en Stat3 peut entraver la métastase du cancer du sein positif à ErbB2. Cependant, le mécanisme reste flou. En effectuant une analyse transcriptomique de cellules cancéreuses du sein positives pour ErbB2 et nulles pour Stat3 dissociées de tumeurs de souris, Lgals3 s'est avéré être une cible de Stat3 qui pourrait avoir médié le phénotype métastatique. Suite à la réduction par ARNsh de Lgals3, les cellules cancéreuses du sein positives à ErbB2 ont démontré une migration et une invasion réduites. Elles ont également formé des niveaux élevés d'adhésions focales qui peuvent mener à une réduction de la migration et des métastases. L'inhibition pharmacologique de Gal-3 conduit à une diminution de la migration et de l'invasion cellulaires. Ceci révèle le potentiel thérapeutique de l'inhibition de Lgals3 dans la prévention des métastases du cancer du sein positif à ErbB2.

Le cancer du sein positif aux récepteurs d'œstrogènes (ER) représente environ 70 % du total des cancers du sein et les métastases de cancer du sein positif à ER comptent pour la majorité de la mortalité liée à ce cancer. Bien que le cancer du sein positif à ER soit le sous-type le plus courant de cancer du sein, il y a un manque de modèles de souris qui récapitulent

fidèlement le cancer du sein induit par les ER. Les recherches publiées par notre laboratoire ont montré que la mutation ESR1Y541S entraîne une activation constitutive des ER, un développement anormal de la glande mammaire, une féminisation de la souris mâle, et une diminution de la survie, mais aucune croissance tumorale n'est associée à ce modèle de souris. La protéine de la boîte à fourche A1 (FOXA1) est un facteur de transcription qui facilite l'association ER-chromatine, et favorise la tumorigenèse par une variété de mécanismes. En surexprimant FOXA1 dans le modèle de souris inductible par la doxycycline, nommé FIC/MTB, et en le croisant avec le modèle de souris ESR1 (FIC/MTB/ESR1), nous pourrions créer un nouveau modèle de souris de cancer du sein positif à ER. Nous avons démontré que les organoïdes dérivés de la glande mammaire de souris FIC/MTB développent une structure de sphère pleine suite à l'induction par la doxycycline, imitant l'hyperplasie de la glande mammaire humaine. De plus, les souris FIC/MTB/ESR1 ont développé une hyperplasie significative après 20 semaines d'induction. Bien que l'étude de la cinétique tumorale *in vivo* soit en cours, nos résultats actuels suggèrent que le nouveau modèle de souris FIC/MTB/ESR1 a le potentiel de développer des tumeurs.

ACKNOWLEDGEMENTS

To begin with I would like to thank my supervisor Dr. William J. Muller, for accepting me as a master's student and allowing me to take initiative in my projects. It's been an honour to be a member of Muller lab and conduct a variety of experiments, especially those pre-clinical ones. I would also like to express my thanks to my committee members, my advisor Dr. Michel Tremblay, committee professors Dr. Vincent Giguere and Dr. Luke McCaffrey, for all the valuable suggestions and encouragement.

Moreover, I would like to thank all my lab members, for your support and all the help during the two years. Firstly, I would like to express my great gratitude to my mentor Ipshita. Your guidance in teaching me all the essential techniques, troubleshooting experimental issues, offering encouragement and support as I chase my dreams has been invaluable. Words fall short of adequately expressing my appreciation. My warmest thanks to Linshan, for always helping me in experiments and in life, supporting me and encouraging me. I will always remember the happy time and hard time that we had together. I would also like to extend my heartfelt thanks to Dongmei, who has consistently been the nurturing presence of our lab. Dongmei's assistance and encouragement have been invaluable to me in every facet of my life. Then, I would like to thank Tarek and Sherif, for sharing your passion for doing research, troubleshooting issues, and teaching me how to solve problems in doing research. Your research has been a profound source of inspiration to me. My sincere gratitude goes to Yu, for always offering help whenever I need. To Hailey, thank you for making the lab environment happy and relaxing. To Adeline and Alice, I really appreciate that you also helped me with many things. To the youngest lab members, Ellie and Elizabeth, thank you for sharing the snacks with us. I would also like to express my thanks to Vasilios, for helping with the mouse work and keeping the order of the lab. And to Virginie,

thank you for discussing the experiments with me, doing FACs for us, and offering help whenever I need.

I would especially like to express my gratitude to my parents, for always being there supporting me, and helping me when I am not feeling well, either emotionally or physically. Without your support, I will never reach this step. And I would like to thank my undergraduate lab supervisor at McGill University Department of Pharmacology, Dr. R. Anne McKinney, and my undergraduate lab mentor, for all the warmest support during my undergraduate and graduate studies.

CONTRIBUTION OF AUTHORS

I hereby state that I have carried out the work presented in this thesis unless stated otherwise.

Mouse stains and other reagents:

Dr. D. Levy provided the conditional Stat3^{flx} mice

Dr. L. Chodosh provided the MMTV-rtTA mice

The FIC, MMTV-NIC, EIC, ESR1 mouse strains were generated in the Muller lab.

Technical services

All paraffin-embedding, sectioning and hematoxylin and eosin (H&E) staining was performed by Goodman Cancer Research Center Histology Core Facilities.

McGill Advanced BioImaging Facility (ABIF) provided the use of all microscopes as well as technical assistance when required.

McGill Animal Facility at the GCRC performed pro-nuclear injections for the generation of the FIC.

In addition, they provided housing services for all mice.

Section 2.1.1

Dr. Jill Ranger and Dr. Laura Jones crossed MMTV-NIC strain to Stat3^{flx/flx} strain, and generated all the experimental mice, did the necropsies, collected tissues for paraffin-embedded sections. Dr. Jill Ranger dissociated tumors and created the Stat3-null NIC cell lines. Dr. Laura Jones sent the WT NIC and Stat3-null NIC cell lines for RNA-seq and did the bioinformatic analysis (Figure 4).

Novogene did the RNA-seq (Figure 4).

Section 2.1.2

Dr. Sherif Attalla crossed EIC/MTB strain to Stat3^{flx/flx} strain, and generated all the experimental mice, monitored them, did the necropsies, collected tissues for flash freezing, paraffin-embedded sections, and the lungs for H&E staining. Dr. Sherif Attalla generated the tumor growth curve and tumor burden graph (Figure 11). Dr. Sherif Attalla sent the EIC/MTB and Stat3^{flx/flx}/EIC/MTB tumors for RNA-seq and Novogene did the RNA-seq and bioinformatic analysis (Figure 14).

Section 2.2.1

Dr. Bin Xiao created the mouse model TetO-FOXA1-Ires-Cre (FIC). The initiation of this project was done by Sierra Lusson, who demonstrated that founder line 3 (FIC3) has higher expression than founder line 1 (FIC1)(Lusson, 2023). Therefore, only FIC2 and FIC3 are compared in this thesis.

Dr. William Muller and Dr. Alain Nepveu reviewed this thesis.

LIST OF FIGURES AND TABLES

Figure 1: Schematic construct of Stat3flx/flx/NIC	54
Figure 2: Apoptosis is increased in Stat3flx/flx/NIC tumors.....	56
Figure 3: Focal adhesion protein expressions are elevated in Stat3flx/flx/NIC cells	58
Figure 4: Transcriptomic study and bioinformatic analysis of WT NIC & Stat3-null NIC cells. 60	
Figure 5: Galectin-3 expression is downregulated in the Stat3-null NIC breast tumors and cells 63	
Figure 6: Knockdown of Lgals3 with shLgals3_1 and shLgals3_3 in WT NIC cell lines	66
Figure 7: Gal-3 knockdown leads to decreased migration and invasion	66
Figure 8: Pharmacological inhibition of Gal-3 leads to decreased migration and invasion	67
Figure 9: Focal adhesion protein expressions are decreased with Gal-3 knockdown in NIC cell lines	68
Figure 10: Schematic construct of Stat3flx/flx/EIC/MTB.....	69
Figure 11: Tumor onset is delayed in Stat3flx/flx/EIC/MTB mice and tumor burden is decreased	70
Figure 12: Lung metastasis is significantly decreased in Stat3flx/flx/EIC/MTB mice compared to EIC/MTB mice.....	72
Figure 13: A trend of decreased proliferation in the Stat3flx/flx/EIC/MTB compared to EIC/MTB mouse breast tumor.....	73
Figure 14: Transcriptomic study and bioinformatic analysis of EIC/MTB and Stat3flx/flx/EIC/MTB tumors	75
Figure 15: Gal-3 protein expression is decreased in Stat3flx/flx/EIC/MTB tumors compared to EIC/MTB tumors	77
Figure 16: Schematic construct of FIC/MTB mouse model.....	79
Figure 17: Representative genotyping blots of FOXA1 and MTB.....	79
Figure 18: Comparison of FOXA1 (Left) and Cre (Right) mRNA levels in the 4-week induced MTB, FIC2/MTB, and FIC3/MTB mice	80
Figure 19: FIC2/MTB mouse mammary gland-derived organoids have higher mRNA expression of FOXA1 and Cre expression in two-week induced organoids with doxycycline induction in FIC2/MTB than FIC3/MTB.....	81
Figure 20: FIC2/MTB mouse mammary glands had significantly higher expression of FOXA1 compared to WT counterparts after 12-week induction	82
Figure 21: Schematic procedures of growing organoids <i>in vitro</i> , timeline and the experiments .	84
Figure 22: FIC2/MTB mouse mammary gland-derived organoid developed a filled sphere structure with doxycycline induction.....	85
Figure 23: 4-week induced MTB and FIC2/MTB mammary gland H&E staining.....	86
Figure 24: 12 week-induced FIC2/MTB mammary gland wholemount, H&E staining, and immunofluorescent staining.....	88
Figure 25: 20-week induced MTB and FIC2/MTB mouse mammary gland wholemounts and H&E staining	89
Figure 26: Schematic construct of FIC/MTB/ESR1	90
Figure 27: Representative genotyping blot of ESR1	91
Figure 28: Excision PCR of FIC/MTB/ESR1 mammary gland-extracted DNA.....	91
Figure 29: 20-week induced FIC/MTB/ESR1 mouse mammary gland showed dramatic hyperplasia	93

Figure 30: Proposed schematic mechanism of Stat3 promoting HER2-positive breast cancer metastasis	98
Table 1: Genotyping PCR primer sequences, programs, and band size	106
Table 2: Excision PCR primer sequences, programs, and band size	107
Table 3: Primers used in qRT-PCR	108
Table 4: List of antibodies	112

LIST of ABBREVIATIONS

ADCC	Antibody-dependent cell-mediated cytotoxicity
ADCs	Antibody-drug conjugates
ADH	Atypical ductal hyperplasia
AIs	Aromatase inhibitors
AIB1	Amplified in breast cancer 1
ALH	Atypical lobular hyperplasia
CC3	Cleaved caspase 3
CCD	Coiled-coil domain
CERM	Conditional estrogen receptor alpha in mammary tissue
CRD	Carbohydrate recognition domains
DBD	DNA binding domain
DB-TFs	DNA-binding transcription factors
DCIS	Ductal carcinoma in situ
DMBA	7,12-dimethylbenz(a)anthracene
DOX	Doxycycline
ECM	Extracellular matrix
EGFR	Epidermal growth factor receptor
EMT	Epithelial-mesenchymal transition
ER	Estrogen receptor
ERK	Extracellular signal regulated kinase
EREs	Estrogen response elements

EtBr	Ethidium Bromide
FOXA1	Forkhead box protein A1
Gal-3	Galectin-3
GAS	Gamma-activated sites
GEMM	Genetically engineered mouse models
GnRHa	Gonadotropin-releasing hormone agonists
GO	Gene ontology
GSEA	Gene Set Enrichment Analysis
H&E	hematoxylin and eosin staining
HER2	Human epidermal growth factor-2
IDC	Invasive ductal carcinoma
IF	Immunofluorescence
IGF1R	insulin-like growth factor receptor
IHC	immunohistochemistry
IHF	Immunohistofluorescence
ILC	Invasive lobular carcinoma
IPA	Ingenuity pathway analysis
JNK	c-Jun N-terminal kinase
LBD	Ligand binding domain
LCIS	Lobular carcinoma in situ
LD	Linker domain
LTR	Long terminal repeat
MAPK	mitogen-activated protein kinase

MMTV	Mouse mammary tumor virus
NTD	N-terminal domain
OFS	Ovarian function suppression
PCR	Polymerase chain reaction
PG	glycosaminoglycans/proteoglycans
PI3K	phosphatidylinositol-4,5,-bisphosphate 3-kinase
PKC	protein kinase C
PRL	Prolactin
PRKP	Prolactin receptor
PyV mT	Polyomavirus middle T antigen
Rb	Retinoblastoma protein
Rpm	Revolutions per minute
rtTA	reverse tetracycline transactivator
Stat3	Signal transducer and activator of transcription 3 (Stat3)
SERMs	Selective estrogen receptor modulators
SERDs	Selective estrogen receptor degraders
SH2	Src-homology domain
TAD	Transcription activation domain
TF	Transcription factor
TME	Tumor microenvironment
TKIs	tyrosine kinase inhibitors
TUNEL	terminal deoxynucleotidyl transferase dUTP nick end labeling
Tyr	Tyrosine

WT	Wildtype
ZEB1	Zinc finger E-box binding homeobox 1

Chapter 1: Literature Review

1.1. Mammary Gland and Breast Cancer

1.1.1. Breast Cancer Epidemiology

As of 2023, cancer is the leading cause of death in Canada. In females, breast cancer constitutes the second most common cause of mortality, following lung cancer (Society, 2023a). It is estimated that in Canada, approximately 1 in 8 women will be diagnosed with breast cancer during their lifetime, and 1 in 36 will die from it (Society, 2023a).

Breast cancer has a high gender specificity (Konduri et al., 2020). Despite the high prevalence of breast cancer in females, it is relatively rare in men, which comprises only less than 1% of all breast cancer (Konduri et al., 2020). Moreover, the prognosis of male and female breast cancer differs (Gnerlich et al., 2011).

Breast cancer survival rate has been drastically improved due to the progression in early stage screening and treatment (Nardin et al., 2020). In Canada, the 5-year net survival for breast cancer patients is 89%, however, it highly varies depending on the stage of diagnosis (Society, 2023b). Although Stage 1 breast cancer has a net 5-year survival rate of 100% in women, it is only 23% for that of Stage 4 breast cancer patients (Society, 2023b). The poor prognosis of Stage 4 breast cancer due to metastasis and resistance to treatments further highlights the importance of breast cancer research and new therapeutic development.

1.1.2. Mammary Gland Anatomy and Basic Structure

Understanding the fundamental anatomy and structure of mammary gland is essential for breast cancer research. Mammary gland is specific to mammals, and has a compound, branched tubuloalveolar structure, which evolved from the epidermal apocrine glands (Biswas et al.,

2022). The primary function of mammary glands is the secretion of milk, which provides essential nutrition for offspring during the postnatal period (Biswas et al., 2022). The mammary glands are fundamentally composed of alveoli, which cluster together to form lobules surrounded by adipose and connective tissues (Biswas et al., 2022). Each lobule is connected to the nipple via a lactiferous duct through which it drains (Biswas et al., 2022).

Several types of cells collectively form the mammary glands (Biswas et al., 2022). The ductal network of the gland, including the lactiferous duct, is composed of epithelial cells, which maximize the surface area within the limited volume available (Biswas et al., 2022). Besides, mammary glands are supported by an array of stromal cells or connective tissues with extracellular matrix (ECM) proteins (Biswas et al., 2022). The stromal connective tissues comprise adipocytes, fibroblasts, vascular endothelial cells, a variety of innate immune cells, and nerves (Biswas et al., 2022).

Epithelium can be further classified into two types, luminal and basal. Luminal epithelium forms the inner layer of the lactiferous duct whereas the basal epithelium, which comprises myoepithelial cells and forms the outer layer of the lactiferous duct (Biswas et al., 2022). During pregnancy, the luminal cells or luminal progenitors can develop alveolar epithelial cells, which act as the major source of milk production (Gieniec & Davis, 2022; Li et al., 2022). After milk is produced, basal cells, which are contractile, are responsible for the ejecting of milk (Gieniec & Davis, 2022; Li et al., 2022). Moreover, basal cells may play a role in tumor suppression, by inhibiting the progression of Ductal Carcinoma In Situ to invasive ductal carcinoma (Li et al., 2022).

1.1.3. Breast Cancer Development

The hypothesis posits that the development of breast cancer follows a stepwise progression. This progression starts with normal mammary glands developing atypical ductal hyperplasia (ADH) or atypical lobular hyperplasia (ALH), which describes the presence of abnormal proliferative lesions (Myers & Walls, 2024). Although these lesions are not qualitatively or quantitatively abnormal enough to be defined as ductal carcinoma in situ (DCIS) or lobular carcinoma in situ (LCIS), ADH or ALH is considered a high-risk factor of DCIS or LCIS (Myers & Walls, 2024). As the names suggest, DCIS or LCIS represent the stages of non-invasive lesions characterized by the transformation of cells into a cancerous state that remains localized at the original site (Buerger et al., 2000). However, DCIS or LCIS, especially high-grade lesions, is the risk factor of invasive ductal carcinoma (IDC) or invasive lobular carcinoma (ILC) (Buerger et al., 2000). Therefore, DCIS and LCIS are sometimes referred to as Stage 0 breast cancer (van Seijen et al., 2019). Once the myoepithelium is breached and cancerous cells escape from the ducts, the DCIS becomes IDC (Tower et al., 2019). This transformation may be attributed to genetic alterations and immune microenvironment alterations (Gil Del Alcazar et al., 2017; Trinh et al., 2021). IDC and ILC are followed by metastasis (Rivenbark et al., 2013). Metastasis is defined as the mobile of cancer cells from their original site to the other organs or tissues of the body, mainly through the blood or lymph system (Seyfried & Huysentruyt, 2013). In breast cancer, the major metastatic sites are bones, livers, lungs, and brain (Wang et al., 2019). Metastasis of breast cancer is associated with relatively poor prognosis, with an only 23% 5-year survival rate in the Stage 4 patients (Society, 2023b).

1.1.4. Histological and Molecular Subtypes of Breast Cancer

Breast cancer can be further categorized into subtypes by histological features and molecular features. The histological type describes the growth pattern of the tumors (Weigelt et al., 2010). Based on the histological features, breast cancer can be classified into in situ carcinoma and invasive carcinoma depending on whether the cancerous cells remain in the original place of occurrence (Malhotra et al., 2010). Depending on whether the carcinoma affects ducts or lobules of the breast, in situ breast cancer can be further classified into DCIS or LCIS (Malhotra et al., 2010). The major invasive carcinoma subtypes include invasive lobular, infiltrating ductal, ductal/lobular, mucinous, medullary, tubular and papillary carcinomas (Malhotra et al., 2010).

Another way to classify breast cancer is based on the molecular subtypes of breast cancer, which is very commonly employed in breast cancer biochemical research. Based on the molecular features, breast cancer can be mainly categorized into luminal A, luminal B, HER2-Positive, and triple-negative breast cancer (Orrantia-Borunda et al., 2022). Luminal A breast cancer is characterized by the presence of ER and/or PR without the expression of HER2, with a prevalence of 28% to 31% of the total breast cancer (Dwivedi et al., 2019; Malhotra et al., 2010; Orrantia-Borunda et al., 2022). Luminal A breast cancers are generally low grade, and proliferate slowly, with a Ki-67 less than 20%, thus having a relatively good prognosis (Orrantia-Borunda et al., 2022). Luminal B breast cancer is also ER and/or PR positive, however, it differs from luminal A breast cancer by the presence of HER2 (Orrantia-Borunda et al., 2022). Luminal B breast tumors are usually higher grade than luminal A breast tumors, thus having a prognosis worse than luminal A breast cancer (Orrantia-Borunda et al., 2022). This luminal B subtype breast cancer accounts for 10-20% of luminal tumor types (Orrantia-Borunda et al., 2022).

Another common subtype of breast cancer is HER2-Positive breast cancer, which is characterized by an overexpressed HER2 (Orrantia-Borunda et al., 2022). They are generally more aggressive and have a high proliferation, so they have a worse prognosis than luminal B breast cancer (Orrantia-Borunda et al., 2022). Triple-negative breast cancer (TNBC), which means ER, PR, HER2 negative, constitutes approximately 20% of all breast cancer and has the worst prognosis (Orrantia-Borunda et al., 2022). It can be further categorized into additional subtypes including basal-like, claudin-low, mesenchymal, luminal androgen receptor, and immunomodulatory subtypes (Orrantia-Borunda et al., 2022). Due to the lack of expression of ER, PR and HER2, the treatment regime is generally more restricted to chemotherapy (Wahba & El-Hadaad, 2015). The 5-year survival of the different breast cancer subtypes differs, with the best survival of 94.4% for luminal A subtype, 90.7% for the luminal B subtype, 84.4% for HER2-Positive subtype, and 77.1% for the TNBC subtype (Orrantia-Borunda et al., 2022).

1.1.5. Genetically Engineered Mouse Models (GEMM) of Breast Cancer

The GEMMs play a critical role in breast cancer research, from the perspectives of understanding the underlying mechanism and exploring potential therapeutics (Sakamoto et al., 2015). They employ the modification of genes to study the molecular events in tumor initiation and progression *in vivo* (Sakamoto et al., 2015). The first transgenic breast cancer mouse model that spontaneously develop breast tumor by the expression of c-myc was generated in 1984 by Stewart et al (Stewart et al., 1984). To ensure the mammary-specific transgene expression, the mouse mammary tumor virus (MMTV)-long terminal repeat (LTR) promoter has been widely employed in the transgenic mouse model of breast cancer (Stewart et al., 1988). Moreover, for the spatial and temporal control of transgene expression, inducible mouse models that can be

controlled with tetracycline and its derivative doxycycline administration have been developed (Hennighausen et al., 1995). Later, in an effort to further improve the inducible system, Chodosh group developed the MTB (MMTV-rtTA) mice that express reverse tetracycline transactivator (rtTA) under the control of MMTV promoter (Gunther et al., 2002). The MTB strain, usually crossed with a mouse strain bearing Tet-On system, brings about a promising inducible system which enables the rapid induction of transgene and permits the titration of transgene expression to a desired level (Gunther et al., 2002). With the administration of doxycycline, rtTA is activated and undergoes a conformational change, which drives its binding to the TRE region of the TetO operator (Das et al., 2016; Gunther et al., 2002). This binding enables the expression of the downstream genes of TetO operator (Das et al., 2016).

A common way to study a specific gene and its regulatory role in disease is to remove this gene from the disease mouse model and monitor the pathogenesis. To accomplish a spatial and temporal removal of the gene, a Cre-loxP system has been widely used (Kim et al., 2018). Cre recombinase was discovered as a 38-kDa DNA recombinase produced from cre gene which works as a cyclization recombinase in bacteriophage P1 (Sauer, 1998; Sternberg & Hamilton, 1981). Cre recombinase can recognize a specific DNA sequence called loxP site and mediates the excision of the DNA sequence flanked by these loxP sites (Sauer, 1998). The activity of Cre recombinase can be regulated through a range of different promoters or operators, resulting in various activation patterns (Kim et al., 2018). For example, coupling Cre with MMTV promoter facilitates the site-specific activation in the mammary epithelium (Yuan et al., 2011). Meanwhile, linking Cre with Tet-O operator only allows for the Cre activation upon doxycycline induction (Kim et al., 2018).

1.2. HER2-Positive Breast Cancer

1.2.1. Mechanism of HER2-Positive Breast Cancer

Human epidermal growth factor receptor-2 (HER2), also known as ERBB2 or neu, belongs to the epidermal growth factor receptor (EGFR) family (Dean & Kane, 2012). HER2 normally plays a key role in various cellular processes including cell proliferation and anti-apoptosis, therefore, its abnormality drives the oncogenic process (Gutierrez & Schiff, 2011). HER2 is an oncogene that is amplified or overexpressed in 15-30% of breast cancers and 10-30% of gastric/gastroesophageal cancers (Iqbal & Iqbal, 2014).

The HER family (also called EGFR family) consists of four transmembrane receptor tyrosine kinases, HER1, HER2, HER3, and HER4, which exist as monomers on the cell surface (Nuciforo et al., 2015). Although HER2 does not have a known ligand that directly activates its activity, it can spontaneously form active dimers or become active through heterodimerization with other HER family members (Iqbal & Iqbal, 2014; Peckys et al., 2019). This dimerization activates a variety of signaling pathways through the autophosphorylation of tyrosine residues within the cytoplasmic domain of the receptors (Iqbal & Iqbal, 2014). These signaling pathways include the mitogen-activated protein kinase (MAPK), phosphatidylinositol-4,5,-bisphosphate 3-kinase (PI3K), and protein kinase C (PKC) (Iqbal & Iqbal, 2014). The activation of these pathways triggers the recruitment of various nuclear factors that drive the transcription of a range of genes (Iqbal & Iqbal, 2014). These particular genes play important roles in modulating cellular processes including cell cycle progression, proliferation, survival and apoptosis (Iqbal & Iqbal, 2014). Under normal circumstances, these processes are the key components of cellular functions and behaviors (Iqbal & Iqbal, 2014).

However, the overexpression of HER2 leads to the constitutive activation of the growth factor signaling pathways, thereby driving breast cells to grow and divide in an uncontrolled way, eventually becoming breast cancer (Gajria & Chandarlapaty, 2011). In 1988, Muller et al. demonstrated that the overexpression of c-neu gene in mouse mammary epithelial cells is sufficient to induce malignant transformation in a single step to drive the tumorigenesis (Muller et al., 1988).

1.2.2. Metastasis of HER2-Positive Breast Cancer

Metastasis is the process of cancer cell dissemination from the original site to other organs or tissues of the body (Hanahan & Weinberg, 2000). It is the major cause of morbidity of breast cancer and accounts for about 90% of cancer deaths (Hanahan & Weinberg, 2000). Beyond the necessary conditions of cancer initiation and progression, additional characteristics are required for metastasis, which have been referred to as the hallmarks of metastasis, including motility & invasion, modulation of microenvironment, plasticity, and colonization (Welch & Hurst, 2019). Motility & invasion play a fundamental role in metastatic cascades, as metastasis occurs in a stepwise manner that highly relies on the migration and invasion of tumor cells (Stuelten et al., 2018). This process encompasses several steps: breaching of the basement membrane and escaping from primary tumors, migrating to blood and lymphatic vessels, intravasation and extravasation, and eventually moving into distant organs (Stuelten et al., 2018). Another key component of metastasis is the tumor microenvironment (TME), which is modulated by a range of immune cells, cancer-associated fibroblasts, and structural elements that constitute the extracellular matrix (ECM) (Neophytou et al., 2021). The cellular and structural component interactions of TME can direct the aggressiveness, dissemination of malignant cells

and promote immune evasion (Neophytou et al., 2021). Moreover, at the metastatic site, the TME plays a role in awakening cancer cells from dormancy, thus promoting the growth of metastatic tumors (Neophytou et al., 2021). In addition, cell plasticity, which refers to the adaptation of cancer cells to different cell states, plays an important role in modulating tumor growth and proliferation, metastasis and drug tolerance (Pérez-González et al., 2023).

Colonization is the last step of metastasis, during which several obstacles need to be overcome, including infiltrating distant tissue, evading immune defences, adapting to supportive niches, surviving as latent tumor-initiating seeds, and eventually breaking out to replace the host tissue (Massague & Obenauf, 2016).

Research has shown that HER2 overexpression can promote the metastatic phenotype and HER2-Positive breast cancer is prone to recurrence and metastasis (Yang et al., 2022). Studies have shown that approximately 94% of samples have consistent HER2 status between primary tumor and metastatic sites (Gancberg et al., 2002). HER2 can promote cell migration by activation of Zinc finger E-box binding homeobox 1 (ZEB1), a transcription factor that enhances tumor invasion and metastasis, and downregulation of E-Cadherin (Zeng et al., 2019). Also, HER2-overexpressing breast cancer cells can secrete extracellular matrix protein 1 (ECM1), which promotes the formation of a vascular niche that accelerates cancer cell migration and invasion (Steinhaeuser et al., 2020). In addition, HER2 encodes protein p185erbB2 which plays a role in cell movement, thus providing the ability of tumor cells to spread and metastasize (De Potter & Quatacker, 1993).

1.2.3. Therapeutics of HER2-Positive Breast Cancer

Although HER2-Positive breast cancer generally has a worse prognosis when compared to luminal A and luminal B breast cancer, the overexpression of HER2 makes it possible for the targeted therapy (Orrantia-Borunda et al., 2022).

Targeting HER2 protein, monoclonal antibodies have been developed and have achieved success in the treatment of HER2-Positive breast cancer (Baselga et al., 1998). Trastuzumab (Herceptin) was the first humanized monoclonal antibody successfully against HER2 (Baselga et al., 1998). It functions by binding to the extracellular domain of HER2, thereby inhibiting the intracellular HER2 signaling pathways and mediating the antibody-dependent cell-mediated cytotoxicity (ADCC) (Baselga et al., 1998; Swain et al., 2023).

Another class of HER2-Positive breast cancer is tyrosine kinase inhibitors (TKIs), which are small molecules targeting the intracellular catalytic kinase domain of HER2, thus blocking phosphorylation and signaling pathways (Paul & Mukhopadhyay, 2004). Lapatinib is a reversible inhibitor of HER1 and HER2, which can still be used in patients with trastuzumab resistance (Konecny et al., 2006). This is because trastuzumab resistance is mediated by upregulation of insulin-like growth factor receptor (IGF1R), but Lapatinib can block the crosstalk between IGF1R and HER2 (Nahta et al., 2007).

In addition to monoclonal antibodies and TKIs, antibody-drug conjugates (ADCs) have gained remarkable success (Swain et al., 2023). ADCs combine the HER2 antibodies that can recognize the specific sites of action, and the cytotoxic drugs that mediate cell death at the target, into a single pharmacological entity (Peters & Brown, 2015). The major purpose of ADCs is to increase the antitumor efficacy at the targeting site and decrease the effects on healthy tissues

(Marei et al., 2022). Indeed, ADCs have a higher efficacy than the sum of antibodies and drug respectively (Peters & Brown, 2015).

Other therapies of HER2-Positive breast cancer include immunotherapy, chemotherapy, radiotherapy, and surgeries (Ayoub et al., 2019). The integration of these therapies has markedly improved the 5-year survival of HER2-Positive breast cancer (Swain et al., 2023).

1.2.4. Mouse Models of HER2-Positive Breast Cancer

Although the importance and relevance of HER2 in breast cancer were discovered in 1980s, there was a lack of evidence that overexpression of HER2 is sufficient to drive tumorigenesis (Muller et al., 1988). Therefore, a mouse model that conditionally overexpressed HER2 in mammary gland was required.

In 1988, the Leder lab generated the first HER2-Positive mouse model by overexpressing activated rat homologue of HER2 (NEU-NT) linked to MMTV promoter (Muller et al., 1988). With a latency of 3 months, these mice spontaneously develop breast tumor that involves the entire mammary epithelium (Muller et al., 1988). Further proved by three independent transgenic lines, these showed that the overexpression of NEU was sufficient to transform mammary epithelial cells (Guy et al., 1996). Moreover, the wildtype proto-oncogene NEU overexpressed mouse model MMTV-NEU showed a longer tumor onset of 7 months, which demonstrated that the wildtype NEU can also promote tumorigenesis (Guy et al., 1992). In another study, the receptors were modified with in-frame deletions within the extracellular domain and these mice (MMTV-Neu-NDL) were able to grow multifocal tumors that frequently metastasize to the lung (Siegel et al., 1999).

The integration of HER2 mouse models with additional transgenic mouse models has been widely used in studying various genes in biological processes of HER2-Positive breast cancer. For this purpose, the Muller lab has generated a transgenic mouse model expressing both activated ErbB2 (NDL2-5) and Cre recombinase, under the control of promoter MMTV (MMTV-NIC) (Ursini-Siegel et al., 2008). MMTV-NIC mouse model has an average tumor onset of 146 days and only develops tumors in mammary glands (Ursini-Siegel et al., 2008). By crossing the NIC mouse model to another transgenic mouse that bears the LoxP site flanked by the target genes, these specific genes are removed, thus making it possible to study the role of specific genes in HER2-Positive mouse model (Ursini-Siegel et al., 2008).

To further study the HER2-Positive breast cancer initiation and progression, the Muller lab has developed another HER2-Positive breast cancer mouse model that faithfully recapitulate the human HER2 breast cancer, the TetO-ErbB2-Ires-Cre (EIC) mouse model (Attalla et al., 2023). Compared to NIC mouse model, EIC mouse model employs human HER2 as the oncogene, features an inducible system by crossing with MTB, and recapitulates human DCIS stage of breast cancer (Attalla et al., 2023).

1.3. ER-Positive Breast Cancer

1.3.1. Mechanism of ER Signaling in Mammary Gland

Estrogen receptor (ER) is activated by estrogen, and plays important roles in maintaining normal female reproductive functions and other metabolic functions (Miziak et al., 2023).

Estrogen receptors can be mainly classified into two categories, nuclear estrogen receptors and membrane estrogen receptors (Miziak et al., 2023). Nuclear receptor ERs can be further

categorized into ER alpha and ER beta, which render different biological effects (Miziak et al., 2023).

ER alpha and ER beta are encoded by ESR1 and ESR2 gene, and located on the sixth and fourteenth chromosome respectively (Fuentes & Silveyra, 2019). The functions of ER alpha and ER beta vary greatly by acting on distinct tissues and cells (Paterni et al., 2014). ER alpha mainly functions in female reproductive systems by expressing in breasts, ovaries, and uterus, whereas the expressions of ER beta are mainly found in nervous system, cardiovascular systems, ovaries, and the male reproductive systems (Paterni et al., 2014). Therefore, the biological functions of ER in mammary glands are predominantly mediated by ER alpha (Paterni et al., 2014).

The signaling of ER can be categorized into genomic signaling and non-genomic signaling (Miziak et al., 2023). In genomic signaling, the signaling of ER is activated by cytoplasmic estrogen binding to the ER monomer in the cytoplasm (Mohibi et al., 2011; Zhang et al., 2014). In classical ER signaling, activated ER forms dimers and translocates into the nucleus, where the complex binds to a specific DNA sequence called the estrogen response elements (EREs), which transactivates specific gene expressions (Kuntz & Shapiro, 1997). Transcription factor Forkhead box A1 (FOXA1) plays a pioneering role in facilitating ER-chromatin association, thus producing transcriptional regulation of ER-regulated genes (Seachrist et al., 2021). Additionally, cyclin D1 binds directly to the hormone-binding domain of the estrogen receptor, increasing the binding of the receptor to ERE sequences, and upregulating ER-mediated transcription (Zwijnsen et al., 1997). Moreover, FOXA1 is required for the estrogen-induced cyclin D1 (CCND1) expression, and they synergistically promote the transcription of genes driven by ER (Albayrak et al., 2018). In the “non-classical” genomic ER signaling pathways, upon the estrogen binding to the ER, they can form a complex and translocate to the

nucleus, where they indirectly bind to the transcription factors (TF) via the TF response elements (Miziak et al., 2023).

In non-genomic signaling, the ER alpha is localized on the cell membrane (Miziak et al., 2023). The process of estrogen binding to the ER-alpha can lead to downstream signaling pathway activation, including PI3K and Ras-MAPK pathways (Mohibi et al., 2011). The activation of the two pathways results in target protein phosphorylation, thereby driving the transcription of a range of genes related to cell growth and proliferation (Mohibi et al., 2011). This process of PI3K and Ras-MAPK pathway activation by estrogen binding to membrane ER is in synergy with TGF-alpha binding to EGFR and Prolactin (PRL) binding to the prolactin receptor (PRLR) (Mohibi et al., 2011). In addition, PRL binding to PRLR also triggers a tyrosine kinase-mediated signaling cascade, which activates Stat1, Stat3, and Stat5, and results in their translocation to the nucleus (Mohibi et al., 2011; Mortlock et al., 2021). In the nucleus, phosphorylated Stat proteins interact with ER alpha and together drive the transcriptional activity of ER target genes (Hou et al., 2018; Siersbæk et al., 2020).

1.3.2. Therapeutics of ER-Positive Breast Cancer

About 70% of breast cancers are ER-Positive breast cancers (Lumachi et al., 2013). Due to the feature of ER-Positive breast cancer, treatments are given mainly to prevent the activation of ER signaling, which are called hormone or endocrine therapy (Lumachi et al., 2015). The drugs in the endocrine therapy can be categorized into two types, including drugs that block ER and drugs that lower estrogen levels (Lumachi et al., 2015). Drugs blocking ER can be further subcategorized into selective estrogen receptor modulators (SERMs) and selective estrogen receptor degraders (SERDs) (Lumachi et al., 2015).

SERMs function by competitively binding to ER, thus blocking the natural estrogen from binding with cancer cells in the breast (Lumachi et al., 2015). They have a mixed agonist/antagonist activity in the interaction with ER varying from tissues to tissues (Lumachi et al., 2015). The SERMs that treat breast cancer act as an antagonist in breast tissues, but they act as partial agonists on the endometrium (Cano & Hermenegildo, 2000). Therefore, one of the adverse effects of SERMs is the possibility of developing endometrial cancer (Cano & Hermenegildo, 2000). Tamoxifen is the most widely used SERM, and studies have suggested that ten-year treatment with Tamoxifen significantly reduces breast cancer recurrence and improves survival (Davies et al., 2013).

In contrast, SERDs are pure antagonist of ER, promoting the degradation of SERD-ER complex via proteasome and blocking the ER signaling (Hernando et al., 2021). Fulvestrant, the first SERD, exhibits higher affinity to ER than Tamoxifen, and disrupts ER signaling through dual mechanism (Hernando et al., 2021). The first mechanism prevents the dimerization of ER, blocking ER from translocating to the nucleus (Hernando et al., 2021). The second makes an unstable Fulvestrant-ER complex that can be easily degraded by the ubiquitin-proteasome system (Hernando et al., 2021).

Another class of drugs in endocrine therapy functions by decreasing estrogen levels. These drugs can be further categorized into aromatase inhibitors (AIs) and ovarian function suppression (OFS) drugs (Lumachi et al., 2015). AIs inhibit the enzyme aromatase, which is mainly expressed in ovary (premenopausal women), testis, placenta, brain, bone and adipose tissue (postmenopausal women), and plays a key role in turning other hormones into estrogen (Lumachi et al., 2015). AIs are only used in postmenopausal women, as they are ineffective in premenopausal women, which is because the ovaries of premenopausal women can compensate

for this by increasing gonadotropin secretion and estrogen production ("Aromatase inhibitors versus tamoxifen in premenopausal women with oestrogen receptor-positive early-stage breast cancer treated with ovarian suppression: a patient-level meta-analysis of 7030 women from four randomised trials," 2022; Lumachi et al., 2015). Based on distinct chemical structures and mechanisms of action, there are two types of AIs, permanent steroidal inhibitors of aromatase and reversible nonsteroidal inhibitors (Lumachi et al., 2015). Studies have shown that in postmenopausal women, AIs are even more effective than Tamoxifen by further decreasing the recurrence rates by 30% ("Aromatase inhibitors versus tamoxifen in premenopausal women with oestrogen receptor-positive early-stage breast cancer treated with ovarian suppression: a patient-level meta-analysis of 7030 women from four randomised trials," 2022).

For decades, OFS has been achieved by performing surgical oophorectomy, which is the surgery that removes one or both ovaries (Lawson & Rentea, 2024; Lumachi et al., 2015). Nowadays, OFS can also be obtained with gonadotropin-releasing hormone agonists (GnRHa), and this reversible drug therapy has largely replaced surgery (Lumachi et al., 2015). In early stage ER-Positive breast cancer, the combination of OFS and AIs has been shown to significantly reduce the recurrence compared to other regimen (Lumachi et al., 2015).

Although endocrine therapy has achieved great success in treating ER-Positive breast cancer, about 20% of patients have innate resistance to endocrine therapy, and others can develop resistance to endocrine therapy over time (Zhou et al., 2023). Therefore, another class of drug, CDK4/6 inhibitors have been given to patients resistant to endocrine therapy, or given together with endocrine therapy to patients with advanced-stage ER-Positive breast cancer (Zhou et al., 2023). CDK4 and CDK6 together with D-type cyclins phosphorylate retinoblastoma protein (Rb), which releases E2F to promote transcription of genes and initiate progression from

the G1 to S phase (Sheikh & Satti, 2021). CDK4/6 inhibitors function by inhibiting the retinoblastoma protein (Rb) phosphorylation, leading to G₁ cell cycle arrest (Zhou et al., 2023). The synergistic effects of CDK4/6 inhibitor and endocrine therapy have been extensively studied, which revealed that the combination of a novel CDK4/6 inhibitor dalpiciclib and fulvestrant significantly prolonged the progression-free survival in ER-Positive, HER2 negative patients (Sheikh & Satti, 2021).

Despite the considerable effectiveness of endocrine therapy and CDK4/6 inhibitors, patients with ER-Positive breast cancer patients who develop resistance to both therapies often face limited treatment options upon recurrence or metastasis (Zhou et al., 2023). The options include chemotherapy, combination therapies that target the PI3K/AKT/mTOR pathway and CDK2 inhibitors (Zhou et al., 2023). However, these therapies generally have a lower efficacy or exhibit significant adverse effects (Zhou et al., 2023). Therefore, there remains an urgent need for the exploration of novel therapies that against ER-Positive breast cancer.

1.3.3. Mouse Models of ER-Positive Breast Cancer

Considering the imperative to delve into the pathogenesis of ER-Positive breast cancer and explore novel therapeutics, it is of great importance to develop mouse models that recapitulate ER-Positive breast cancer initiation and progression.

Several ER-Positive breast cancer mouse models have been established, which can be classified into five types based on the underlying mechanism driving tumor growth (Dabydeen & Furth, 2014b).

The first category is the mouse models developing ER-Positive mammary tumor from direct over-expression or constitutive activation of ER alpha (Dabydeen & Furth, 2014b). One of

these mouse models is the conditional estrogen receptor alpha in mammary tissue (CERM), *Tet-op-Esr1^{MMTV-rtTA}*, which is regulated with MMTV-LTR promoter and tetracycline-inducible system, and overexpress ER alpha expression by two times higher than normal (Frech et al., 2005; Miermont et al., 2012). However, only 3-5% of mice develop mammary cancers between 10 to 12 months, and 50% of the mammary tumors are ER-Positive (Frech et al., 2005; Miermont et al., 2012). By introducing an oncogene Simian virus 40 to the ER alpha transgene, the MMTV-tTA/tetop-TAg/tetop-ER-alpha triple transgenic mouse model was established (Tilli et al., 2003). The addition of the oncogene SV40 brings the percentage of mice developing mammary tumors to 37% between 10-12 months, and all of the tumors are ER-Positive (Tilli et al., 2003). However, more than 50% of mice develop salivary adenocarcinoma and other cancers, making it impossible to study the survival of ER-Positive breast cancer (Tilli et al., 2003).

The second category of ER-Positive breast cancer mouse model is developed as a result of genetic alterations of molecules impacting estrogen signaling (Dabydeen & Furth, 2014b). The majority of the ER-Positive mouse models belong to this category (Dabydeen & Furth, 2014b). From the study of ER signaling, many molecules play a role in ER functions, such as cyclinD1, Wnt, Stat1, PRL, and AIB1 (Dabydeen & Furth, 2014b). Amplified in breast cancer 1(AIB1) is a steroid receptor coactivator that is overexpressed in breast cancer and recruited by ER to promote its function (Azorsa et al., 2001). MMTV-AIB1 mouse model conditionally overexpress AIB1 gene in the mouse mammary gland (Torres-Arzayus et al., 2004). In this mouse model, about 76% of mice developed mammary tumors between 12 to 25 months, and 40% of them are ER-Positive tumors (Torres-Arzayus et al., 2004). In this AIB1 overexpressing mouse model, the PI3K/AKT pathway is activated, which plays a role in promoting tumorigenesis (Torres-Arzayus et al., 2004). Another mouse model is the Stat1^{-/-} mouse model

(Chan et al., 2012). Stat1 expression level was higher in the normal breast tissue adjacent to the malignant lesion, indicating that Stat1 expression is downregulated in tumor progression (Chan et al., 2012). The mouse model with Stat1 knockout spontaneously develops mammary tumors in 62% of mice and more than 90% of the tumors are ER-Positive (Chan et al., 2012). Despite the relatively high tumor penetrance and high ER positivity, the tumor onset is between 18 months and 26 months (Chan et al., 2012). Reintroducing Stat1 into Stat1^{-/-} tumor cells lead to apoptosis, indicating the role of Stat1 in promoting apoptosis and thus tumor suppression (Chan et al., 2012).

The third category of ER-Positive breast cancer mouse model combines the pharmacological treatment and genetic alterations of molecules impacting estrogen signaling (Dabydeen & Furth, 2014b). *Brca1^{f11/f11/p53+/-/MMTV-Cre}* mouse model introduces anticancer drug peroxisome proliferator-activated receptor gamma (PPARgamma) agonist efatutazone into BRCA1 conditional loss, TP53 insufficiency mouse model at the age of 4 months (Nakles et al., 2013). This mouse model 100% develops breast tumor between 10 and 12 months, whereas only 23% of the tumors are ER-Positive (Dabydeen & Furth, 2014b; Nakles et al., 2013). The introduction of the drug efatutazone decreased the total number of cancers and increased the rate of well-differentiated cancers, making the pathological features closer to the ER-Positive breast cancer (Beikman et al., 2013; Nakles et al., 2013).

The fourth category of ER-Positive breast cancer mouse model relies on carcinogen exposure in combination with genetic alterations to develop breast tumor (Dabydeen & Furth, 2014b). The mouse model, MMTV-myrAkt1, which overexpress the activated Akt1 (myristoylated AKT), was treated with carcinogen 7,12-dimethylbenz(a)anthracene (DMBA) for 5 weeks beginning at 9 weeks of age, developing mammary tumors in 40% of mice and all of the

tumors are ER-Positive (Blanco-Aparicio et al., 2007). Meanwhile, the tumor onset is between 6 and 12 months (Blanco-Aparicio et al., 2007). However, due to the exposure of carcinogen, a range of other cancers also develop in a large percentage of mice (Blanco-Aparicio et al., 2007). For instance, ovary tumors are found in more than 50% of mice of the MMTV-myrAkt1 mouse model (Blanco-Aparicio et al., 2007).

The last category of ER-Positive breast cancer mouse model is driven by the brother-sister matings (Dabydeen & Furth, 2014b). As an uncommon method to establish mouse model, Kumar et al. used an NIH nude mouse that spontaneously developed tumor as the founder and continuous brother-sister mating (Kumar et al., 2007). About 62% of heterozygous mutated NIH nude female mice develop mammary tumors from 3.5 to 12 months, and all of them have high ER expression (Kumar et al., 2007). Although this mouse model has a relatively high tumor rate and high ER-Positive tumor rate, this mouse model requires parity to develop breast tumor because they don't develop tumors until they give birth to at least one litter (Kumar et al., 2007).

Here we analyzed five categories of ER-Positive breast cancer mouse models, which reveals a diverse spectrum of the existing ER-Positive breast cancer mouse models. However, all these mouse models exhibit one or more of the following limitations, including long latency, low tumor rate, low ER-Positive tumor rate, parity required, insensitive to Tamoxifen treatment, growth defects, multiple cancer types, and molecular features not fully consistent with ER-Positive human breast cancer (Dabydeen & Furth, 2014b). Given that ER-Positive breast cancer accounts for about 70% of total breast cancer and the lack of a faithful mouse model, the development of a novel ER-Positive breast cancer mouse model is critically important.

1.3.4. A novel ESR1 point mutation mouse model that drives male mouse feminization

In an effort to create a mouse model that faithfully recapitulates ER-Positive breast cancer, the Muller lab recently created a novel mouse model with ESR1^{Y541S} mutation (Simond et al., 2020). Mouse ESR1^{Y541S} mutation happens in the ligand binding domain (LBD) and is equivalent to ESR1^{Y537S} mutation in human, which leads to the constitutive activation of ER alpha, and accounts for up to 20% of endocrine-resistant metastatic tumors (Simond et al., 2020). Also, although ESR1^{Y537S} mutation is not implicated in primary ER-Positive breast tumor, it is frequently observed in the metastatic ER-Positive breast cancer (Dustin et al., 2019). The germline expression of ESR1^{Y541S} mutation results in runting in both female and male transgenic mice (Simond et al., 2020). Moreover, the male mice bearing ESR1^{Y541S} mutation exhibit feminization, which is represented by prominent nipples and a closer anal-genital region (Simond et al., 2020). Female mice have defects in the reproductive system and display abnormality in bone development (Simond et al., 2020). Also, the survival rate of the female transgenic mice (15%) is significantly lower than control mice (100%) at 150 days, whereas the survival of male counterparts is minimally affected (Simond et al., 2020). Despite the abnormalities in the reproductive system and survival, the mice with ESR1^{Y541S} mutation do not grow mammary tumors, making it difficult to study the tumorigenesis with this novel ESR1 mouse model (Simond et al., 2020).

1.4. Transcription Factors in Breast Cancer

1.4.1. Overview of Transcription Factors in Breast Cancer

Transcription factors are the proteins that bind to specific DNA sequences and promote or suppress transcription (Barnes, 2009). They mainly bind to DNA-regulatory sequences

including enhancers and silencers, which usually localize in the 5-upstream region of target gene (Barnes, 2009). Based on the structures of transcription factors, they can be classified into helix-turn-helix, helix-loop-helix, zinc finger, basic protein-leucine zipper, and beta-sheet motifs families (Barnes, 2009).

The activation of transcription factors is complicated. It is believed that they can get activated through multiple intracellular signal transduction pathways, such as MAPK/ERK pathway, JAK/STAT pathway, kinases PKA, and PKC pathways (Barnes, 2009). In the MAPK/ERK signaling, kinases such as extracellular signal regulated kinase (ERK), c-Jun N-terminal kinase (JNK), and p38 kinase drives the transmitting of extracellular signals into the cell (Nagini, 2014). However, other studies have suggested that they may be directly activated by ligand binding such as glucocorticoids (Barnes, 2009).

To study the genes altered in breast cancer, multiplatform genomic analyses were conducted and revealed 93 frequently altered genes, among which 49 genes are directly or indirectly involved in transcription, and 13 of them are DNA-binding transcription factors (DB-TFs) (Zacksenhaus et al., 2017). Moreover, the 13 DB-TFs in this study can be further classified to constitutive TFs and inducible TFs (Zacksenhaus et al., 2017). In this study, the constitutive TFs include MYC, GATA3, ZNF217, TBX3, RUNX1, CIC, and PRDM1, and inducible TFs include TP53, ESR1, FOXA1, FOXP1, XBP1, and SMAD4 (Zacksenhaus et al., 2017). This study demonstrates that TFs are frequently altered in breast cancer, and may play critical roles in breast cancer initiation and progression (Zacksenhaus et al., 2017). However, certain TFs that are altered in breast cancer are missing in this study, such as Stat3 and Stat5 (Zacksenhaus et al., 2017).

Transcription factors play a critical role in regulating cancer cell proliferation, metastasis, metabolism, resistance to therapies, modulating tumor microenvironment, and as prognostic markers of cancer (Vishnoi et al., 2020).

1.4.2. Signal Transducer and Activator of Transcription 3 (Stat3)

Signal transducer and activator of transcription (Stat) proteins are transcription factors that comprise 7 genes, Stat1, Stat2, Stat3, Stat4, Stat5a, Stat5b, and Stat6 in mammals (Mitchell & John, 2005). The Stat family proteins share a conserved structure consisting of 6 domains, the N-terminal domain (NTD), coiled-coil domain (CCD), DNA binding domain (DBD), linker domain (LD), Src-homology (SH2) domain and transcription activation domain (TAD) (Guanizo et al., 2018). All of these domains are critical for the JAK-Stat pathway activation and functioning (Guanizo et al., 2018). The NTD plays a role in Stat protein dimerization and translocation into the nucleus, and the CCD domain coordinates with other proteins to assist nuclear import and export (Guanizo et al., 2018). The DBD domain makes it possible for Stat protein to bind to the promoters of target genes and initiate transcription (Guanizo et al., 2018). Moreover, SH2 domain is highly conserved in the Stat protein family, as it is required for the Stat proteins to be recognized for tyrosine phosphorylation (Guanizo et al., 2018). In addition, the tyrosine and serine phosphorylation sites of the C-terminal TAD allow for maximal transcriptional activation of target genes (Guanizo et al., 2018).

The Stat family proteins are activated by JAK kinases, and this activation plays important roles in immunity, proliferation, differentiation and survival (Mitchell & John, 2005).

Dysregulation of the JAK-Stat pathway plays an important role in increasing angiogenesis, enhancing tumor cell survival and immunosuppression (Mitchell & John, 2005). Cytokine-

induced JAK activation phosphorylates Stat, and it translocates to the nucleus, where it binds to consensus DNA-recognition motifs called gamma-activated sites (GAS), leading to the transcription of target genes (Mitchell & John, 2005). Recent studies have suggested that non-phosphorylated Stat proteins can shuttle between cytoplasm and nucleus, whereas phosphorylated Stat protein is retained in the nucleus (Mitchell & John, 2005).

Within the Stat protein family, aberrant Stat3 signaling has been implicated in various cancer types, which defines Stat3 as an oncogene (Zou et al., 2020). In normal tissues, the Stat3 activation and signaling are critical for maintaining normal cellular functions and behaviors responding to external cues (Zou et al., 2020). In contrast, the hyperactivation of Stat3 is found in various malignant tumors and is related to poor prognosis (Zou et al., 2020). Due to its role in oncogenesis, targeting Stat3 signaling pathway has emerged as a promising therapeutics in cancer treatment (Zou et al., 2020). Also, given its immune regulatory roles, targeting Stat3 may play a role in enhancing immune therapy (Zou et al., 2020). These all suggest that Stat3 may be an important target to study in breast cancer research.

1.4.2.1. Canonical and Non-canonical Stat3 Signaling

The canonical Stat3 signaling relies on the phosphorylation of the Y705 residue of Stat3 (Sellier et al., 2013). The Stat3 is recruited through the cytokine IL-6 activation of JAK, which in turn phosphorylates and activates Stat3 at the Y705 site. Upon activation, the phosphorylated Stat3 homodimerizes and translocates into the nucleus (Sellier et al., 2013). In the nucleus, phosphorylated Stat3 binds to DNA and promotes the transcription of a range of genes associated with cell proliferation, differentiation, survival, and other functions (Sellier et al., 2013). Stat3 controls proliferation by regulating genes such as Bcl-2, Bcl-xL, Survivin, Cyclin D1, c-Myc,

and Mcl-1; it influences angiogenesis through Hif1alpha and VEGF; and it governs for epithelial-mesenchymal transition (EMT) via Vimentin, TWIST, MMP-9, and MMP-7 (Banerjee & Resat, 2016). Moreover, it is believed that tumors without Y705 phosphorylated form are not addicted to the oncogene Stat3 (Sellier et al., 2013). Therefore, patients without expression of Y705 phosphorylated form are not considered candidates for Stat3-targeting therapies (Sellier et al., 2013).

Recently, studies have suggested that the activation of Stat3 does not only rely on Y705 phosphorylation because Stat3 can activate transcription even without Stat3 Y705 phosphorylation (Sellier et al., 2013). Another phosphorylation site, S727, may also play a role in gene transcription through the interaction with transcriptional coactivators such as SRC, cdk9, and CBP (Sellier et al., 2013). Another paper demonstrated that in the absence of Y507 phosphorylation, the phosphorylation of S727 is necessary for its normal functioning (Hazan-Halevy et al., 2010). The phosphorylation of S727 site either alone or together with Y705 site is considered the non-canonical signaling of Stat3 (Sellier et al., 2013). Interestingly, in an ER-Positive breast cancer cell line MCF-7, the survival of the cancer initiating cells relies on the Stat3 S727 phosphorylation, together with mTOR kinase (Sellier et al., 2013). However, in a basal-like cancer cell line, the survival of CD44+CD24- cells relies on the phosphorylation of Y705 site by JAK2 (Sellier et al., 2013).

Besides, Stat3 also plays a role in mitochondria functioning, and even unphosphorylated Stat3 can work as a transcription factor, which is also considered non-canonical signaling of Stat3 (Srivastava & DiGiovanni, 2016). Stat3 localizes in mitochondria, interacts with electron transport chain, influences mitochondrial respiration, and alters ROS production and apoptosis (Srivastava & DiGiovanni, 2016). The functioning of Stat3 is highly dependent on tumor

suppressor GRIM-19 (Srivastava & DiGiovanni, 2016). GRIM-19 is a retinoic-interferon-beta induced cancer cell mortality protein (Srivastava & DiGiovanni, 2016). GRIM-19 plays a role in importing Stat3 into mitochondria and acts as a chaperone protein of Stat3 in the through an interaction with S727 phosphorylation (Srivastava & DiGiovanni, 2016; Tammineni et al., 2013). Also, it directly interacts with the NLS-domain of Stat3, thereby inhibiting the Stat3 nuclear localization and transcriptional activity (Srivastava & DiGiovanni, 2016).

1.4.2.2. Stat3 in Breast Cancer Initiation and Progression

To study the roles of Stat3 in breast cancer initiation and progression, the Muller lab crossed the Stat3^{flx/flx} strain to the MTB/MIC (MMTV-rtTA/TetO-PyV mT-IRES-Cre) mouse strain, a doxycycline-inducible mouse model that develops malignant breast tumors driven by conditional expression of polyomavirus middle T antigen (PyV mT) in mammary epithelial cells, recapitulating luminal B subtype of human breast cancer (Jones et al., 2016). Although both MTB/MIC and Stat3^{flx/flx}/MTB/MIC mice developed a comparable extent of hyperplasia and adenomas at 2 weeks post-induction, the hyperplasia and adenomas had begun to regress at 4 weeks post-induction in Stat3^{flx/flx}/MTB/MIC mice (Jones et al., 2016). Moreover, at a 6-week time point, the Stat3^{flx/flx}/MTB/MIC mice were completely devoid of hyperplasia or adenomas, whereas the MTB/MIC mice showed continuous aggravating hyperplasia and adenomas (Jones et al., 2016). Also, by doing the immunohistochemistry of Ki67, Cleaved-caspase 3, and terminal deoxynucleotidyl transferase dUTP nick end labeling (TUNEL) markers, no difference in proliferation and apoptosis was detected between Stat3^{flx/flx}/MTB/MIC and MTB/MIC mammary gland at two-week time point (Jones et al., 2016). Eventually, the MTB/MIC mice developed mammary tumors within an average of 20 days, whereas Stat3^{flx/flx}/MTB/MIC mice developed

tumors with an average tumor onset of 275 days (Jones et al., 2016). These suggested that in this luminal B-like breast cancer mouse model, Stat3 may not be necessary for initiation of the early lesions but is required for the progression into invasive carcinomas (Jones et al., 2016). Further study suggested that the role of Stat3 in tumor progression is attributable to its effects in establishing an immunosuppressive tumor microenvironment (Jones et al., 2016). The Stat3 deficiency leads to increased specific myeloid populations and increased T cell recruitment and activation (Jones et al., 2016).

Also, in another study published by the Muller lab, the researchers crossed the Stat3^{flx/flx} strain to the MMTV-NIC mouse model, an ErbB2-overexpressing mouse model that recapitulates human HER2-Positive breast cancer (Ranger et al., 2009). No difference in the breast cancer initiation was observed (Ranger et al., 2009). This demonstrated that consistent with the findings in luminal B-like breast cancer, Stat3 is not required for HER2-Positive breast cancer initiation.

1.4.2.3. Stat3 in Breast Cancer Metastasis

The Muller lab identified the key roles of Stat3 in breast cancer progression in the luminal B-like breast cancer mouse model (Jones et al., 2016). To study the roles of Stat3 in metastasis, the lung metastasis of MTB/MIC mice and Stat3^{flx/flx}/MTB/MIC were quantified, which showed significantly less lung metastasis in Stat3^{flx/flx}/MTB/MIC (Jones et al., 2016). Remarkably, none of the Stat3^{flx/flx}/MTB/MIC mice developed lung metastasis at the tumor end point, whereas all the MTB/MIC mice developed lung metastasis (Jones et al., 2016).

In addition, in the Stat3^{flx/flx}/NIC mice, there were significantly fewer Stat3^{flx/flx}/NIC mice that developed lung metastasis at the breast tumor end point, and significantly smaller size of

lung metastasis, compared to their Stat3-proficient counterparts (Ranger et al., 2009). To further study the role of Stat3 in ErbB2 positive breast tumor metastasis, tail vein injection of the dissociated breast tumor cells of Stat3^{flx/flx}/NIC and NIC were performed on the immunocompromised mice, which showed defects of lung colonization of the Stat3-deficient cell lines (Ranger et al., 2009).

These suggest that Stat3 plays a key role in driving the metastasis of ErbB2 positive breast cancer and luminal B breast cancer. However, the underlying mechanism remains unclear.

A previous Ph.D. student from the Muller lab has shown that the dissociated tumor cells of Stat3^{flx/flx}/NIC breast tumors have significantly decreased migration and invasion (Jones, 2018). Also, the focal adhesion markers, including phosphorylated-FAK (Y925), vinculin, paxillin and phosphorylated-paxillin (Y118) were expressed at a higher level in Stat3^{flx/flx}/NIC cells than WT NIC cells (Jones, 2018). Remarkably, the Stat3^{flx/flx}/NIC cells exhibited a markedly higher assembly rate of focal adhesions compared to their disassembly rate than WT NIC cells, thereby enhancing the stability of the focal adhesion in the Stat3^{flx/flx}/NIC cells (Jones, 2018). These may account for the decreased metastasis in the Stat3^{flx/flx}/NIC mice.

1.4.2.4. Stat3 target gene Lgals3

1.4.2.4.1. Biology and Signaling of Galectin-3

Galectin-3 (Gal-3) is a 30kD protein encoded by the gene Lgals3, and belongs to the galectin family which is a family of β -galactoside-binding lectins (Hara et al., 2020). Mammalian galectins share one or two conserved carbohydrate recognition domains (CRDs), allowing them to recognize β -galactoside residues, bind to them, and form complexes (Hara et al., 2020). Galectins can be classified into three subgroups based on their CRD number and functions,

including proto-type galectins (Gal-1, -2, -5, -7, -10, -11, -13, -14, and -15), tandem-repeat galectins (Gal-4, -6, -8, -9, and -12), and chimera-type galectin (Gal-3) (Hara et al., 2020). Gal-3 protein is an oligomer composed of monomers with one CRD and an amino-terminal polypeptide tail region (Hara et al., 2020).

Based on the localization, Gal-3 can be categorized into extracellular Gal-3 and intracellular Gal-3 (Hara et al., 2020). Extracellular Gal-3 is involved in functions including inflammation and allergy, cell-to-cell contacts, cell-to-matrix contacts, and AGE receptor function, and intracellular Gal-3 is involved in pre-mRNA splicing activity, cell cycle control, and protection from apoptosis (Hara et al., 2020).

Gal-3 plays an important role in mediating cell-cell interaction, and cell-matrix interaction (Fortuna-Costa et al., 2014). It is found to upregulate the detachment of cancer cells from the primary tumor (Fortuna-Costa et al., 2014). This may be attributable to its interaction with integrins (Margadant et al., 2012). Gal-3 is believed to regulate the lateral mobility of the integrins at least partially (Yang et al., 2017). Studies have suggested a feedback relation between $\beta 1$ integrins and Gal-3, which is a process involved in the epigenetic induction of Gal-3 expression promoting the integrin-induced EMT and cell scattering (Margadant et al., 2012). In endometrial cells, Gal3 contributes to regulating integrin $\beta 3$ mediating the cell adhesion to fibronectin (Lei et al., 2009). The administration of recombinant Gal-3 to endometrial cells significantly decreased their adhesion, followed by a further decrease with the addition of integrin $\beta 3$ (Lei et al., 2009). However, in the endometrial cells, $\beta 1$ was shown to have no effect in the adhesion process (Lei et al., 2009). Moreover, silencing Gal-3 is incorporated with elevated expression of integrin $\beta 3$, indicating a negative feedback relation (Lei et al., 2009). Another study investigated on the role of Gal-3 as an extracellular ligand in cell-matrix adhesion (Sedlář

et al., 2021). The researchers found that the cell adhesion to the preabsorbed Gal-3 was attributable to $\beta 1$ and αV integrins including $\alpha 5\beta 1$, $\alpha V\beta 3$, and $\alpha V\beta 1$ integrins at least partially (Sedlář et al., 2021). Also, Gal-3 regulates the integrin $\alpha 2\beta 1$ -mediated adhesion to collagen-I and IV by alteration of receptor clustering (Friedrichs et al., 2008).

1.4.2.4.2. Galectin-3 in Cancer

The role of Gal-3 in cancer metastasis has been controversial. Galectin-3 has been considered a potential target to prevent cancer metastasis by several mechanisms, including antiapoptosis, promoting neoangiogenesis, promoting homotypic aggregation, and inducing apoptosis of cancer-infiltrating T cells (Ahmed & AlSadek, 2015). In hepatocellular carcinoma, Gal-3 favors tumor metastasis by activating the Galectin-3- β -catenin-OGFBP3/vimentin signaling cascade, thus being a potential therapeutic target (Mengjia Song et al., 2020). In the lung adenocarcinoma, both the genetic and pharmacological inhibition of Gal-3 significantly decreases metastasis, inhibits tumor growth, and enhances the response to PD-L1 blockade (Vuong et al., 2019). However, in a triple-negative breast cancer cell line 4T1, the downregulation of Gal-3 increases the metastatic potential of tumor cells through the regulation of glycosaminoglycans/proteoglycans (PG) (Pereira et al., 2019). Moreover, the role of Galectin-3 in HER2-Positive breast cancer metastasis remains unclear.

Galectin-3 is a known target of Stat3, and a high expression level of Gal-3 has been related to poor prognosis in HER2-Positive breast cancer patients (Chen et al., 2022). Gal-3 deficiency reduces tumor proliferation and improves the sensitivity to trastuzumab (Chen et al., 2022). In addition, it appears a protective role in cancer cell survival by repairing the DNA

damage or inhibiting apoptosis, thus preventing the cancer cells from being cleared by chemotherapy (Boutas et al., 2019).

1.4.2.5. Experimental rationale

Studies have suggested a key role of Stat3 in promoting metastasis in HER2-Positive breast cancer, however, the underlying mechanism remains unclear. We are interested in exploring the key mediators of the metastatic phenotype in the Stat3 proficient ErbB2 positive mice, and the cellular events that drive the metastasis. For this purpose, we performed the transcriptomic analysis to explore the mediator of the metastatic phenotype in ErbB2 positive breast cancer.

1.4.3. Forkhead Box A1 (FOXA1)

Forkhead Box proteins belong to a large family of the transcriptional regulators that share the evolutionarily conserved DNA-binding domain (DBD) known as forkhead box or winged helix domain (Myatt & Lam, 2007). In humans, there are 17 Fox gene subfamilies (FoxA-R) with at least 41 genes (Myatt & Lam, 2007). Although the Fox genes share the same DBD binding, the functions of Fox genes vary significantly depending on the different sequences outside of DBD, which makes it possible for differential regulation (Myatt & Lam, 2007). The Fox genes work in synergy and contribute significantly to a wide range of biological processes, including development, proliferation, differentiation, apoptosis, migration, invasion, and metabolism (Myatt & Lam, 2007). Due to the significant roles of Fox genes in cellular functions and behaviors, specific Fox subfamilies have been implicated in tumorigenesis and progression of certain cancers, such as FoxO, FoxM, FoxA, FoxC, and FoxP (Myatt & Lam, 2007).

Among the Fox proteins, FoxA family was the first identified mammalian forkhead type proteins (Myatt & Lam, 2007).

1.4.3.1. FOXA1 in mammary gland development

The FOXA1 gene, also known as HNF-3 α , was originally discovered in the liver in an effort to identify the transcriptional regulators for the tissue-specific expression of genes (Costa et al., 1989). A DNA-binding protein, named HNF-3 α , together with C/EBP- β , was found to be responsible for the transcription of the liver-specific genes transthyretin (*Ttr*) and α 1-antitrypsin (*Serpina1*), and the liver morphogenesis (Costa et al., 1989). Around the same time, Weigel et al. determined the *Drosophila* forkhead (*fkf*) DNA-binding protein which is essential for the fly development (Weigel et al., 1989). The *fkf* and HNF-3 α showed a high homology of a 100-amino acid region, which includes the DNA-binding domain of the two factors (Lai et al., 1991). This region is different from the known transcriptional regulators by a lack of homeodomain and zinc-finger motifs, making it a new class of transcription factor (Weigel & Jäckle, 1990). Later, based on a new systemic nomenclature, the protein HNF-3 α was given a name of FOXA1, as the founding member of the FOXA subclass (Seachrist et al., 2021).

FOXA1 coordinates with ER and plays a fundamental role in the development of the mammary glands (Seachrist et al., 2021). In the developing postnatal glands, FOXA1 is mainly expressed in the cells of the terminal end bud that contains the luminal progenitor cells (Seachrist et al., 2021). Then, along with the gland development, FOXA1 expression is found in the ductal epithelial cells of the virgin gland, which is similar to the expression pattern of ER (Seachrist et al., 2021). Also, the expression of both FOXA1 and ER is reduced in alveolar structures, further decreased during pregnancy, and gradually restored following involution (Seachrist et al., 2021).

The impact of FOXA1 on mammary gland development was further studied by homozygous knockout of FOXA1 in mice (Bernardo et al., 2010). Although FOXA1 deficient mice exhibit similar mammary gland morphology as FOXA1 proficient mice at birth, the pups are growth retarded and die shortly due to hypoglycemia and dehydration (Behr et al., 2004; Bernardo et al., 2010; Kaestner et al., 1999; Vatamaniuk et al., 2006). To further study the role of FOXA1, embryonic fat pads lacking FOXA1, with only rudimentary ductal structures, were transplanted in the renal capsules (Seachrist et al., 2021). In these mice, although the fat pads grow, the ductal trees fail to extend further into the surrounding fat pads (Seachrist et al., 2021). This suggested the essential role of the FOXA1 in the mammary epithelium in mammary gland development (Seachrist et al., 2021). In addition, the conditional ablation of FOXA1 in the specific mammary epithelial cells demonstrates that FOXA1 expression is fundamental for the ductal formation (Liu et al., 2016). Remarkably, FOXA1 deficiency and ESR1 deficiency mice share similar phenotypes, further indicating coordination between FOXA1 and ER (Seachrist et al., 2021).

1.4.3.2. FOXA1 and ER-Positive Breast Cancer

Genetic studies of breast cancer cell lines and primary tumor tissues show that FOXA1 is selectively upregulated in luminal breast cancers, and about 84% of ER-positive breast cancer express high levels of FOXA1 (Seachrist et al., 2021).

FOXA1 is known as the pioneering factor for ER binding to chromatin (Pavithran & Kumavath, 2021). This is because FOXA1 binding to DNA opens up the condensed chromatin and facilitates the access of ER to the chromatin and its binding to the ERE region, thereby activating the transcription of downstream genes (Pavithran & Kumavath, 2021). Also, studies

have shown that siRNA knockdown of FOXA1 drastically decreases the activity of ER-related genes upon estrogen induction, such as XBP1, TFF1, and NRIP1 (Carroll et al., 2005).

Moreover, Studies have shown that FOXA1 is necessary for almost all ER binding events in breast cancer cells although only about half of the ER-binding sites overlap with FOXA1 binding sites (Hurtado et al., 2011). This may be because FOXA1 is indirectly involved in the stabilization of additional ER binding events (Hurtado et al., 2011).

FOXA1 can promote breast cancer tumorigenesis through multiple mechanisms (Metovic et al., 2022). It plays the pioneering role and promotes the binding of ER to the ERE region and the recruitment of other transcription factors, thus activating the transcription of the downstream genes, including specific genes that are involved in promoting the proliferation and survival of the cells (Pavithran & Kumavath, 2021). Also, FOXA1 mediates the uptake of extracellular lipid precursors through the regulation endothelial lipase (LIPG) which allows the import of lipid precursors specifically in breast cancer cells (Slebe et al., 2016). Downregulation of either LIPG or FOXA1 results in decreased proliferation and impaired synthesis of intracellular lipids in the cancer cells (Slebe et al., 2016). Moreover, FOXA1 also binds to the ESR1 promoter, thereby modulating ER activity by enhancing both the transcription and translation of ER in breast cancer cells (Laganière et al., 2005). In addition, FOXA1 is crucial in driving the cell-cycle progression of the G1-S phase by regulating the expression of cyclin D1 (CCND1) (Eeckhoute et al., 2006). ER alpha collaborates with transcription factors including FOXA1 and NFIC to drive cell-specific cis- and trans-regulators of CCND1 expression (Eeckhoute et al., 2006). FOXA1 recruits MyBL2 or CREB1 to the cyclin E2 and E2F1 genes also contribute to the G1-S phase transition (Robinson & Carroll, 2012). Furthermore, FOXA1 regulates a range of downstream

genes that are involved in promoting the luminal phenotype of breast cancer such as CDH1, and repressing basal differentiation (Anzai et al., 2017).

1.4.3.3. Experimental Rationale

ER-Positive breast cancer accounts for about 70% of the total breast cancer, but there is still not a faithful ER-Positive breast cancer mouse model (Lumachi et al., 2013). Given that FOXA1 plays a critical role in ER functioning and that FOXA1 is involved in many aspects of tumorigenesis, our lab has created a novel FOXA1-overexpressing mouse model called FIC (TetO-FOXA1-Ires-Cre) (Lusson, 2023). By overexpressing FOXA1 itself, or by crossing the FIC mouse model with the ESR1^{Y541S} mouse model, we may be able to create a novel ER-Positive breast cancer mouse model that faithfully recapitulates the features of human ER-Positive breast cancer.

Chapter 2: Results

2.1. Stat3 promotes metastasis in HER2-Positive Breast Cancer through the regulation of Lgals3

2.1.1. Stat3 deficiency results in a significant decrease in metastasis in MMTV-Neu-Ires-Cre (NIC) mouse models

To study the role of Stat3 in breast cancer initiation and progression, our lab has obtained a conditional Stat3 knockout mouse strain (Stat3^{flx/flx} or Stat3-null), and was crossed to the NIC mouse model (Figure 1). Our lab has found that there is no significant difference in the tumor onset between Wildtype (WT) NIC mice and Stat3^{flx/flx}/NIC mice (Ranger et al., 2009). However, significantly lower metastasis in Stat3^{flx/flx}/NIC mice has been observed, from the perspectives of both the number of metastases and the percent area of the lung occupied by metastasis (Ranger et al., 2009). This was further confirmed by doing the tail vein injection of the primary tumor-dissociated Stat3^{flx/flx}/NIC and WT NIC cell lines into immune-deficient NCr mice (Ranger et al., 2009). The Stat3^{flx/flx}/NIC cell lines had drastically impaired capacity in lung colonization compared to WT NIC cell lines (Ranger et al., 2009). These all suggest that Stat3 can promote ErbB2 positive breast cancer metastasis. However, the mechanism remains unclear.

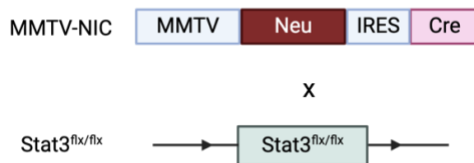


Figure 1: Schematic construct of Stat3^{flx/flx}/NIC

In mammary epithelial cells, Neu and Cre recombinase are expressed and Cre recombinase mediates the excision of LoxP-flanked Stat3. Created with Biorender.com.

2.1.1.1. Stat3 deficiency increases apoptosis in NIC mouse model

To understand the mechanism that Stat3 deficiency decreases metastasis, immunohistofluorescence staining was performed on the paraffined slides of Stat3^{flx/flx}/NIC breast tumors and WT NIC breast tumors (Figure 2). Two markers were used, ki67, a marker for proliferation, and cleaved caspase-3 (CC3), a marker for apoptosis, and the percent number of ki67 or CC3 were quantified. Although there is a trend of higher ki67 in Stat3^{flx/flx}/NIC tumors, no significant difference was observed. However, there is a significantly higher percent number of CC3 positive cells (WT NIC 0.62%±0.28%, n=6 vs. Stat3^{flx/flx}/NIC 3.28%±1.23%, n=5, p=0.046, student's t-test), indicating a higher apoptosis in Stat3-deficient NIC tumors.

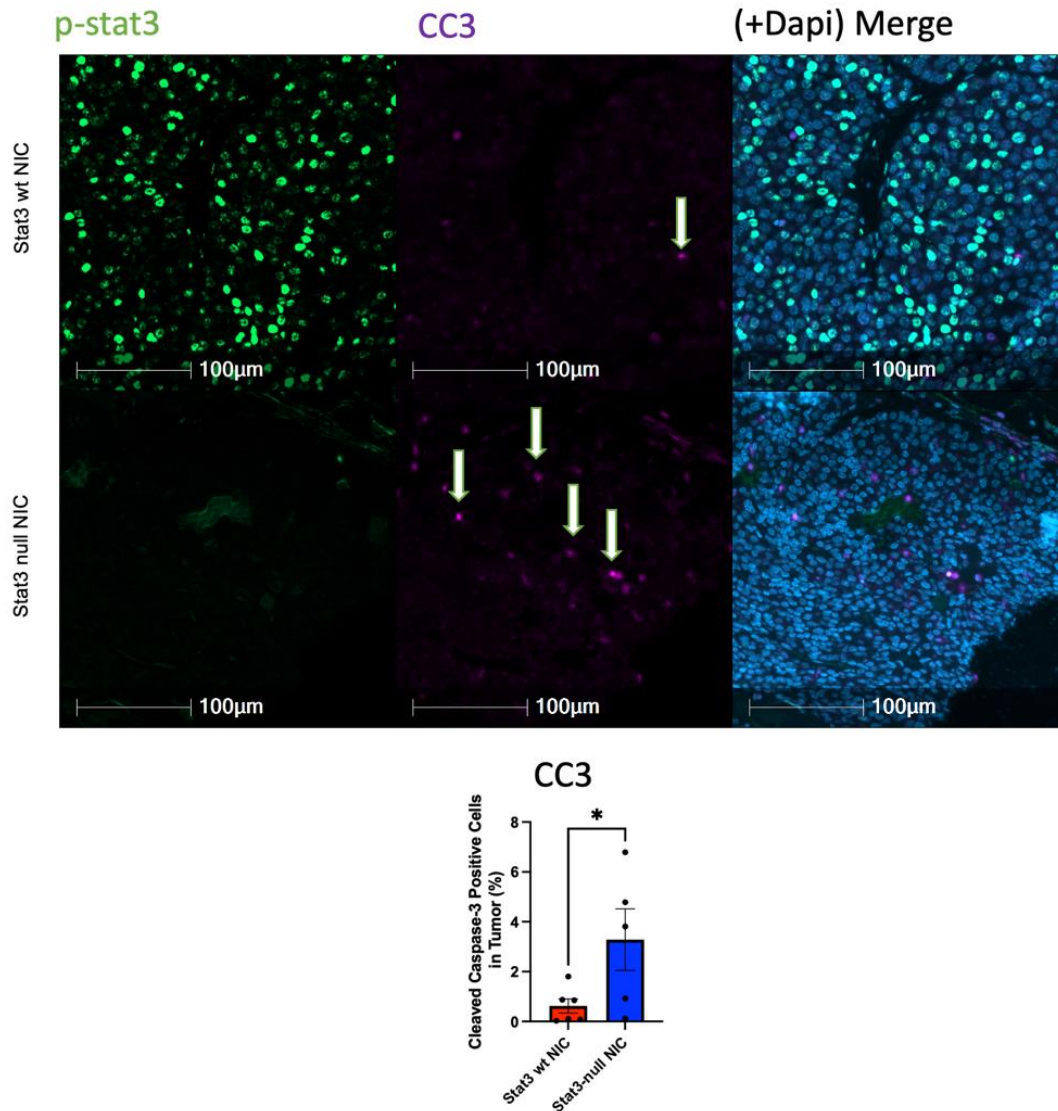


Figure 2: Apoptosis is increased in Stat3flx/flx/NIC tumors

(Upper) Immunohistofluorescence staining (IHF) of p-STAT3, Cleaved caspase 3, and DAPI in WT NIC and Stat3-null NIC breast tumors. (Below) Quantification of Cleaved Caspase 3. * $p < 0.05$, student's t-test. A significantly higher level of cleaved caspase 3 was observed on Stat3-null NIC breast tumor than WT NIC breast tumor.

2.1.1.2. Stat3-deficiency leads to elevated focal adhesion level

A previous Ph.D. student from the Muller lab has reported in her thesis that the expressions of focal adhesion (p-FAK, vinculin, p-paxillin, paxillin) are increased in Stat3 deficiency NIC cell lines (Jones, 2018). To confirm that the cells still exhibit the same properties, we did the immunoblotting on the key focal adhesion markers (Figure 3). Consistent with the previous findings, the Stat3^{flx/flx}/NIC cells express a higher level of focal adhesion markers, including phosphorylated-FAK (Y925), vinculin, phosphorylated-paxillin (Y118), and paxillin.

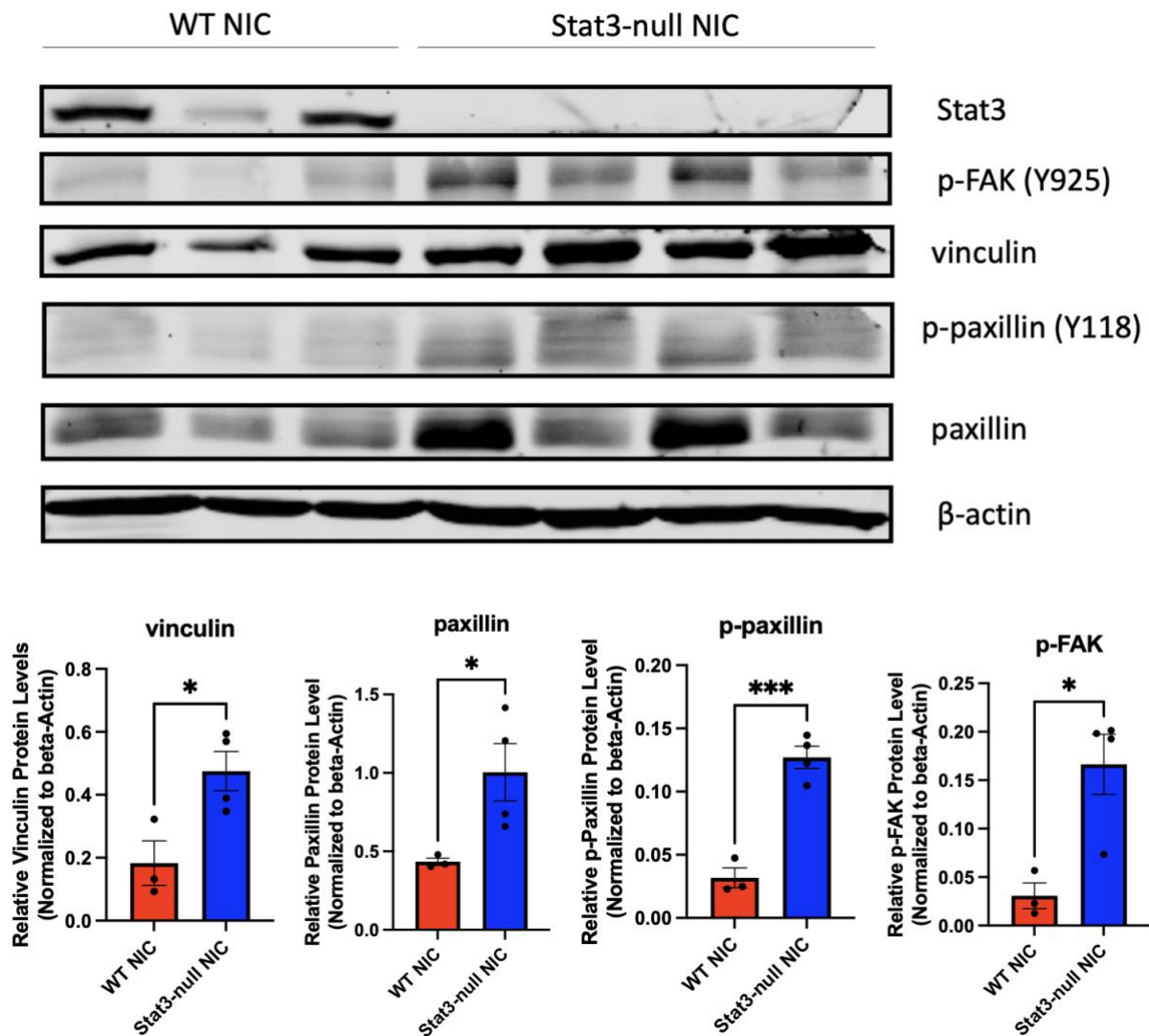


Figure 3: Focal adhesion protein expressions are elevated in Stat3flx/flx/NIC cells

(Upper) Immunoblotting of Stat3, p-FAK (Y925), vinculin, p-Paxillin, Paxillin, and beta-Actin; (Below) Quantification of relative protein levels of vinculin, Paxillin, p-Paxillin, p-FAK. Immunoblotting on the WT NIC cells (n=3), and Stat3-null NIC cells (n=2 in duplicate) of Stat3, phosphorylated-FAK (Y925), vinculin, phosphorylated-paxillin (Y118), paxillin, and beta-actin. Vinculin: WT NIC vs. Stat3-null NIC: 0.18 ± 0.07 vs. 0.47 ± 0.06 , $p=0.027$, Student's t-test; Paxillin: WT NIC vs. Stat3-null NIC: 0.43 ± 0.023 vs. 1.00 ± 0.18 , $p=0.046$, Student's t-test; p-Paxillin: WT NIC vs. Stat3-null NIC: 0.031 ± 0.0068 vs. 0.13 ± 0.0087 , $p=0.0006$, student's t-test; p-FAK: WT NIC vs. Stat3-null NIC: 0.031 ± 0.013 vs. 0.17 ± 0.03 , $p=0.0167$, Student's t-test.

2.1.1.3. Transcriptomic and bioinformatic analysis

The Stat3-null NIC tumors and cells turned out to have a higher level of apoptosis, higher expression level of the anti-metastatic marker, decreased migration and invasion, and can form more robust focal adhesions that may prevent metastasis. These all suggest an anti-metastatic phenotype. However, the mechanism that mediates the phenotype remains unclear. Given that Stat3, as a transcription factor, can regulate the transcription of selected downstream gene, transcriptomic analysis was performed on the dissociated tumor cells from Stat3-null NIC and WT NIC cells breast tumors. This was followed by bioinformatic analysis.

Transcriptomic studies showed differentially regulated gene profiles. Hierarchical cluster analysis of the expression profiles from both WT and Stat3-null NIC cell lines revealed distinct clustering, indicating a significant difference in gene expression between Stat3-deficient and proficient cells (Figure 4a). From the Ingenuity pathway analysis (IPA) analysis, cell spreading emerged as the most significantly altered function, and 39 molecules associated with this process exhibited changes in response to the Stat3 deficiency (Figure 4b). GO pathway analysis was also launched, and two major processes were enriched, including ribosomal components and cell adhesions (Figure 4c). Cell adhesions have been widely documented to be related to metastasis, with the loss of cell-cell adhesion being recognized as a major hallmark of cancer (Janiszewska et al., 2020). The types of cell adhesions that have been extensively altered with the Stat3 deficiency include adherens junction, anchoring junctions, cell-substrate junctions, cell-substrate adherens junctions, and focal adhesions. Furthermore, GSEA analysis suggested that there are large enrichments in the ribosomal signatures and ErbB2 metastatic signatures (Figure 4d). These bioinformatic analysis together demonstrated that Stat3 deficiency is associated with an alteration of metastasis, and this metastasis may be related to a change in cell adhesions.

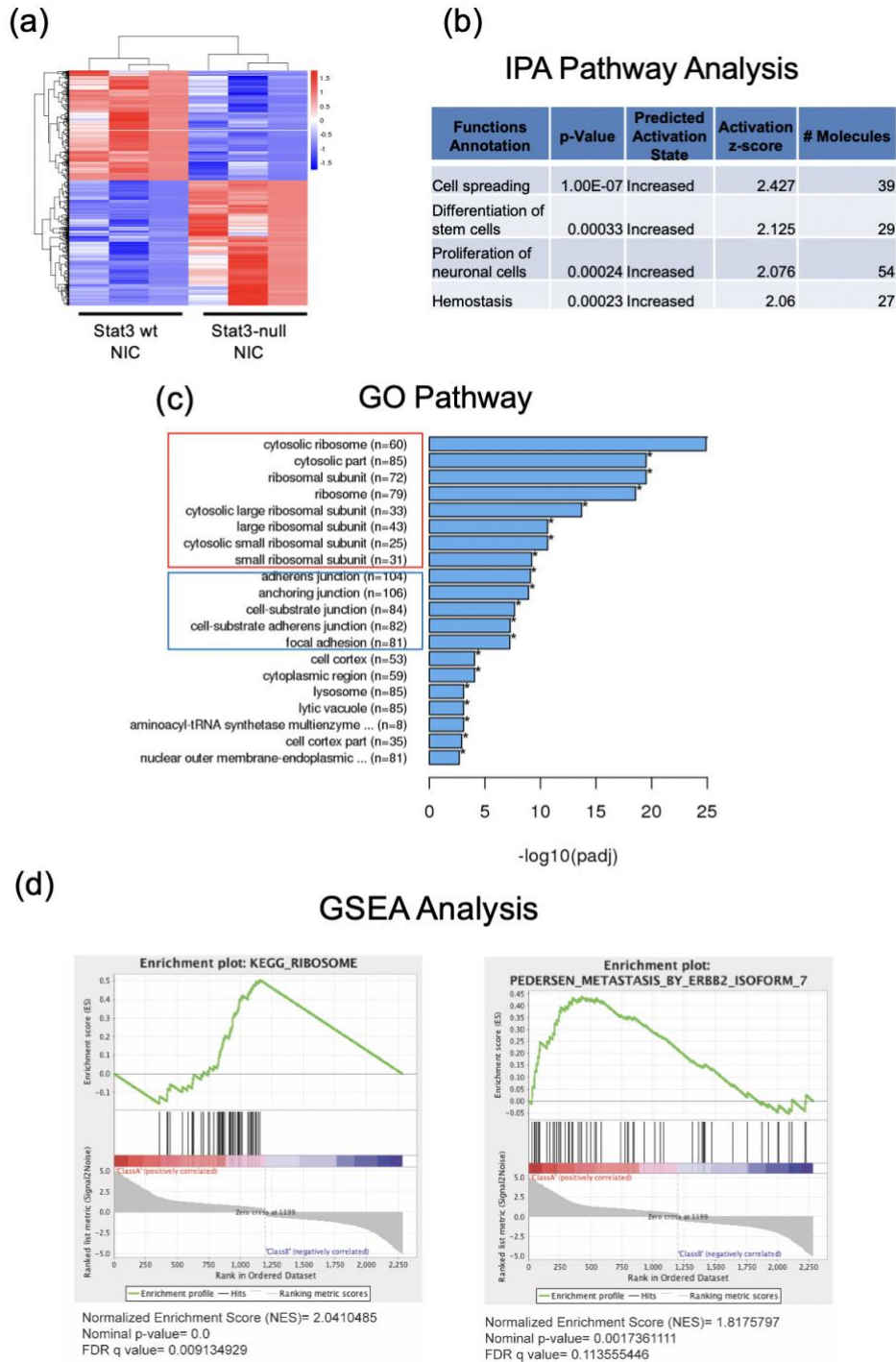


Figure 4: Transcriptomic study and bioinformatic analysis of WT NIC & Stat3-null NIC cells

(a): Cluster analysis of transcriptomic study of WT NIC and Stat3-null NIC cells suggests a differentially regulated gene profiles; (b): IPA analysis suggests a significant alteration in the cell-spreading function in the Stat3-null NIC cells compared to WT NIC cells; (c)GO analysis suggests an enrichment in the ribosomal proteins and cell adhesions in the Stat3-null NIC cells compared to WT NIC cells; (d): GSEA analysis suggests an enrichment in ErbB2 metastatic signature.

2.1.1.4. Lgals3 is the most significantly down-regulated gene in the Stat3-deficient lesions

Among the myriad genes that exhibit different RNA expression levels between WT NIC and Stat3-null NIC cell lines, Lgals3 turned out to be the most significantly down-regulated gene. From the RNA-sequencing results, the RNA level of Lgals3 decreased from more than 10,000 to approximately 0 with Stat3 deficiency (Figure 5a).

The protein encoded by Lgals3, galectin-3 (Gal-3), has been extensively implicated in tumor metastasis via multiple mechanism (Funasaka et al., 2014; Pereira et al., 2019; M. Song et al., 2020). To validate that galectin-3 protein level is reduced in Stat3-null NIC cell lines compared to WT NIC cell lines, we first performed an immunoblotting on ErbB2, Stat3, Gal-3, and the reference β -actin (figure 5b). We found that, the knockout of Stat3 by Cre recombinase was successful. Also, in both WT NIC and Stat3-null NIC, the ErbB2 expression levels remained approximately unchanged despite Stat3 deficiency, indicating Stat3 deficiency did not affect ErbB2 expression. Moreover, there was an overexpression of ErbB2 (Neu) in both mouse models, which validated the mouse models. Regarding Gal-3, in the WT NIC cell lines, there was a high expression level of Gal-3, whereas in Stat3-null NIC cell lines, the expression was markedly diminished, approaching undetectable levels. This demonstrated that Gal-3 expression was dramatically reduced upon Stat3 deficiency.

To further support this conclusion, immunofluorescence was performed on the monolayer cells comparing WT NIC and Stat3-null NIC cell lines (Figure 5c). It showed that, in WT NIC cells, there is high level of Gal-3 (green). By comparing with Dapi staining (blue), we can conclude that Gal-3 proteins are localized in the cytoplasm. In contrast, in Stat3-null NIC cells, there is no detectable level of Gal-3 expression. This is consistent with the conclusions from immunoblotting.

We now know that the Gal-3 expression level is reduced in Stat3-null NIC cell lines; however, it is also important to quantify the Gal-3 expression level in primary WT NIC and Stat3-null NIC breast tumors. Therefore, immunohistofluorescence was performed on the paraffin-embedded tissue sections of WT NIC and Stat3-null NIC breast tumors (Figure 5d). We stained for phospho-Stat3 (Tyr705), an activated form of Stat3, and we observed nuclear staining (green) of it in WT NIC breast tumor section, whereas no phospho-Stat3 was detected in Stat3-null NIC breast tumor. We also stained for Gal-3 (red), and we found that there was a drastic decrease of Gal-3 in the Stat3-null NIC tumor compared to WT NIC tumor. The percent number of Gal-3 positive cells in Stat3-null NIC and WT NIC tumors were quantified by HALO, which revealed a four-fold reduction in the Stat3-null NIC tumors compared to their WT NIC counterparts ((WT NIC 24.52%±4.54%, n=7 vs. Stat3^{flx/flx}/NIC 5.42%±1.61%, n=5, p=0.0067, student's t-test). In addition, we also observed that the Gal-3 proteins are predominantly localized in cytoplasm. This is in consistent with the immunofluorescence findings on the monolayer cells. Furthermore, colocalization of Stat3 and Gal-3 can be observed in the WT NIC breast tumors, indicating a potential regulatory relation between Stat3 and Gal-3.

These all suggested that Gal-3 expression level is significantly decreased with Stat3 deficiency.

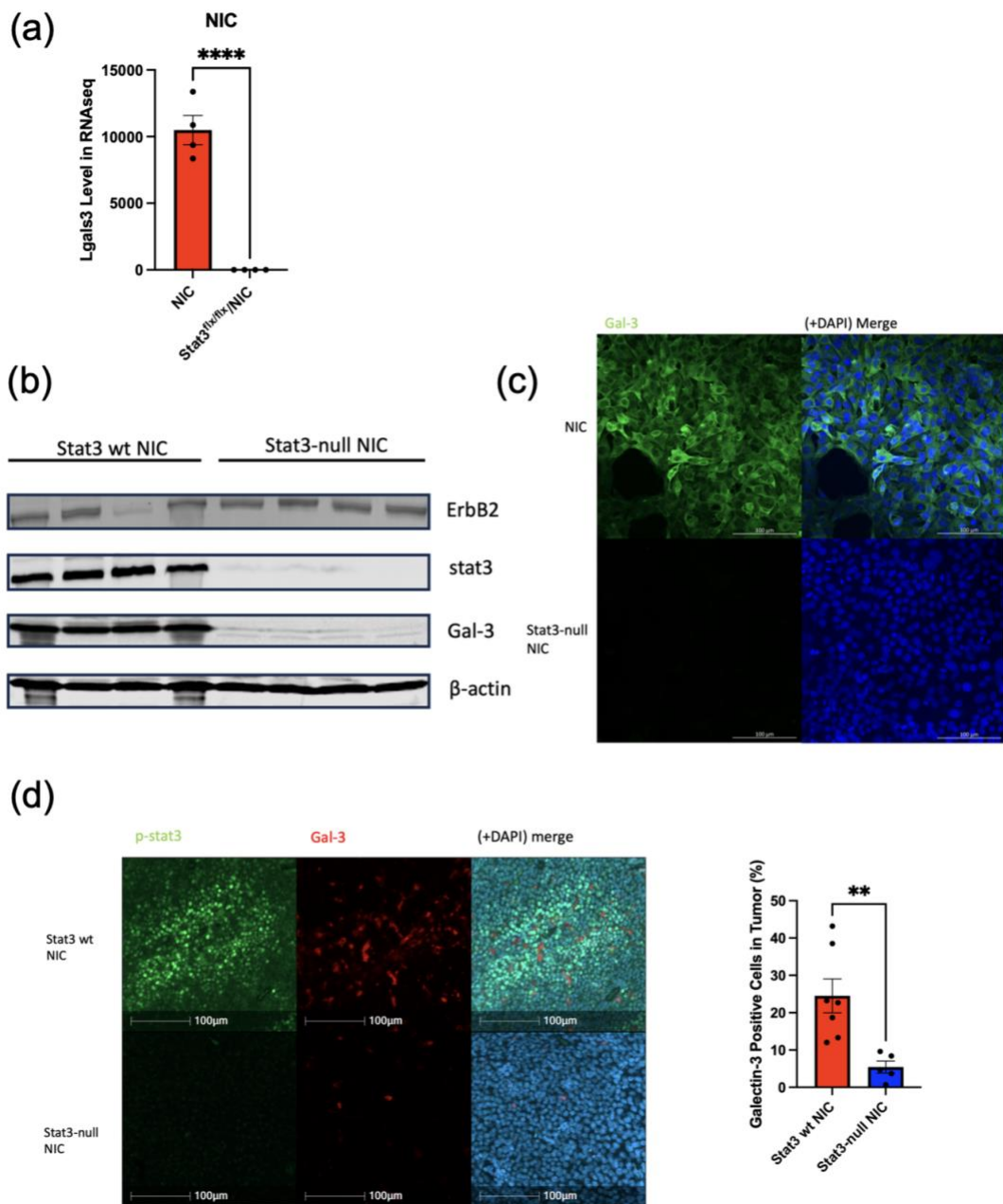


Figure 5: Galectin-3 expression is downregulated in the Stat3-null NIC breast tumors and cells

(a): Lgals3 RNA levels in the WT NIC and Stat3-null NIC cell lines from transcriptomic analysis (RNA sequencing); (b): Immunoblotting of ErbB2, Stat3, Gal-3, beta-actin in WT NIC and Stat3-null NIC cell lines suggests a dramatic decrease of Gal-3 protein level in the Stat3-null NIC cells; (c) Immunofluorescence staining on the monolayer WT NIC and Stat3-null NIC cells on Gal-3 (green) and merge with DAPI (blue) suggests a dramatic decrease of Gal-3 protein level in the Stat3-null NIC cells, scale bar 100 μ m; (d): Immunohistofluorescence staining on p-Stat3 (green), Gal-3 (red), and merge with DAPI (blue), scale bar 100 μ m, with quantification of Gal-3 positive cells in tumor. WT NIC vs. Stat3-null NIC: 24.52% \pm 4.54%, n=7 vs. 5.42% \pm 1.61%, n=5, p=0.0067, student's t-test.

2.1.1.5. Knockdown of Lgals3 decreases migration and invasion

Given the critical relation between Stat3 and Gal-3, we used shRNA to knock down gene expression of Lgals3 in WT NIC cells for phenotype analysis.

To validate the shRNA knockdown, we performed immunoblotting on the Gal-3 and beta-actin of shControl, shLgals3_1, shLgals3_2, and shLgals3_3 NIC cells (Figure 6).

Immunoblotting suggested that in this NIC cell line, shRNA knockdown was effective with shLgals3_1 and shLgals3_3 on protein levels.

Then to study the role of Gal-3 in cancer cell metastasis, we first performed a migration assay to study the mobility of shLgals3 NIC cells (Figure 7). shLgals3 NIC cells and shControl NIC cells were placed in the transwell upper chamber, and were incubated for 16 hours. After the incubation, the transwell bottom surfaces were stained and imaged, followed by the quantification of number of cells migrated. The image of the migration assay suggested a decrease in the number of cells migrated in the shLgals3 NIC cells compared to shControl NIC cells.

Besides the migration ability, invasion capacity is another critical determinant of metastatic potential. Although migration and invasion abilities are frequently discussed in tandem, they are distinct concepts used to describe cellular behavior. Migration is the movement of cells on the 2D surface without any obstructive fiber network, whereas invasion is the cell movement through a 3D matrix, with the reconstruction and interaction with extracellular matrix (ECM) (Kramer et al., 2013). Therefore, it is also critical to study the role of Lgals3 in the invasion.

To study invasion, 5% Matrigel was placed at the bottom of the transwell upper chamber, and shLgals3 NIC cell and shControl NIC cells were placed on the upper chamber of the transwell and incubated for 16 hours to ensure sufficient invasion (Figure 7).

The image of the invasion assay suggested a dramatic decrease in the number of cells migrated in the shLgals3 NIC cells compared to shControl NIC cells. After the 16-hour invasion, the bottom surfaces of the chambers with shControl NIC cells were densely populated and almost saturated, in contrast to sparsely distributed shLgals3 NIC cells on the bottom surfaces of their chambers.

Therefore, both migration and invasion were decreased with the shRNA knockdown of Lgals3.

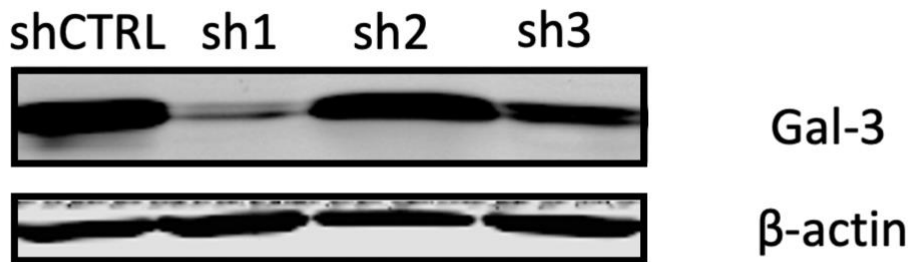


Figure 6: Knockdown of Lgals3 with shLgals3_1 and shLgals3_3 in WT NIC cell lines

Immunoblotting of Gal-3 and beta-actin with shRNA knockdown of Lgals3 in NIC cells, suggests a decrease of Gal-3 protein level with shLgals3_1 and shLgals3_3 in this cell line.

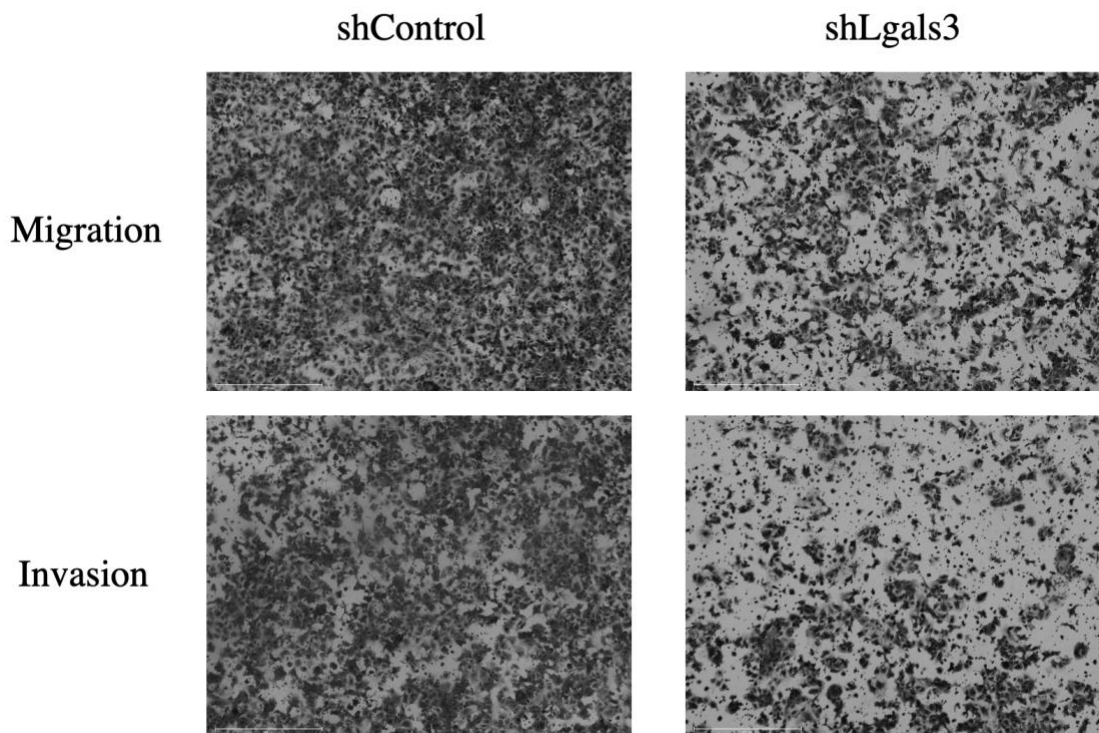


Figure 7: Gal-3 knockdown leads to decreased migration and invasion

(Upper) Representative figures of migration assay of 16 hours with shControl and shLgals3 in the NIC cell lines, and (Lower) Representative figures of invasion assay of 16 hours with shControl and shLgals3 in the NIC cell lines. Scale bar 650um.

2.1.1.6. Pharmacological inhibition of Gal-3 decreases migration and invasion

From the previous section, the knockdown of Gal-3 with shRNA decreases migration and invasion. Therefore, we are also interested in whether pharmacological inhibition of Gal-3 affects migration and invasion. We treated the WT NIC cells with a selective small molecule Gal-3 inhibitor GB1107, and while in treatment, subjected the DMSO-treated and 10uM GB1107-treated WT NIC cells to migration and invasion assay (Vuong et al., 2019). Images from 16-hour migration and invasion assay suggest decreased migration and invasion (Figure 8a). Also, we subjected the WT NIC cell lines to DMSO and a range of GB1107 doses (5uM, 7.5uM, and 10uM) and conducted a proliferation assay, which showed no significant difference in proliferation at 10uM GB1107 (Figure 8b). Therefore, both genetic knockdown and pharmacological inhibition of Gal-3 decrease migration and invasion.

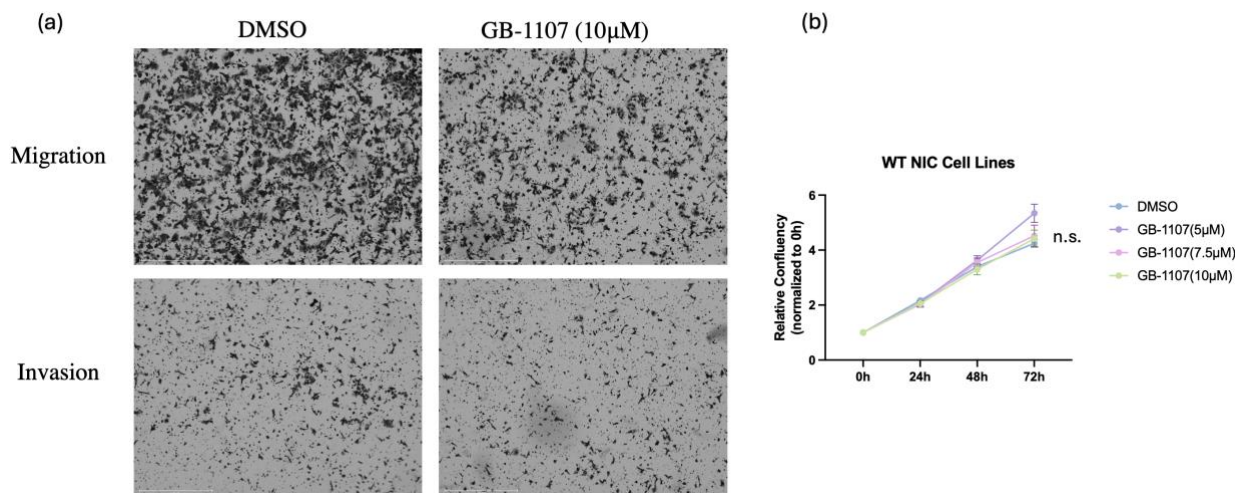


Figure 8: Pharmacological inhibition of Gal-3 leads to decreased migration and invasion

(a): Representative images of migration and invasion assay of 16 hours treated with DMSO or 10uM GB1107 in the WT NIC cells lines, suggested a decrease of migration and invasion with Gal-3 pharmacological inhibition. Scale bar 650um. (b): Proliferation assay shows no difference in proliferation between DMSO-treated or 10uM GB1107-treated WT NIC cells. Student's t-test.

2.1.1.7. Knockdown of Lgals3 increases focal adhesion markers

We have shown that in Stat3^{flx/flx}/NIC cells, the focal adhesion expression levels are elevated, and Gal-3 level is significantly downregulated in the Stat3-deficient cells. Therefore, we are interested in if the Gal-3 downregulation exhibits the same features as Stat3-deficient cells. We performed immunoblotting on the focal adhesion markers that were altered in the Stat3-deficient NIC cells (Figure 9). Remarkably, shLgals3_1 and shLgals3_3 demonstrated better knockdown of Gal-3, and these two cell lines exhibited high levels of phosphorylated-FAK, vinculin, phosphorylated-paxillin, and paxillin expression, compared to shControl and shLgals3_2. This suggests that Gal-3 recapitulates the capacity of Stat3 in down-regulating the expression of focal adhesion markers.

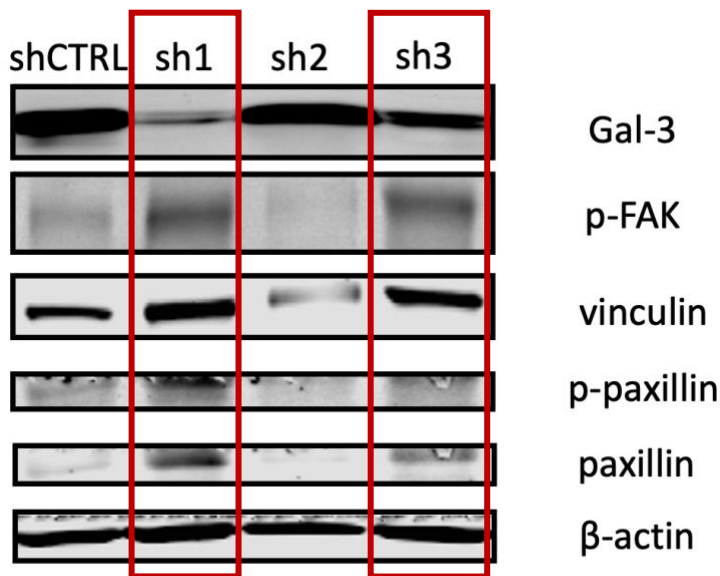


Figure 9: Focal adhesion protein expressions are decreased with Gal-3 knockdown in NIC cell lines

Immunoblotting of Stat3, p-FAK, vinculin, p-paxillin, paxillin, and beta-Actin protein in shControl and shLgals3 cell lines. Successful knockdown of Gal-3 can be observed with shLgals3_1 and shLgals3_3. With shLgals3_1 and shLgals3_3 knockdown, the protein levels of p-FAK, vinculin, p-Paxillin, and Paxillin are higher. However, with an unsuccessful knockdown of Gal-3 with shLgals3_2, the expression of focal adhesions mentioned above is not increased.

2.1.2. Stat3 deficiency results in a significant delay in tumor onset and a decrease in metastasis in TetO-ErbB2-Ires-Cre (EIC) mouse models

More recently, the Muller lab has generated a novel HER2-Positive breast cancer mouse model, TetO-ErbB2-Ires-Cre (EIC) (Attalla et al., 2023). Compared to the NIC mouse model, EIC mouse model exhibits more advantages (Attalla et al., 2023). It is a doxycycline-inducible mouse model and employs human version of ErbB2 as an oncogene (Attalla et al., 2023). By crossing EIC strain to MTB strain and inducing with doxycycline, the EIC/MTB mice follow a stepwise malignant transformation, and recapitulate the human breast cancer DCIS stage (Attalla et al., 2023).

To further study the role of Stat3 in HER2-Positive breast cancer initiation and progression, we crossed Stat3^{flx/flx} with EIC/MTB mouse model, and administered doxycycline to induce the activation of transgenes (Figure 10). Upon administration of doxycycline, the rtTA gets activated and binds to the Tet-ON operator, thereby activating expression of the ErbB2 and Cre, and the Cre recombinase excises the sequence between the LoxP sites flanked by Stat3 gene.

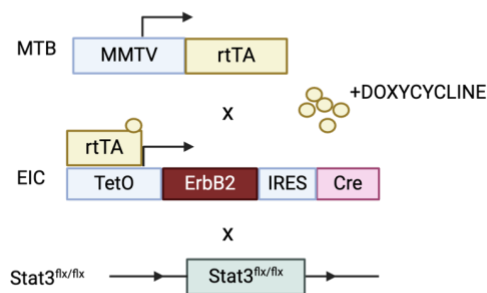


Figure 10: Schematic construct of Stat3^{flx/flx}/EIC/MTB

Upon doxycycline induction, rtTA binds and activates TetO operator, which activates the transcription of ErbB2 and Cre recombinase. Cre recombinase mediates the excision of LoxP-flanked Stat3. Created with Biorender.com.

2.1.2.1. Stat3 deficiency results in a delay in tumor onset and decreased tumor burden

To study the role of Stat3 in HER2-Positive breast cancer initiation and progression, the EIC/MTB/Stat3^{flx/flx} and EIC/MTB mice were induced with doxycycline and palpated for tumor kinetics. To study the tumor initiation, the tumor onset curve was generated (Figure 11a). The average tumor onset for EIC/MTB mice was 105.4±5.1 days (n=34), whereas the average tumor onset for significantly longer than EIC/MTB mice (p<0.0001, student's t-test). The penetrance was 100% for both EIC/MTB/Stat3^{flx/flx} and EIC/MTB mice.

Tumor burden is an important indicator of tumor progression, which refers to the ratio of tumor mass to body mass at the tumor end point (Figure 11b). At the experimental end point, the average tumor burden was 16.4%±0.9% for EIC/MTB mice, and 12.8%±1.4% for EIC/MTB/Stat3^{flx/flx} mice. The tumor burden for EIC/MTB mice was significantly heavier than EIC/MTB/Stat3^{flx/flx} mice (p=0.039, student's t-test).

The tumor onset curve and tumor burden graph suggested that Stat3 deficiency in the EIC HER2-Positive mouse model results in delayed tumor onset and decreased tumor burden.

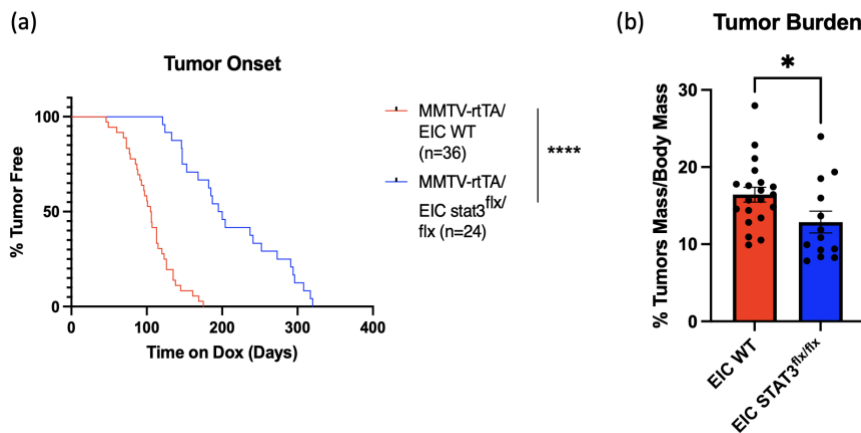


Figure 11: Tumor onset is delayed in Stat3^{flx/flx}/EIC/MTB mice and tumor burden is decreased

(a). Tumor onset was significantly delayed in Stat3^{flx/flx}/EIC/MTB mice compared to EIC/MTB mice, p<0.0001, student's t-test; (b). Tumor burden was significantly decreased in Stat3^{flx/flx}/EIC/MTB mice compared to EIC/MTB, p=0.039, student's t-test

2.1.2.2. Stat3 deficiency results in decreased metastasis

Besides the roles of Stat3 in tumor initiation and progression, it is also critical to study the roles of Stat3 in metastasis. At the tumor end point, one of the major sites of breast cancer metastasis, the lungs, were collected, embedded in paraffin, and sectioned for subsequent H&E staining (Figure 12a) (Jin et al., 2018). The extent of lung metastasis in the H&E-stained slides was then quantified (Figure 12b).

We first quantified the incidence of lung metastasis in EIC/MTB and EIC/MTB/Stat3^{flx/flx} mice, and we found that 84.6% of EIC/MTB mice (n=13) developed lung metastasis at the breast tumor end point, whereas only 50% of EIC/MTB/Stat3^{flx/flx} mice (n=8) developed lung metastasis. Therefore, there was a lower incidence of lung metastasis in EIC/MTB/Stat3^{flx/flx} mice compared to EIC/MTB mice. In addition, the size of lungs occupied by metastasis was also quantified. In EIC/MTB mice, 9.1%±2.8% of lungs (n=13) were occupied by metastasis, whereas in EIC/MTB/Stat3^{flx/flx} mice, only 1.3%±0.5% of lungs (n=8) were occupied by metastasis. Therefore, the size of lungs occupied by metastasis of EIC/MTB/Stat3^{flx/flx} mice was significantly smaller than that of EIC/MTB mice (p=0.043, student's t-test).

To summarize, the deficiency of Stat3 results in decreased metastasis, from the perspectives of both incidence and size of metastasis. This is consistent with the findings from NIC/Stat3^{flx/flx} mouse model, demonstrating a role of Stat3 in promoting HER2-Positive breast cancer.

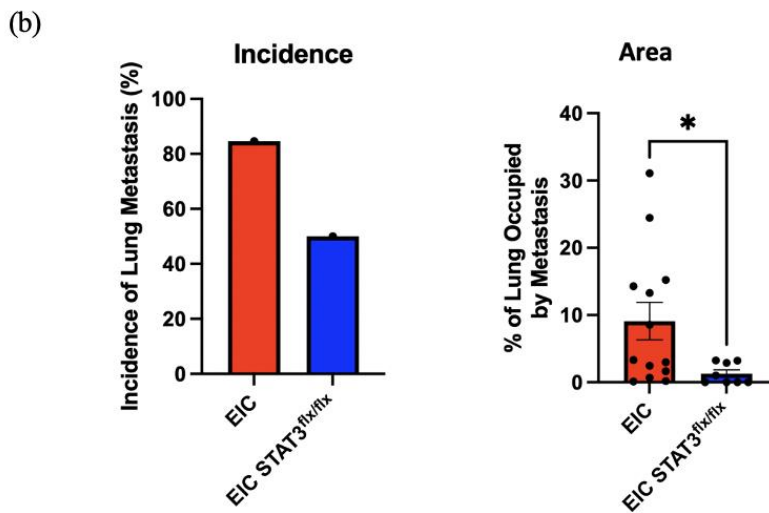
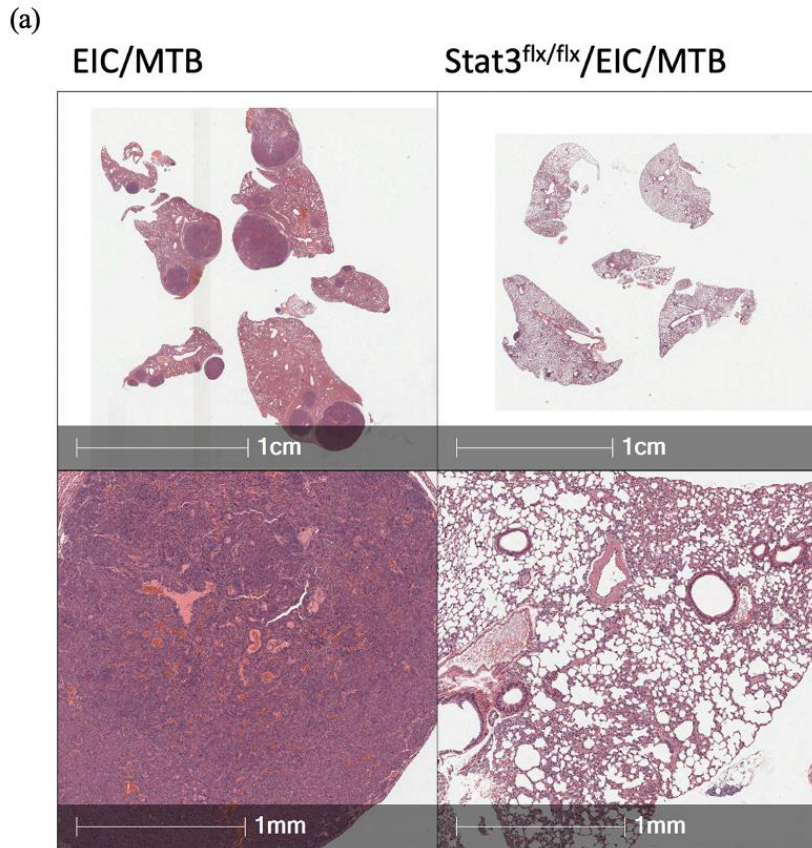


Figure 12: Lung metastasis is significantly decreased in Stat3^{flx/flx}/EIC/MTB mice compared to EIC/MTB mice

(a): Representative images of lung metastasis in EIC/MTB and Stat3^{flx/flx}/EIC/MTB, scale bar 1cm (upper), and 1mm (below); (b): quantification of incidence of lung metastasis and percent area occupied by lung metastasis in EIC/MTB and Stat3^{flx/flx}/EIC/MTB, for the percent area: p=0.043, student's t-test

2.1.2.3. Stat3 deficiency results in a trend of decreased proliferation

To study the proliferation and apoptosis of the EIC/MTB and EIC/MTB/Stat3^{flx/flx} breast tumor, immunohistofluorescence staining of ki67 and cleaved-caspase 3 was performed on the paraffin-embedded tissue sections (Figure 13). The ki67 positive cells in EIC/MTB breast tumor accounts for 17.4%±3.8%, whereas they only accounts for 9.2%±1.4% in EIC/MTB/Stat3^{flx/flx} breast tumor. Therefore, there is a marginal significance of decreased proliferation in the EIC/MTB/Stat3^{flx/flx} breast tumor (p=0.07, student's t-test). Meanwhile, to study the apoptosis of the tumor cells in the EIC/MTB and EIC/MTB/Stat3^{flx/flx} breast tumor, cleaved-caspase 3 staining was performed. Although there is a trend of lower cleaved-caspase 3 level in the EIC/MTB/Stat3^{flx/flx} breast tumor, no significant difference was observed.

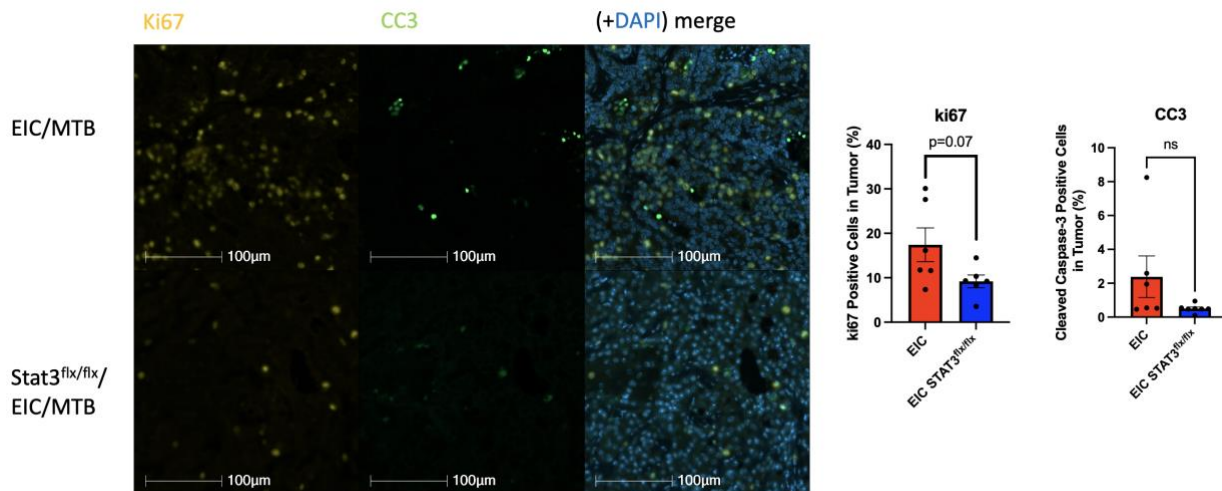


Figure 13: A trend of decreased proliferation in the Stat3^{flx/flx}/EIC/MTB compared to EIC/MTB mouse breast tumor

(Left) Representative figure of immunofluorescence staining of EIC/MTB and Stat3^{flx/flx}/EIC/MTB of Ki67 (yellow), cleaved caspase-3 (green), and merge with DAPI (blue). (Right) Quantification of Ki67 and Cleaved caspase 3 positive cells by immunohistofluorescence staining on breast tumors of EIC/MTB and Stat3^{flx/flx}/EIC/MTB, p>0.05, student's t-test

2.1.2.4. Transcriptomic and bioinformatic analysis

We have found that Stat3^{flx/flx}/EIC/MTB mice had a significantly delayed tumor onset compared to EIC/MTB mice, and they had significantly reduced lung metastasis. To study the underlying mechanism, transcriptomic and bioinformatic analysis were performed on the Stat3^{flx/flx}/EIC/MTB and EIC/MTB breast tumors. Transcriptomic studies showed differentially regulated gene profiles. Among the cellular functions and behaviors that are altered in the Stat3-deficient EIC/MTB tumors, the biological process of antigen processing and presentation appeared to be upregulated to a large extent. GO analysis demonstrated that 30 genes involved in this process were altered, such as Tap1, Tap2, and Gm11127 (Figure 14a and b) (Agrawal et al., 2004; Qu et al., 2023). Furthermore, GSEA analysis suggested that there are large enrichments in the antigen processing and presentation (Figure 14c). In addition, a similar finding was obtained with KEGG analysis, and 38 genes were altered and involved in antigen processing and presentation (Figure 14d).

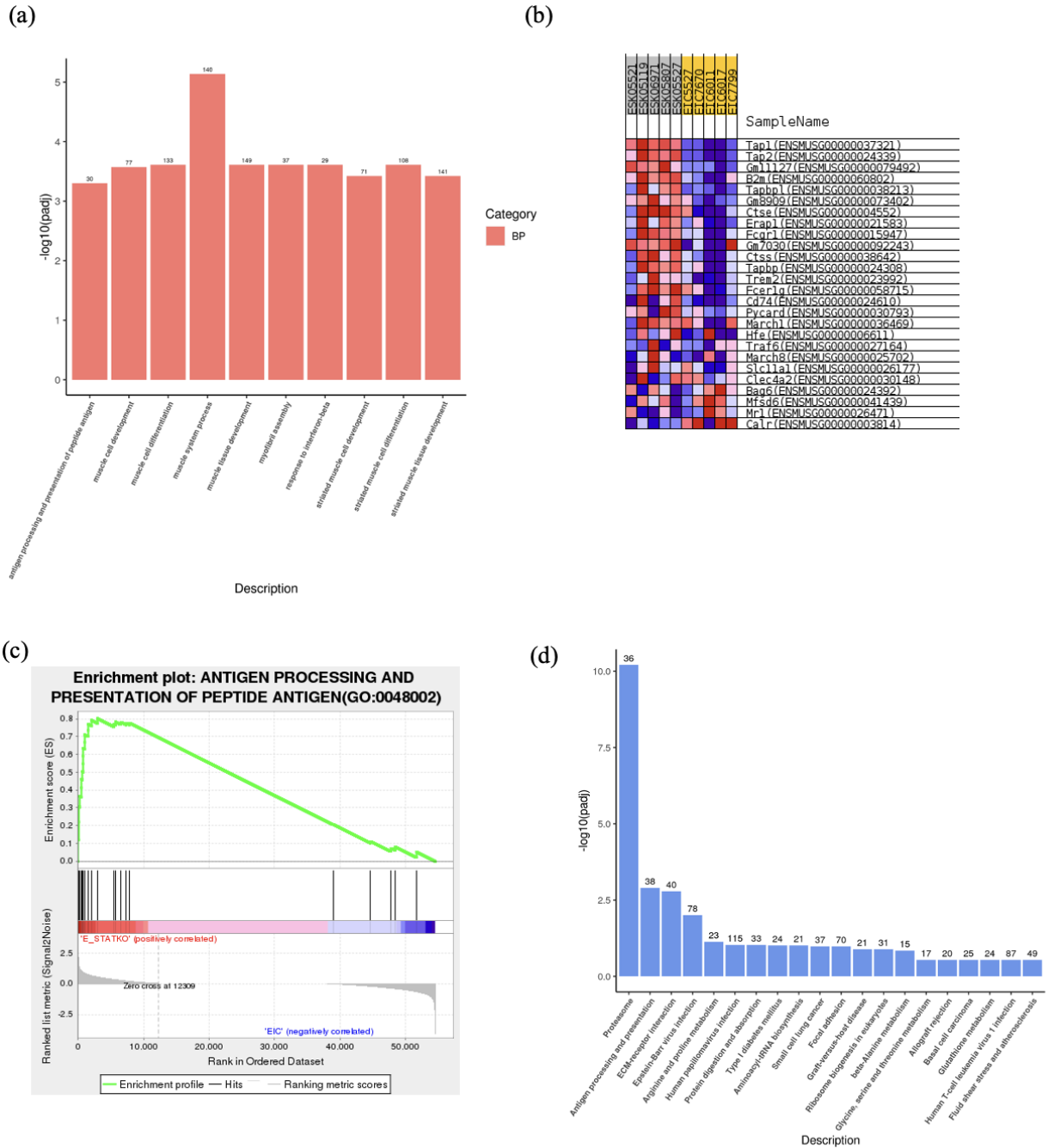


Figure 14: Transcriptomic study and bioinformatic analysis of EIC/MTB and Stat3flx/flx/EIC/MTB tumors

(a): GO analysis revealed that antigen processing and presentation was significantly upregulated in Stat3^{flx/flx}/EIC/MTB tumors; (b): The genes that are altered and involved in antigen processing and presentation revealed by GO analysis; (c): GSEA enrichment analysis revealed an enrichment in antigen processing and presentation; (d): KEGG analysis suggested a significant alteration in antigen processing and presentation

2.1.2.5. Lgals3 is significantly down-regulated in the Stat3-deficient lesions

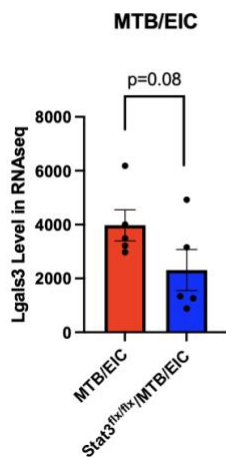
We have demonstrated in the NIC mouse model that Stat3 may promote HER2-Positive breast cancer metastasis through the regulation of Lgals3. To further study the mechanism of Stat3 promoting HER2-Positive breast cancer metastasis, we studied the expression of Lgals3 in EIC/MTB and EIC/MTB/Stat3^{flx/flx} breast tumor. We first examined the Lgals3 level from the transcriptomics analysis of EIC/MTB and EIC/MTB/Stat3^{flx/flx} breast tumor, and we observed a trend of lower Lgals3 level in the EIC/MTB/Stat3^{flx/flx} breast tumor ($p=0.08$, $p_{adj}=0.26$) (Figure 15a).

To study the protein levels of Gal-3, we performed an immunohistofluorescence staining of phospho-Stat3, Gal-3, and HER2 on EIC/MTB and EIC/MTB/Stat3^{flx/flx} breast tumor paraffin-embedded tissue sections (Figure 15b). We observed nuclear staining of phospho-Stat3 (green) in the EIC/MTB breast tumor, while no phospho-Stat3 was detected in EIC/MTB/Stat3^{flx/flx} breast tumor. In addition, similar levels of HER2 expression (purple) was observed in both EIC/MTB and EIC/MTB/Stat3^{flx/flx} breast tumor, indicating the presence of mammary gland epithelial cells, where the transgenes are expressed.

In EIC/MTB breast tumors, we observed the expression of Gal-3 protein (red) expression both in epithelial cells and stromal cells, and the expression is predominantly cytoplasmic. In contrast, EIC/MTB/Stat3^{flx/flx} breast tumor exhibited markedly low expression of Gal-3 in the epithelial cells. By the HALO program quantification, we found that $28.0\% \pm 7.4\%$ of EIC/MTB breast tumor epithelial cells were Gal-3 positive, whereas only $8.8\% \pm 1.5\%$ of EIC/MTB/Stat3^{flx/flx} breast tumor cells exhibited Gal-3 positivity. This indicated a significantly lower Gal-3 expression in EIC/MTB/Stat3^{flx/flx} breast tumor epithelial cells ($p=0.029$, student's t-test).

However, although the Gal-3 expression is low in epithelial cells of EIC/MTB/Stat3^{flx/flx} breast tumor, its expression is very high in stromal cells. This may explain why in transcriptomics analysis, the Lgals3 is not significantly lower in EIC/MTB/Stat3^{flx/flx} breast tumor. Moreover, this elevated level of Gal-3 in stromal cells may be related to an altered immune profile of EIC/MTB/Stat3^{flx/flx} breast tumor.

(a)



(b)

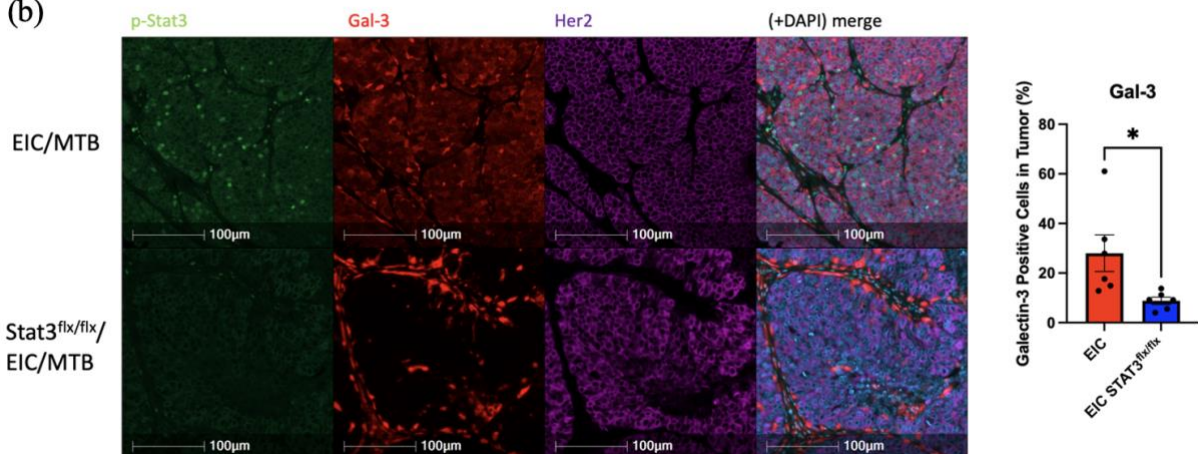


Figure 15: Gal-3 protein expression is decreased in Stat3^{flx/flx}/EIC/MTB tumors compared to EIC/MTB tumors

(a): Level of Lgals3 by transcriptomic analysis (RNA sequencing), $p=0.08$, $p_{adj}=0.26$; (b): Immunohistochemistry staining of p-Stat3 (green), Gal-3 (red), ErbB2 (purple), and merge with DAPI (blue), Quantification of Gal-3 positive cells in tumors. $p=0.029$, student's t-test.

2.2. Creating a novel ER-Positive Breast Cancer Mouse Model: TetO-FOXA1-Ires-Cre (FIC)

Estrogen receptor (ER) positive breast cancers, primarily luminal A, luminal B, and some HER2-positive types, comprise roughly 70% of all breast cancers (Mohibi et al., 2011). While ER-Positive breast cancer is predominant, there's a significant void in mouse models that genuinely mimic ER-driven breast cancer (Dabydeen & Furth, 2014a). This makes comprehensive ER-positive breast tumor initiation and progression studies challenging, given factors like extended tumor development latency, low ER-positive tumor rates, growth defects, and resistance to endocrine therapies in current models (Dabydeen & Furth, 2014a). Recognizing the imperative role of accurate mouse models, our lab seeks to develop new ER-positive breast cancer mouse models. FOXA1 is a transcription factor facilitating ER-chromatin association, and it may promote tumorigenesis through multiple mechanisms (Seachrist et al., 2021).

2.2.1. FIC/MTB mouse model

To create a novel ER-Positive breast cancer mouse model that faithfully recapitulates the features of human ER-Positive breast cancer, our lab has generated a novel TetO-FOXA1-Ires-Cre (FIC) mouse model that overexpresses the FOXA1 gene. By crossing to the rtTA-MMTV (MTB) strain, FIC/MTB mice conditionally overexpress the FOXA1 gene in the mammary epithelial cells upon the doxycycline induction, and activate the Cre recombinase protein expression at the same time (Figure 16). We had two founder lines, namely FIC2 and FIC3, which were selected for a higher level of transgene expression.

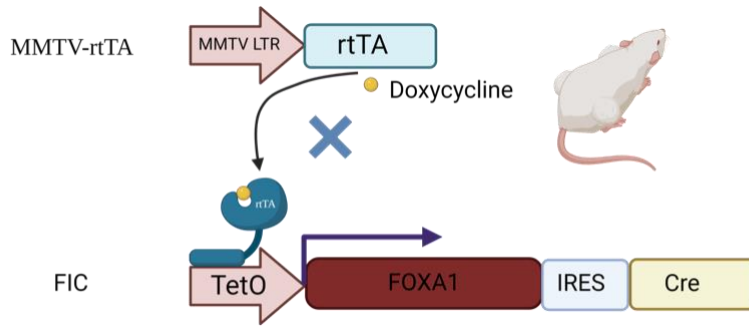


Figure 16: Schematic construct of FIC/MTB mouse model

Upon doxycycline induction, rtTA gets activated and binds to TetO operator, which drives the transcription of FOXA1 and Cre recombinase. Created by Biorender.com.

2.2.1.1. Validation of FOXA1 expression and comparisons of founder lines

To generate the female cohorts of FIC/MTB, the progenies of FIC and MTB mice were subjected to genotyping at the age of three weeks, only mice that were positive for both FOXA1 and MTB genes were considered FIC/MTB mice (Figure 17).

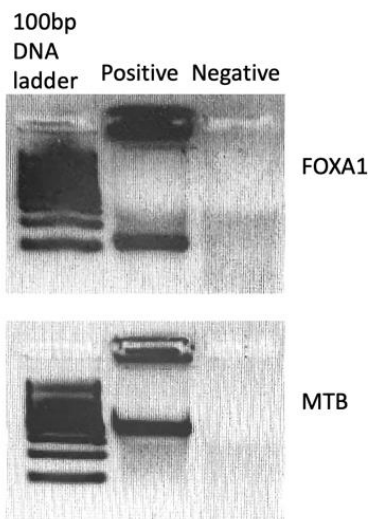


Figure 17: Representative genotyping blots of FOXA1 and MTB

Mice bearing FIC transgene in their mammary glands appear a band at around 100bp (Upper), and mice bearing MTB transgene appear a band at around 500bp (Below). Only mice that are positive for both FIC and MTB are considered the FIC/MTB experimental mice.

The FIC2/MTB and FIC3/MTB mice were induced with doxycycline for 4 weeks after 2-month old, followed by the validation of FOXA1 and Cre expression. The mammary glands from FIC2/MTB and FIC3/MTB were harvested and extracted for RNA and proteins. FIC2/MTB had an approximately three-time increase in the FOXA1 mRNA level compared to the control MTB mice, and FIC3/MTB had an approximately one-time increase in the FOXA1 mRNA level to that of the MTB mice (Figure 18). Also, compared to MTB mice, FIC2/MTB mice had an approximately six-time increase in the Cre mRNA level, and FIC3/MTB mice had an approximately one-time increase in the Cre recombinase mRNA level (Figure 18). This demonstrated that from the mRNA level, founder line 2 (FIC2/MTB) has a higher expression of the transgene FOXA1 and Cre.

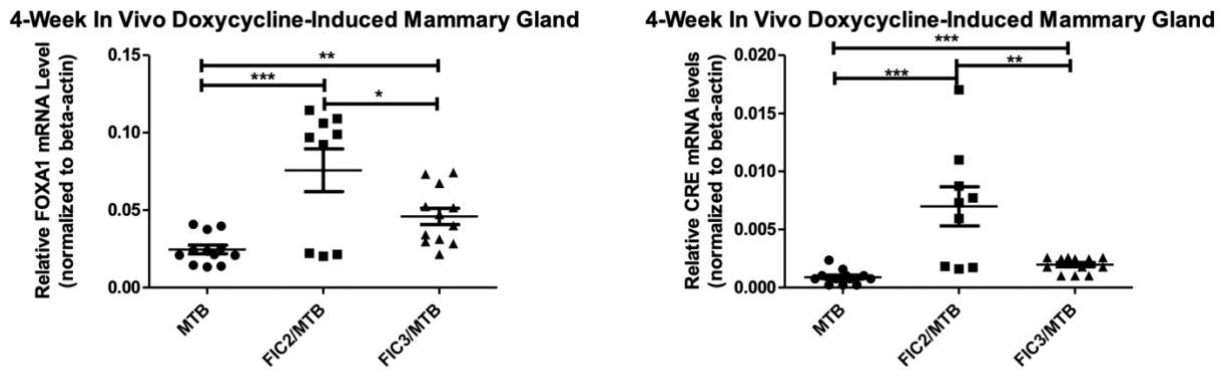


Figure 18: Comparison of FOXA1 (Left) and Cre (Right) mRNA levels in the 4-week induced MTB, FIC2/MTB, and FIC3/MTB mice

The FOXA1 (Left) and Cre (Right) mRNA levels were quantified in MTB, FIC2/MTB, and FIC3/MTB mouse mammary glands. Both FOXA1 and Cre mRNA levels are significantly higher in the FIC2/MTB compared to MTB and FIC3/MTB.

FOXA1: MTB vs. FIC2/MTB: $p=0.0005$, MTB vs. FIC3/MTB: $p=0.0016$, FIC2 vs. FIC3: $p=0.038$;

Cre: MTB vs. FIC2/MTB: $p=0.0005$, MTB vs. FIC3/MTB: $p=0.0004$, FIC2 vs. FIC3: $p=0.0028$;

Student's t-test

To further validate this conclusion, we grew the uninduced FIC/MTB mammary gland-derived organoids on the polyHEMA-coated plates, and induced with doxycycline *in vitro*. After inducing for 14 days, the organoids were harvested and extracted for RNA for real-time PCR (RT-PCR), for the comparisons of FIC2/MTB and FIC3/MTB transgene expression (Figure 19). We found that upon doxycycline induction, the organoids from FIC2/MTB express significantly higher mRNA levels of FOXA1 and Cre compared to the control group without doxycycline induction. However, in the FIC3/MTB, there is no difference in the FOXA1 and Cre mRNA levels between the with and without doxycycline induction groups.

This further demonstrated that founder line 2 (FIC2/MTB) has a higher expression of FOXA1 and Cre gene. Therefore, FIC2/MTB mice were used for further study.

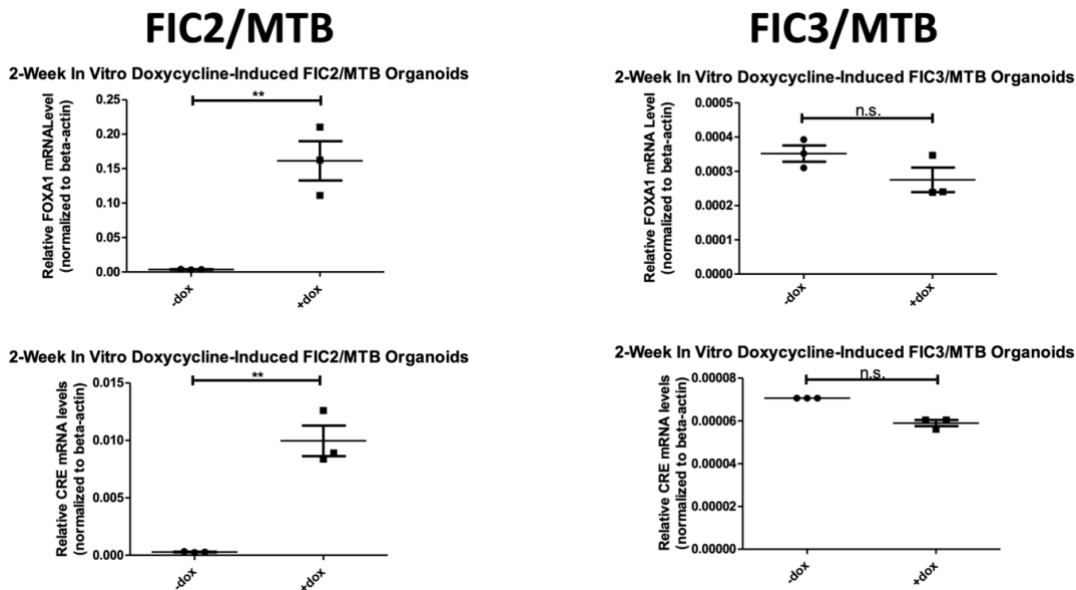


Figure 19: FIC2/MTB mouse mammary gland-derived organoids have higher mRNA expression of FOXA1 and Cre expression in two-week induced organoids with doxycycline induction in FIC2/MTB than FIC3/MTB

(Left) In FIC2/MTB mouse mammary gland-derived organoids, relative FOXA1 mRNA level with doxycycline vs. without doxycycline: $p=0.0049$, student's t-test; Cre mRNA level with doxycycline vs. without doxycycline: $p=0.0019$, student's t-test; (Right) In FIC3/MTB mouse mammary gland-derived organoids, relative FOXA1 mRNA level with doxycycline vs. without doxycycline: n.s., student's t-test; Cre mRNA level with doxycycline vs. without doxycycline: n.s., student's t-test

The FIC2/MTB mice were further induced for 12 weeks, and we validated the expression of FOXA1 by RT-PCR (Figure 20). By RT-PCR, there is an approximately two-time increase in the mRNA level of FOXA1 in the FIC2/MTB compared to MTB.

From here on, all the FIC/MTB and FIC/MTB/ESR1 studies are conducted with founder line FIC2.

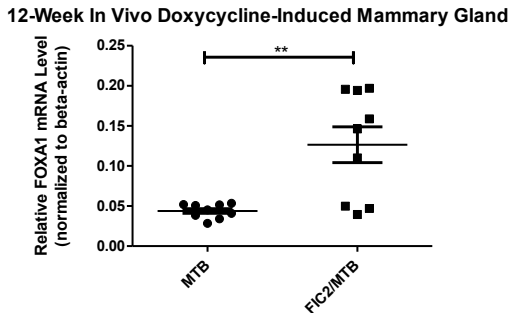


Figure 20: FIC2/MTB mouse mammary glands had significantly higher expression of FOXA1 compared to WT counterparts after 12-week induction

Comparison of FOXA1 mRNA level in 12-week induced MTB and FIC/MTB mouse mammary glands demonstrated significantly higher expression in FIC2/MTB compared to MTB, $p=0.0021$, student's t-test.

2.2.1.2. *In vitro* study of mammary gland-derived organoids showed abnormal filled sphere structure upon doxycycline induction

To study the growth and abnormality of FOXA1-overexpressing mammary gland *in vitro*, we harvested the mammary glands of the FIC/MTB mice and dissociated into single cells. With these mammary gland-derived single cells, we grew into organoids on the 24 well plates coated with Geltrex (Figure 21). The organoids were grown on the Geltrex for 6 days, followed by with or without doxycycline induction for 15 days. At day 15 and day 21, we performed immunofluorescence staining and imaged with confocal microscope on the organoids. In

addition, the size of the organoids was measured and the morphology of the organoids was recorded.

Immunofluorescence staining was performed on FIC2/MTB-derived organoids grown on 24-well plate. We found that, at day 15, FOXA1 expression (red) was well detected in the doxycycline-induced organoids, whereas no Foxa1 expression was observed in the non-induced control organoids (Figure 22a). Meanwhile, the FOXA1 protein was detected in the nucleus. Moreover, the non-induced organoids developed a hollow sphere-like structure that mimicked normal mammary glands, however, the doxycycline-induced organoids developed a filled sphere structure that mimicked the mammary gland hyperplasia. At day 21, in the induced group, although the organoids had largely lost their expression of FOXA1, which could be due to the restriction of organoid lifetime, the filled sphere structures were also observed in the doxycycline-induced group (Figure 22b). This abnormality may indicate that *in vivo*, overexpression of FOXA1 can lead to hyperplasia in mammary gland. Furthermore, a decreased expression of E-cadherin (purple) was observed, which might indicate a potential epithelial-to-mesenchymal (EMT) process.

Furthermore, the diameter of induced (not exclusive to FOXA1-expressed organoids) and non-induced organoids were measured on day 18 (Figure 22c). The measurement has shown that the doxycycline-induced organoids have a significantly larger diameter ($57.3 \pm 2.2 \mu\text{m}$) than non-induced organoids ($41.0 \pm 1.4 \mu\text{m}$) at day 18 ($p=0.0001$, student's t-test). This may indicate a higher proliferation of FOXA1-overexpressing organoids compared to normal organoids.

In conclusion, *in vitro* study demonstrated that overexpression of FOXA1 in mammary gland-derived organoids led to an abnormal filled sphere structure, and FOXA1 promoted proliferation in mammary glands *in vitro* upon doxycycline induction.

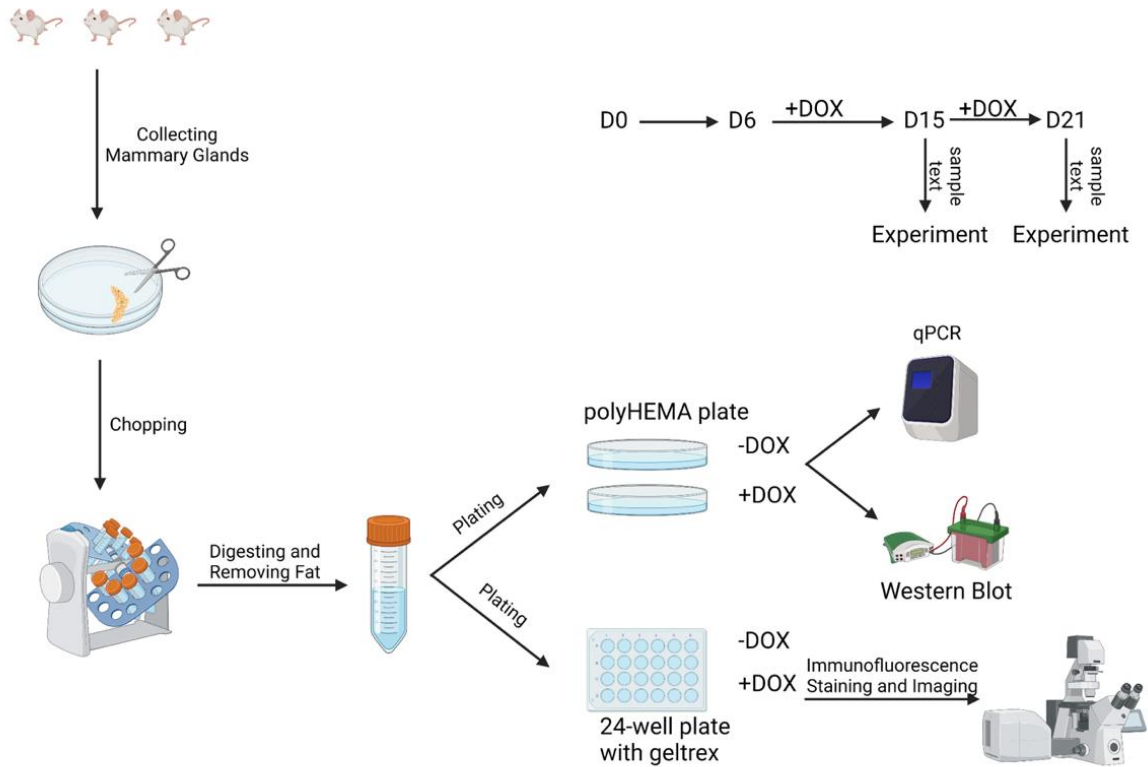
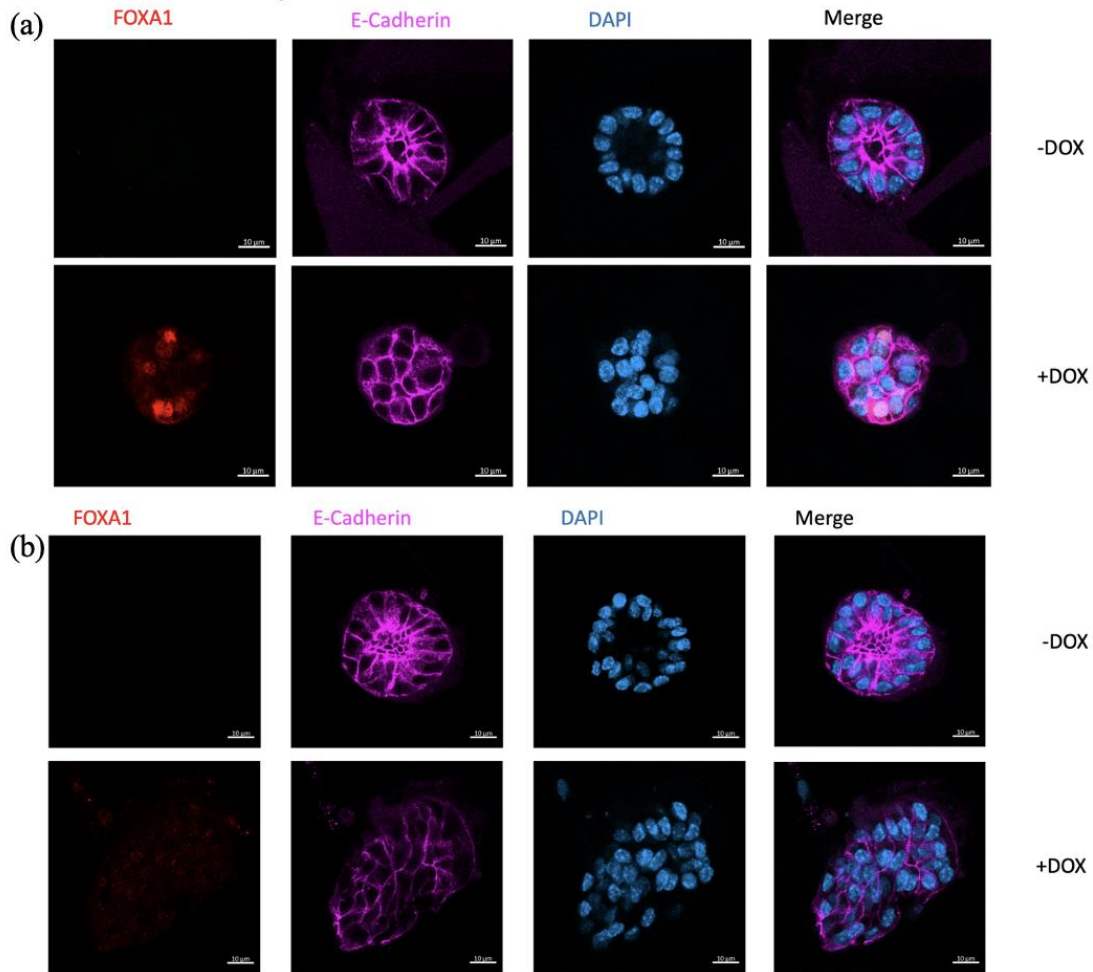


Figure 21: Schematic procedures of growing organoids *in vitro*, timeline and the experiments

The mammary glands were harvested following necropsies, and were chopped with scissors for 10-15 minutes. The chopped tissues were digested in digestion media on rotator. After several washes and trypsinization, the single cells were grown on polyHEMA plate in which single cells/organoids were suspended in the media, and on 24-well plate with geltrex to which single cells/organoids attach and grow. The single cells were allowed to grow for 6 days to become organoids, and then treated with or without doxycycline for 15 days. 9 days and 15 days post-induction, the organoids were fixed and immunofluorescent stained. Also, 15 days post-induction, the organoids in the polyHEMA plate was collected for qRT-PCR. Created with Biorender.com.



(c) 2-Week In Vitro Doxycycline-Induced FIC2/MTB Organoids

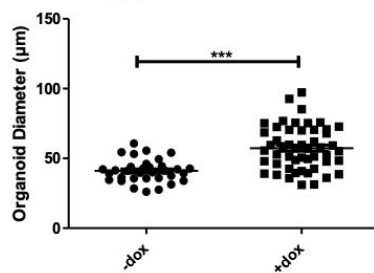


Figure 22: FIC2/MTB mouse mammary gland-derived organoid developed a filled sphere structure with doxycycline induction

(a): Immunofluorescence on the FIC2/MTB mouse mammary gland-derived organoids with and without doxycycline on FOXA1 (red), E-cadherin (purple), DAPI (blue), and merge on Day 9 post-induction. The organoids developed a filled sphere structure with doxycycline induction; (b): Immunofluorescence staining of organoids on Day 15 post-induction. The organoids also had the filled sphere structure; (c): Quantification of the diameters of the organoids with and without doxycycline. $P < 0.0001$, student's t-test.

2.2.1.3. *In vivo* 4-week induction

Although *in vitro* study of FOXA1 overexpression in mammary gland-derived organoid has shown the role of FOXA1 in proliferation, we are also interested in the role of FOXA1 overexpression *in vivo*. Therefore, we induced the FIC/MTB and MTB mice with doxycycline for 4 weeks and harvested their mammary glands. The H&E staining was performed on the mouse mammary gland tissue sections (Figure 23). From the H&E staining of MTB mouse mammary gland, we observed a hollow lumen that is surrounded by epithelial cells. Although the majority of FIC2/MTB mouse mammary glands also had normal hollow lumen structures, there was one out of four FIC2/MTB mice that had mammary glands with early hyperplasia. These abnormal mammary glands were infiltrated with many immune cells, which can be observed surrounding the mammary glands.

However, given that the abnormality was at a very early stage, longer doxycycline induction was performed on FIC/MTB mice to further study the role of FOXA1 in mammary glands.

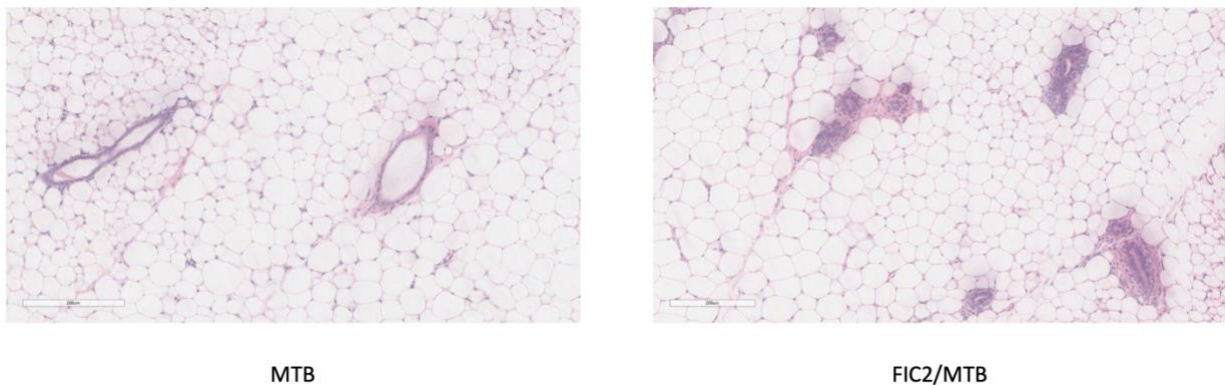


Figure 23: 4-week induced MTB and FIC2/MTB mammary gland H&E staining

After 4-week induction, MTB mouse mammary glands (left) had normal lumen ducts, whereas one of the FIC2/MTB (right) out of four mice, developed an early hyperplasia, and the ducts seemed to be surrounded by immune cells. Other FIC2/MTB mammary glands appeared normal. Scale bar 200um.

2.2.1.4. *In vivo* 12-week induction

We further induced the FIC2/MTB mice for 12 weeks and harvested the mammary glands. The mammary glands were subjected to wholemount, H&E staining of the tumor sections, and immunofluorescence staining.

The wholemount of mammary glands did not show a difference in the morphology between FIC/MTB and MTB mice. Meanwhile, no hyperplasia can be observed from the mammary gland wholemount (Figure 24a).

In addition, the H&E staining of the paraffin-embedded slide sections showed that there was no hyperplasia in FIC/MTB mouse mammary glands, given their hollow lumen structures (Figure 24b). No significant difference can be observed in the H&E staining between FIC/MTB and MTB mice after 12 weeks of doxycycline induction.

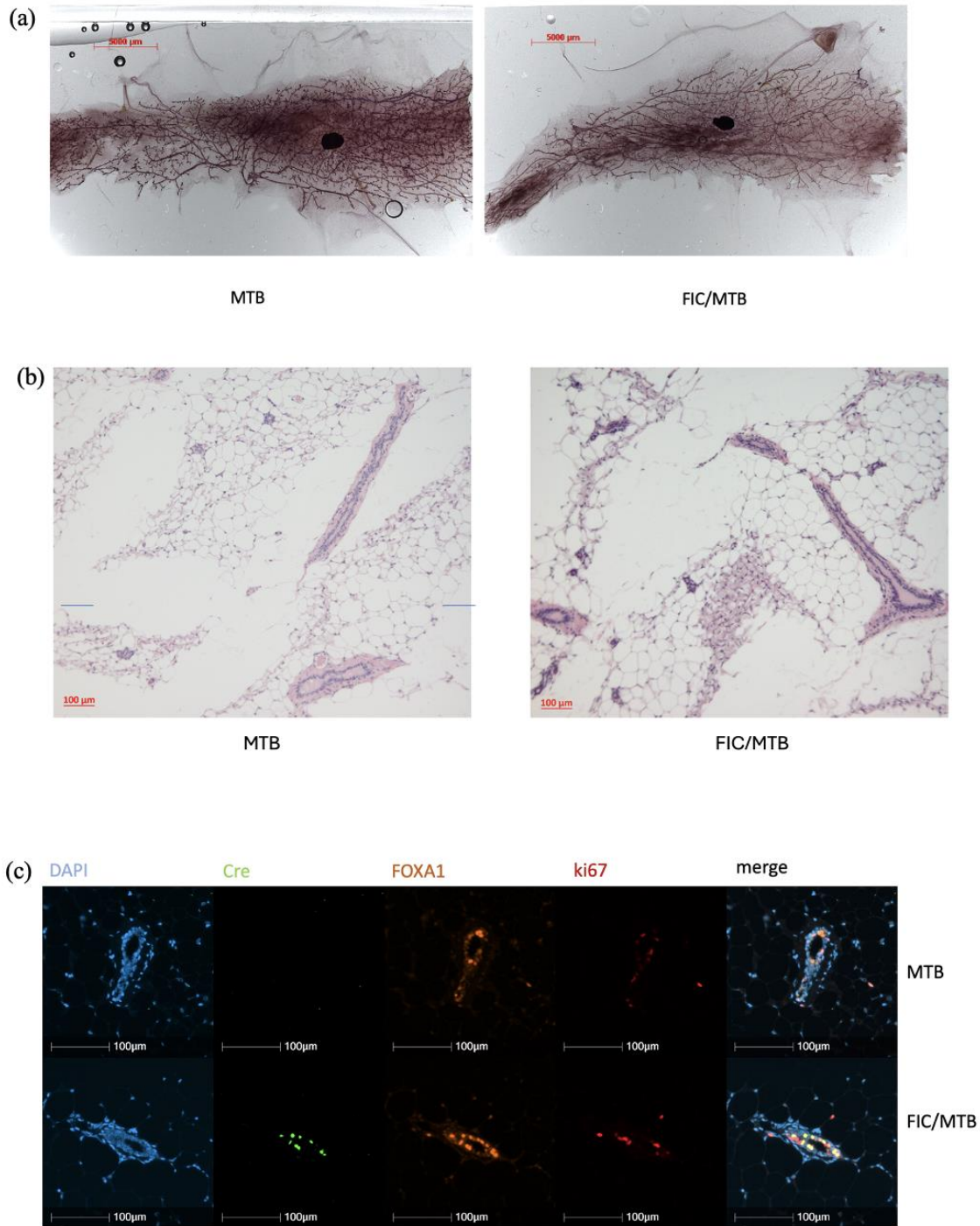


Figure 24: 12 week-induced FIC2/MTB mammary gland wholemount, H&E staining, and immunofluorescent staining

(a): Representative wholemounts of 12-week induced MTB and FIC/MTB mammary glands, scale bar 5000um; (b): Representative H&E staining of 12-week induced MTB and FIC/MTB mammary glands, scale bar 100um;(c): Immunofluorescence staining of DAPI (blue), Cre (green), FOXA1 (orange), and ki67 (red) on paraffin-embedded sections of MTB and FIC/MTB mammary glands.

2.2.1.5. *In vivo* 20-week induction

We further induced the FIC/MTB mice for 20 weeks and harvested the mammary glands. The mammary glands were subjected to wholemount, H&E staining of the tumor sections (Figure 25).

No hyperplasia can be observed in either MTB or FIC/MTB mouse mammary glands from wholemounts and H&E staining of mammary gland sections. However, there may be increased immune cells infiltrating the mammary ducts of FIC/MTB mice, as we observed many cells surrounding mammary ducts.

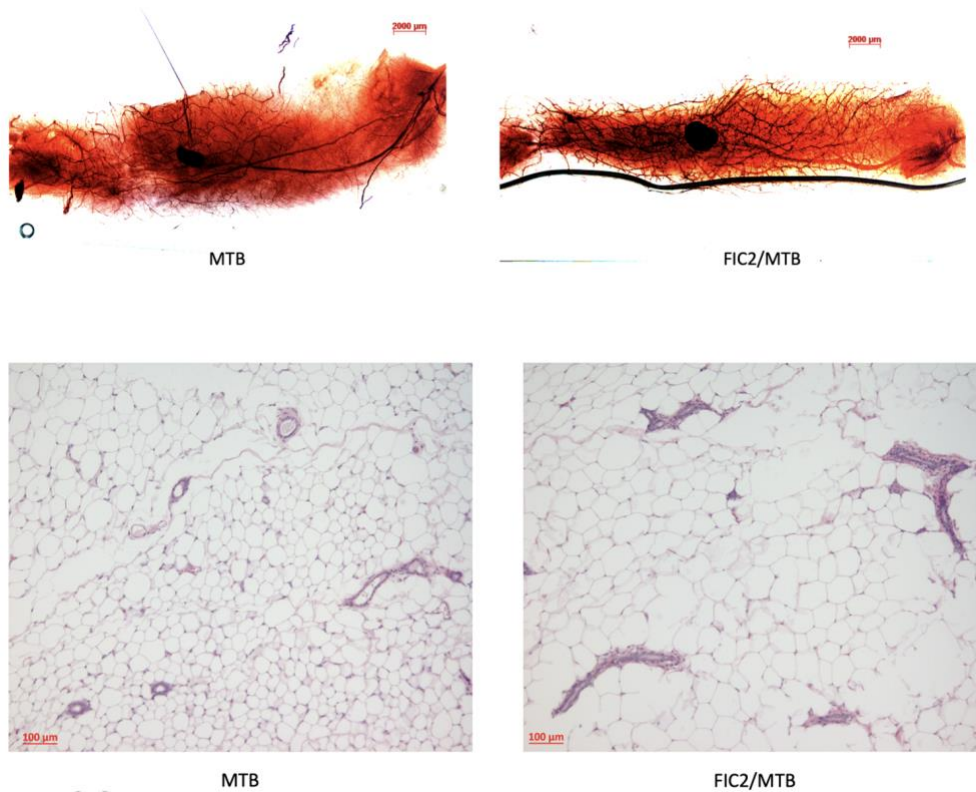


Figure 25: 20-week induced MTB and FIC2/MTB mouse mammary gland wholemounts and H&E staining

(Upper) Wholemounts of 20-week induced MTB and FIC2/MTB mouse mammary glands with hematoxylin staining. Scale bar 2000um. (Below) H&E staining of the mammary gland sections of 20-week induced MTB and FIC2/MTB. There may be increased immune cells infiltrating FIC2/MTB mouse mammary ducts. Scale bar 100um.

2.2.2. FIC/MTB/ESR1 mouse model

To speed up the oncogenesis process, the FIC/MTB mouse model was crossed to the ESR1^{Y541S} (ESR1) mouse model, which mutates the ESR1 gene and results in constitutive activation of ER (Simond et al., 2020) (figure 26). Only mice that are genotyped to be positive for all FOXA1, MTB, and heterozygous ESR1^{Y541S} are considered FIC/MTB/ESR1 for doxycycline induction and following experiments (Figure 27).

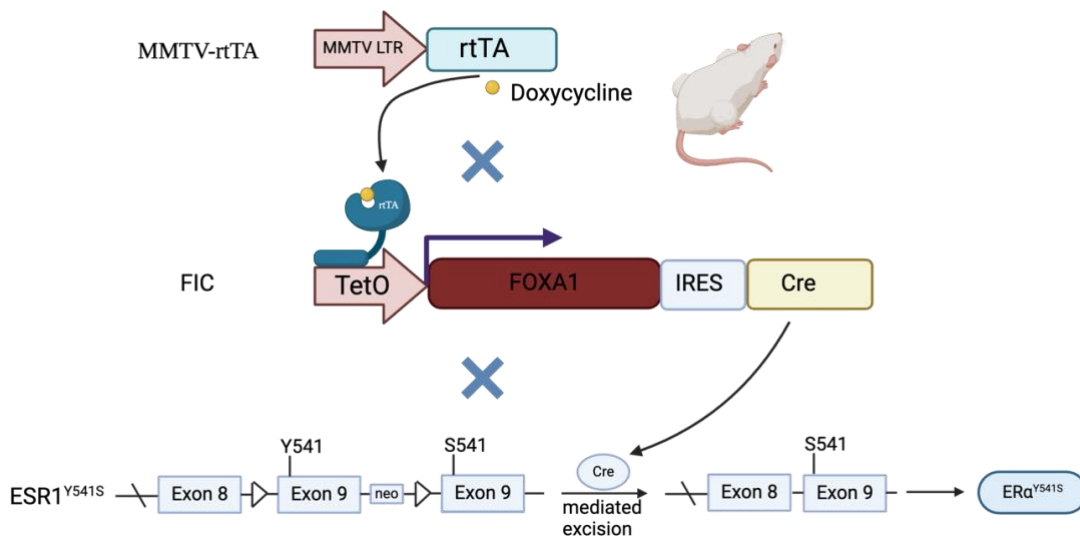


Figure 26: Schematic construct of FIC/MTB/ESR1

Upon doxycycline induction, rtTA binds and activates TetO operator, which activates the transcription of FOXA1 and Cre recombinase. Cre recombinase mediates the excision of WT exon 9 of ESR1 and activates the mutated exon 9, thereby leading to constitutive activation of ERα. Created by Biorender.com.

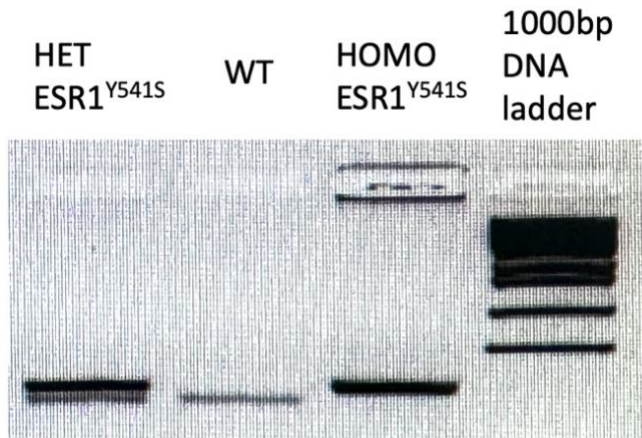


Figure 27: Representative genotyping blot of ESR1

Homozygous ESR1 shows one band at approximately 160bp; heterozygous ESR1 shows two bands at 126bp and 160bp; and WT ESR1 shows one band at 126bp. In this study, heterozygous ESR1 has been used as experimental mice.

2.2.2.1. Excision PCR

To validate the Cre recombinase function, an excision PCR was performed with 8-week induced FIC2/MTB/ESR1 mice mammary glands. The positive control is MIC/MTB/ESR1 mouse mammary glands which are known to successfully express Cre recombinase (Rao et al., 2014). This experiment demonstrated successful Cre excision of the WT exon 9 of the ESR1 gene, leaving the mutated exon 9 with Y541S mutation (Figure 28) (Simond et al., 2020).

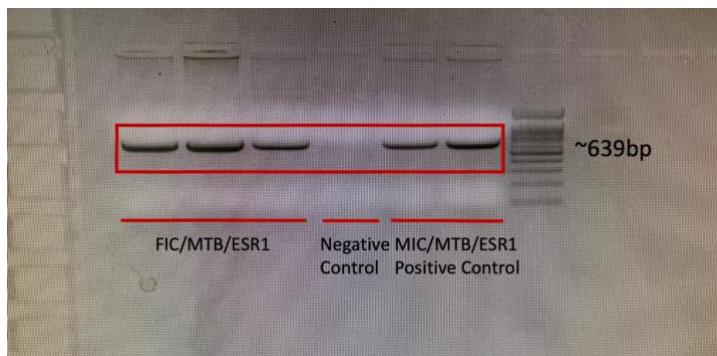


Figure 28: Excision PCR of FIC/MTB/ESR1 mammary gland-extracted DNA

FIC/MTB/ESR1, and positive control MIC/MTB/ESR1 after excision PCR, appeared the band with size around 639bp, which indicated proper Cre function (excising), whereas in negative control, there is no band.

2.2.2.2. 20-week induced FIC2/MTB/ESR1 mouse mammary glands

The FIC/MTB/ESR1 mice were induced for 20 weeks with doxycycline. The mice were sacrificed, and the mammary glands were harvested. Wholemounts with hematoxylin staining of the 20 week-induced MTB and FIC/MTB/ESR1 mouse mammary glands showed dramatic differences. In the MTB mice, the mammary glands appeared a normal morphology, and we observed normal branches in the mammary glands. However, in the FIC/MTB/ESR1 mice, the mammary glands exhibited some extent of hyperplasia (Figure 29a).

Moreover, in the H&E staining of FIC/MTB/ESR1 mammary gland sections, we observed a dramatically increased number of ducts compared to MTB counterparts, and they account for a dramatically large area of the mammary gland (Figure 29b). These ducts did not exhibit normal lumen structures, instead, they formed significant hyperplasia, and they seemed to be well-differentiated hyperplasia based on the shapes of the ducts. Also, these ducts were generally small, however, they had many bubble-like holes within the filled ducts.

Interestingly, the lymph node of FIC/MTB/ESR1 mammary gland was enlarged and appeared an irregular shape, which might be related to malignant transformation.

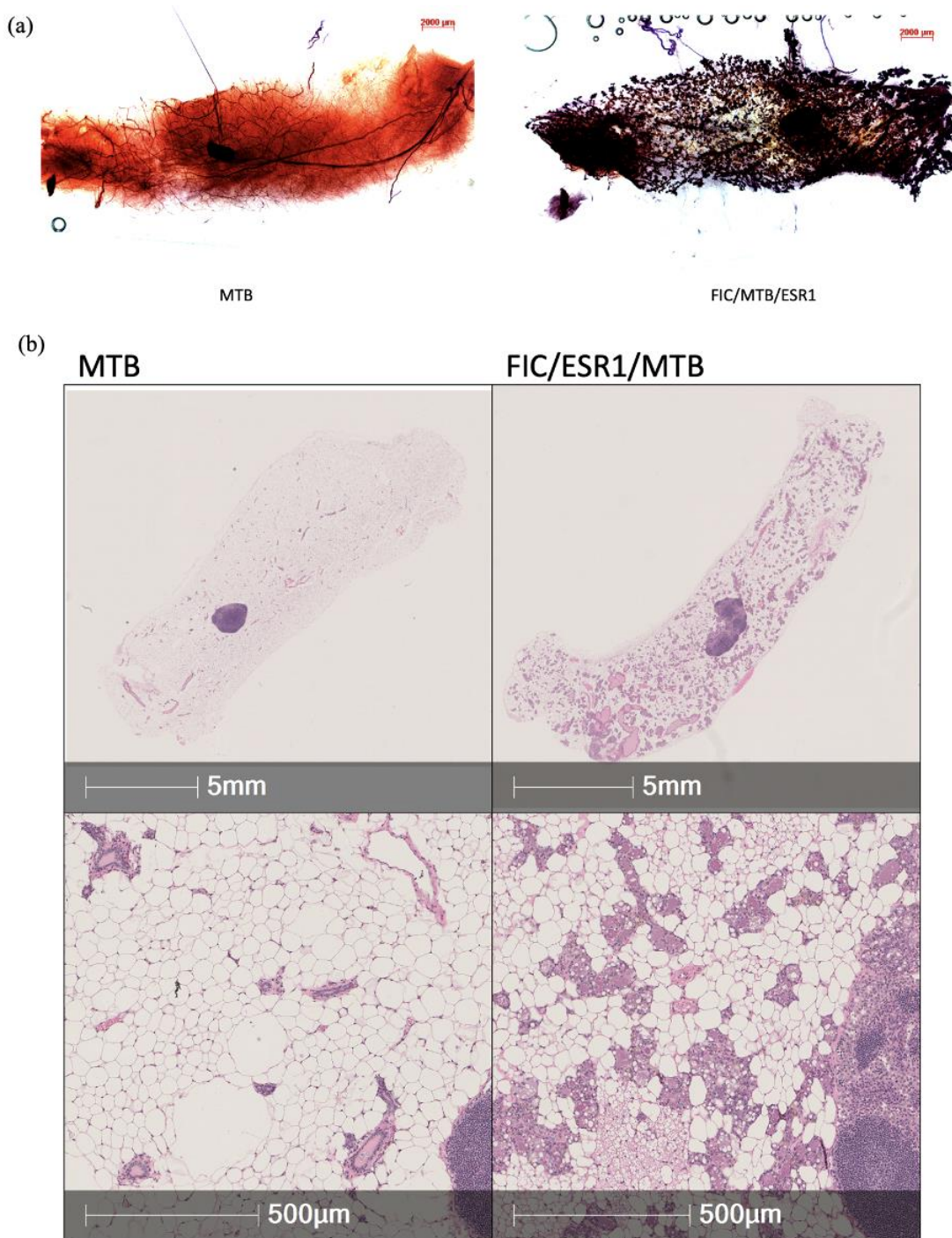


Figure 29: 20-week induced FIC/MTB/ESR1 mouse mammary gland showed dramatic hyperplasia

(a): Representative hematoxylin-stained wholemounts of MTB and FIC/MTB/ESR1 mammary glands, scale bar 2000µm; (b): Representative H&E staining of MTB and FIC/MTB/ESR1 mammary gland sections, scale bar 5mm (upper) and 500µm (below). Well-differentiated hyperplasia can be observed in the mammary glands of FIC/MTB/ESR1.

Chapter 3: Discussion and Concluding Statements

3.1. Summary

We have discussed two transcription factors, Stat3 and FOXA1, and their regulatory roles in breast cancer initiation and progression.

Previous studies have suggested the roles of Stat3 in promoting ErbB2 positive breast cancer metastasis as well as tumor cell migration and invasion (Jones, 2018). However, the mechanism remains unclear. Based on our study, Stat3 deficiency results in increased apoptosis in the primary breast tumor, and higher expression of the focal adhesions, including phosphorylated FAK (Y925), vinculin, paxillin, and phosphorylated paxillin (Y118). Taken together, these may be attributable to the decreased metastasis in the Stat3^{flx/flx}/NIC mice. To further study the mediator of this metastatic phenotype, we did the transcriptomic study and bioinformatic analysis on the dissociated WT NIC and Stat3^{flx/flx}/NIC cells. The transcriptomic study suggested very differentially regulated gene profiles. The GSEA analysis demonstrated enrichments in ErbB2 positive metastatic signatures. The IPA analysis showed altered cell spreading, and GO pathway analysis suggested large enrichments in cell adhesions. From the transcriptomic study and bioinformatic analysis, we may infer that the anti-metastatic phenotype in Stat3-deficient NIC cells may be attributable to altered cell spreading and cell adhesions. Moreover, among the genes that are differentially regulated between WT NIC and Stat3^{flx/flx}/NIC cells, Lgals3 appeared to be the most downregulated gene, and it was known for modulating cell-cell and cell-matrix adhesions. Therefore, we studied the expression of Gal-3 in both cell lines and primary breast tumors, and these showed a dramatic decrease of Gal-3 protein level in Stat3^{flx/flx}/NIC compared to WT NIC. We were also interested in whether Gal-3 deficiency in NIC cells recapitulates the features of Stat3-deficient NIC cells. Therefore, we used shRNA to

knockdown Lgals3. The shLgals3_NIC cells exhibited decreased migration and invasion, and they expressed higher levels of focal adhesion proteins phosphorylated-FAK, vinculin, paxillin, and phosphorylated-paxillin, mimicking the features of Stat3^{flx/flx}/NIC cells. Therefore, we may infer that Stat3 regulates Galectin-3, which inhibits apoptosis and decreases the expression of focal adhesions, thereby promoting cell migration and invasion, and eventually ErbB2 positive breast tumor metastasis. However, further studies are still required to validate this conclusion *in vivo*.

To further study the role of Stat3 in ErbB2 positive breast cancer, the Stat3^{flx/flx} strain was crossed to EIC/MTB mouse model. We found that, different from in the NIC mouse model, the Stat3 deficiency in the EIC/MTB results in delayed tumor onset, and a decreased tumor burden. Also, there is a trend of decreased proliferation of Stat3^{flx/flx}/EIC/MTB breast tumors compared to EIC/MTB tumors. However, Stat3 deficiency in both NIC and EIC/MTB mouse models leads to decreased lung metastasis, from the perspectives of both incidence and size of the metastasis. To investigate the underlying mechanism, we also conducted the transcriptomic study and bioinformatic analysis, which suggested that the antigen processing and presentation was upregulated. To verify the regulatory role of Stat3 on Gal-3, we performed immunohistofluorescence staining of the Gal-3 on the EIC/MTB and Stat3^{flx/flx}/EIC/MTB breast tumors, and the Gal-3 protein level was significantly downregulated in the Stat3^{flx/flx}/EIC/MTB breast tumors. Interestingly, in the Stat3^{flx/flx}/EIC/MTB breast tumors, the Gal-3 protein level was upregulated in the stroma.

Another transcription factor that we investigated is FOXA1, an ER-associated protein (Seachrist et al., 2021). To create a novel ER-Positive breast cancer mouse model, and to study the roles of FOXA1 in tumorigenesis, our lab has generated a novel doxycycline-inducible

mouse model FIC (FOXA1-IRES-Cre). By crossing FIC to the MTB (MMTV-rtTA) strain and administering doxycycline, the mice conditionally express FOXA1 and Cre in the mammary epithelial cells. We compared two founder lines FIC2 and FIC3, and determined that FIC2 has a higher expression level of both FOXA1 and Cre. We continued the further experiments with FIC2. To study the roles of FOXA1 overexpression *in vitro*, we derived epithelial cells from FIC/MTB mammary gland, grew into organoids, and induced with doxycycline. In the doxycycline-induced group, the organoids had developed a filled sphere structure nine days post-induction, which mimics the human mammary gland hyperplasia. In contrast, in the control group, the organoids developed a hollow sphere structure, which mimics the normal lumen of the mammary ducts. We also observed larger diameters of organoids with doxycycline induction, indicating a role of FOXA1 in promoting proliferation. In addition, a lower expression of E-cadherin was observed in the doxycycline-induced group 15 days post-induction, which may indicate an EMT phenotype. This *in vitro* study demonstrated that FOXA1 played a role in promoting proliferation, and overexpression of FOXA1 in mammary epithelial cells has the potential to develop hyperplasia in mammary glands.

To study the role of FOXA1 *in vivo*, we induced the FIC/MTB and MTB mice with doxycycline for 4 weeks. One out of four FIC/MTB mice developed an early stage of hyperplasia, and the ducts seemed to be infiltrated by many immune cells. The other FIC/MTB mice and all the MTB mice appeared normal. We further induced the FIC/MTB and MTB mice for 12 weeks, however, no significant difference was observed in the wholemount or H&E staining of the mammary gland sections between FIC/MTB and MTB mice. Until now, the FIC/MTB mice have been induced for 170 days, and no tumor growth has been observed.

To speed up the oncogenesis process, we crossed FIC/MTB mouse model with the ESR1^{Y541S} (ESR1) mouse model, and induced the FIC/MTB/ESR1 and MTB mice with doxycycline. The excision PCR demonstrated the proper functioning of Cre recombinase in removing the WT exon 9 of ESR1 gene and activating mutated exon 9 with Y541S mutation. After 20-week induction, the mammary glands were harvested for wholemount, H&E staining of the sections. We observed a dramatically increased number of ducts with well-differentiated hyperplasia in the FIC/MTB/ESR1 mouse mammary glands. Also, we noticed that the lymph node was enlarged and appeared an irregular shape, which might be related to malignant transformation. These suggest that the FIC/MTB/ESR1 mouse model has the potential to develop malignant tumors.

3.2. Discussion

Stat3-deficient NIC mice develop dramatically less metastasis than WT NIC mice, and the dissociated Stat3-deficient NIC tumor cells have significantly reduced migration and invasion (Jones, 2018). Also, we have shown that Stat3-deficient NIC breast tumor has significantly higher apoptosis, and Stat3-deficient NIC tumor cells form higher levels of focal adhesions which makes it hard for tumor cells to disseminate. In addition, transcriptomic analysis has revealed that Lgals3 is the most downregulated gene upon the Stat3 deficiency, and we have validated this downregulation in both in cell lines and primary breast tumor. We also used shRNA to knockdown Lgals3 in the NIC cell lines, which appeared to have lower migration and invasion, and exhibited higher expression of focal adhesions. The knockdown of Gal-3 recapitulates the phenotypes of Stat3-knockout NIC cells. Given the known antiapoptotic role of Gal-3 (Harazono et al., 2014), we propose that in the ErbB2-positive breast cancer cells, Stat3

targets and activates Gal-3, which decreases apoptosis and lowers focal adhesion expressions, thereby reducing migration and invasion, and eventually decreasing metastasis (Figure 30).

However, future studies are still required to further validate this mechanism.

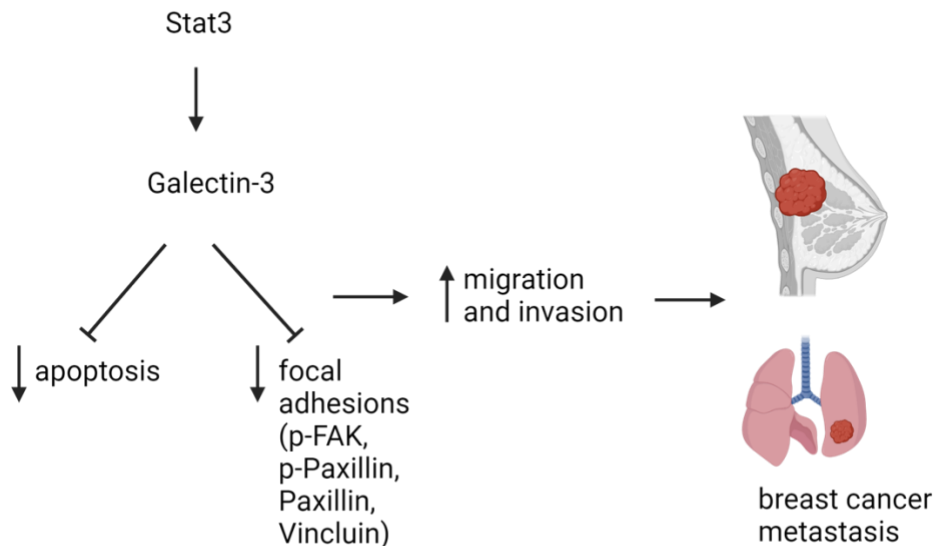


Figure 30: Proposed schematic mechanism of Stat3 promoting HER2-positive breast cancer metastasis

Based on the findings mentioned above, we propose that Stat3 targets Gal-3, the activation of which decreases apoptosis and inhibits focal adhesion formation, thereby promoting migration and invasion, eventually driving breast cancer metastasis. Figure created with Biorender.com.

The role of Stat3 in promoting metastasis has been implicated in several breast cancer mouse models, such as MTB/MIC, a luminal B-like breast cancer mouse model, and here we showed that, in NIC and EIC/MTB, two ErbB2-Positive breast cancer mouse models (Jones et al., 2016). However, the mechanism remains unclear. Moreover, Gal-3 is a known target of Stat3, and Stat3-Lgals3 axis has been implicated in various biological functions and behaviors such as macrophage polarization, inflammatory responses, and trastuzumab resistance (Chen et al., 2022; Jeon et al., 2010; Shirakawa et al., 2018). However, the role of Stat3-Lgals3 axis in metastasis of

HER2-Positive breast cancer is yet to be understood. Here we showed that in the NIC and EIC/MTB mouse model, Gal-3 expression is dramatically downregulated with Stat3 deficiency. Regarding the roles of Gal-3 in cancer metastasis, Gal-3 is required for many steps or functions during tumor metastasis, such as cell growth, angiogenesis, immune function, apoptosis and endocytosis. Also, inhibition of Gal-3 is considered a potential therapeutic in various cancers such as lung cancer and liver cancer (Funasaka et al., 2014; Mengjia Song et al., 2020; Vuong et al., 2019). Moreover, extensive studies suggest that Gal-3 plays an important role in modulating cell-cell and cell-matrix adhesions (Sedlář et al., 2021). Given that bioinformatic analysis revealed that cell adhesions are significantly altered in Stat3^{flx/flx}/NIC tumor cells compared to WT NIC tumor cells, we think that Stat3 may decrease the expression of focal adhesions through regulation of Gal-3.

Focal adhesion protein expression (p-FAK, Vinculin, Paxillin, p-Paxillin) are upregulated in the Stat3-deficient NIC tumor cells, and Lgals3 is the most downregulated gene in the Stat3-deficient NIC cells. Therefore, we were interested in the relation between Gal-3 and focal adhesion protein expressions. According to previous studies, the regulatory roles of Gal-3 on phosphorylated-FAK, vinculin, paxillin, and phosphorylated-paxillin are unclear. Although some studies suggest that Gal-3 activates and stabilizes FAK, other studies demonstrated that FAK phosphorylation is increased with Gal-3 deficiency (Melo et al., 2011; Meng et al., 2015; Tao et al., 2020; Yang et al., 2020). This difference in the roles of Gal-3 in modulating FAK activation may be attributable to the various systems or diseases that have been investigated. In our study, Gal-3 knockdown increases the expression of phosphorylated-FAK, which is consistent with some studies (Melo et al., 2011; Tao et al., 2020). For example, in a study of Alzheimer's disease, the hippocampus of Gal-3-knockout mice had higher expression of phosphorylated-FAK

and phosphorylation of its downstream target CREB, compared to WT mice (Tao et al., 2020). Another study on sarcoma suggests that Gal-3 decreases cell adhesion and promotes cell migration, as extracellular Gal-3 recruits SHP-2 phosphatase to focal adhesion plaques, followed by a decrease in the p-FAK and p-Paxillin level in the lamellipodia of migrating cells (Melo et al., 2011). This study also demonstrates that this promigratory activity of Gal-3 is related to PI3K pathway and AKT phosphorylation (Melo et al., 2011). The FAK-Src complex drives the phosphorylation of paxillin and p130 Crk-associated substrate, which recruit other molecules to regulate cell adhesions and actin cytoskeleton (Webb et al., 2004). Paxillin is regulated by FAK, and similar to FAK, the regulatory roles of Gal-3 on paxillin are controversial (López-Colomé et al., 2017). Although some studies showed that Gal-3 inhibition was related to decreased paxillin expression, there is a study that demonstrated that extracellular Gal-3 led to decreased paxillin activity (Melo et al., 2011; Tian et al., 2021). In our study, we showed that both paxillin and phosphorylated-paxillin expression level is increased with Gal-3 knockdown. Regarding vinculin, few studies have been done on the relation between Gal-3 and vinculin, although a study suggests that vinculin expression is not altered with Gal-3 knockdown in the non-small cell lung cancer cell lines (Kataoka et al., 2019). Our study contributes to the knowledge that upon Gal-3 knockdown, vinculin is upregulated in the NIC cell line, a mouse ErbB2-positive cancer cell line. The elevated expression of focal adhesions including phosphorylated-FAK, vinculin, paxillin, and phosphorylated-paxillin in Stat3-deficient NIC breast tumor cells may play an important role in preventing metastasis by holding the tumor cells at the original sites. For example, extensive studies have shown that cells lacking vinculin are highly metastatic and motile (Raz & Geiger, 1982; Rüdiger, 1998). However, many studies suggest that elevated FAK and Paxillin activity are associated with increased migration and metastasis, which is opposite

from our findings (Lu et al., 2023; Mousson et al., 2021). From our understanding, focal adhesions such as FAK and Paxillin can play a role as a double-edged sword. For one thing, although the mechanism is poorly understood, focal adhesions may hold the cells to their original places and prevent their migration. For another, focal adhesions are essential for the movement of cells because they are the “foots” of cell migration (Mitra et al., 2005). To understand whether focal adhesions play a predominant role in promoting or preventing migration and metastasis in the specific context, another factor is of great importance, the assembly and disassembly rate of the focal adhesions (Yue et al., 2016). This is because efficient and coordinated assembly and disassembly of focal adhesions are essential for the directional movement of cells, whereas a greater assembly rate than disassembly rate may anchor the cells and prevent their movement (Yue et al., 2016). Indeed, the previous studies from the Muller lab have shown that Stat3-deficient NIC cells have a significantly greater assembly than the disassembly rate of focal adhesion (Jones, 2018). Further studies are still required to identify if Gal-3 knockdown NIC cells exhibit the same feature as Stat3-deficient NIC cells.

Interestingly, in the Stat3^{flx/flx}/EIC/MTB mice, there is a significantly delayed tumor onset compared to the EIC/MTB counterparts, however, there is no difference in tumor onset between Stat3^{flx/flx}/NIC and NIC mice. This might be caused by the immune responses in the Stat3^{flx/flx}/EIC/MTB mice since EIC/MTB mice employ human ErbB2 as the oncogene, which may be more immunogenic (Attalla et al., 2023). This is further supported by the transcriptomic study and bioinformatic analysis on the Stat3^{flx/flx}/EIC/MTB mouse breast tumors, which suggested a drastic alteration in the antigen processing and presentation compared to EIC/MTB counterparts. Also, we observed an elevated level of Gal-3 expression in the stroma of the Stat3^{flx/flx}/EIC/MTB breast tumors, which may be also related to immune responses. Studies

suggest that Gal-3 plays a role in recruiting innate immune cells to the site of inflammation, and it may regulate macrophage adhesion, chemotaxis, and apoptosis (Di Gregoli et al., 2020; Díaz-Alvarez & Ortega, 2017).

The 20-week induced FIC/MTB/ESR1 mice developed well-differentiated hyperplasia. The well-differentiated tumors in breast cancer, usually grade 1, tend to grow slowly with a better prognosis (Rakha et al., 2010). Also, the well-differentiated tumors are more commonly seen in luminal A breast cancers which are ER-Positive (Chikarmane et al., 2015). This well-differentiated hyperplasia phenotype corresponds to the underlying mechanism of this FIC/MTB/ESR1 mouse model, which is predominantly driven by ER activation, as FOXA1 plays an important role in facilitating ER functions, and ESR1^{Y541S} mutation leads to constitutive activation of ER (Hurtado et al., 2011; Simond et al., 2020). Given the significant hyperplasia in this mouse model after 20-week induction, the FIC/MTB/ESR1 mice have the potential to develop ER-Positive breast tumor, however, the latency may be long. In contrast, FIC/MTB mice do not develop observable hyperplasia after 20-week induction, which indicates either a synergistic role of FOXA1 overexpression and ESR1^{Y541S} mutation, or a predominant role of ESR1^{Y541S} mutation in driving this hyperplasia. To understand whether it is the synergistic role of FOXA1 overexpression and ESR1^{Y541S} mutation or the predominant role of ESR1^{Y541S} mutation, inducible Cre strain (TetO-Cre) may be crossed to ESR1 mouse model, and we can compare the phenotypes of FIC/MTB/ESR1 and TetO-Cre/ESR1 at the specific time points post-induction.

3.3. Future Directions

We have demonstrated that Gal-3 knockdown results in a decreased migration and invasion. To study the effects of Gal-3 inhibition on metastasis *in vivo* and further validate the mechanism of Stat3 promoting ErbB2-positive breast cancer that we proposed, we will perform tail vein injection and mammary fat pad injection of shLgals3_NIC cells and study the lung metastasis. If there is eventually breast tumor or lung metastasis, the breast tumor and lung sections will be subjected for immunohistochemistry staining for apoptosis and proliferation analysis. Also, we will administrate the neutralizing antibody of Gal-3 in mice bearing ErbB2 positive breast tumors and study its role in tumor growth and metastasis. If both genetic knockdown and pharmacological inhibition of Galectin-3 lead to reduced metastasis, Gal-3 is a potential therapeutic target for HER2-positive breast cancer patients.

To study the immune responses in the Stat3^{flx/flx}/EIC/MTB breast tumors, we will perform immunohistofluorescence on the immune profiles, such as CD3, CD4, CD8, F4/80, p-Stat1, CD206. By studying the immune responses, we may be able to explain the delayed tumor onset and reduced metastasis in the Stat3^{flx/flx}/EIC/MTB mice.

For the FIC/MTB and FIC/MTB/ESR1 mouse model, we will continue with the doxycycline induction for tumor kinetics, such as Kaplan-Meier survival curve and tumor growth curve. We will perform transcriptomic study on the tumors and explore the potential mechanism underlying tumor growth.

Chapter 4. Materials and Methods

4.1. Animal Work

4.1.1. Animal maintenance

All the mice were housed in the animal facility of the Goodman Cancer Research Center and all experiments were done under the animal care guidelines at the Animal Resource Center of McGill. The mouse strains utilized in sections in sections 2.1 and 2.2.: the MTB (MMTV-rtTA) (Gunther et al., 2002), and ESR1 (ESR1^{Y541S}) (Simond et al., 2020), NIC (MMTV-NIC) (Ursini-Siegel et al., 2008), conditional Stat3 (Stat3^{flx}) (Jones, 2018), EIC (TetO-EIC) (Attalla et al., 2023) strains have all been well characterized and were maintained on the FVB background. The TetO-FIC strain was generated by the Muller lab (Lusson, 2023). The experimental doxycycline-inducible mice in sections 2.2. (MTB/TetO-FIC, MTB/TetO-FIC/ESR1) were induced with water containing doxycycline (200mg/mL, Wisent) between 8-12 weeks of age and maintained on doxycycline until sacrifice.

4.1.2. Tumor monitoring

Tumor onset and growth in the transgenic mice was assessed once a week before the tumor onset, and twice a week after tumorigenesis by physical palpation or caliper measurements, respectively. Animals were sacrificed at determined time point as stated, or at an ethical maximum tumor burden, defined as a single tumor of 2.5cm³ or multiple tumor summed to a total of 6.0cm³. Tumor volume was calculated using the formula $V = (4/3)\pi (L/2)(W/2)^2$, in which L and W represent the length and width by caliper measurements.

4.1.3. Necropsy and tissue collection

The tumors, mammary glands, and lungs were collected following euthanasia. Mammary glands, tumors, and lungs were fixed in 10% neutral buffered formalin for 48 hours and paraffin-

embedded. Fixed mammary gland, tumors, or lungs were sectioned into 4uM thickness and stained with Hematoxylin and Eosin (H&E) or left unstained for IHC or IHF. Embedding, sectioning, H&E staining were performed by the Goodman Cancer Research Center Histology Core. Also, mammary glands are used for wholemount, which will be discussed in 4.1.4. The rest tissues were flash frozen and stored with liquid nitrogen.

4.1.4. Wholemount of mammary glands

At certain time points, the mice were sacrificed, and the inguinal mammary glands were harvested. The whole mammary glands were mounted on glass slides and incubated in acetone overnight. The next day, the mammary glands were stained with Harris Modified Hematoxylin (Fischer) overnight, followed by several destaining washes with 70% EtOH with 1% HCl until no color change in the destaining solution. The mammary glands were dehydrated with EtOH and mounted using ClearMount Mounting Media (American MasterTech). Slides were imaged using AxioZoom 16 microscope equipped with digital camera (Carl Zeiss, Inc).

4.2. DNA Analysis

4.2.1. DNA extraction and genotyping

DNA was extracted from either pieces of tail or pieces of ear by incubating in 500uL Tail Buffer (100nM NaCl, 10mM Tris, 10mM EDTA, 0.5% SDS) with 10uL proteinase K at 55°C overnight or longer. Then, 170uL of 5M NaCl was added to the digested tail or ear pieces, and the solution was centrifuged for 10 mins at 13000 revolutions per minute (RPM). The supernatant was transferred to a new tube and 100% EtOH was added to the top of the 1.5mL Eppendorf tube. The solution was mixed and centrifuged for 15 mins at 13000 RPM at 4°C. The supernatant was discarded and the DNA pellet was resuspended in 100uL TE buffer (10mM Tris,

0.5mM EDTA, pH7.8). The extracted DNA is stored in room temperature (short-term) or 4°C (long-term).

Genotyping was performed by PCR to identify experimental mice or requisite breeders through the presence or absence of various transgenes. After DNA extraction, 2uL of DNA was added to 24uL PCR mix containing 10x EasyTaq buffer (Civic Bioscience AP111), 5mM dNTPs, 10uM primers, and 0.5units Taq DNA polymerase. And the mix was run through PCR programs, followed by being run on 2% agarose gel with EtBr and imaged by UV light.

Table 1: Genotyping PCR primer sequences, programs, and band size

Transgene	Primer sequence (5' to 3')	PCR program	Band size
FOXA1	F: ATGAGAGCAACGACTGGAACA R: TCATGGAGTTCATAGAGCCCA	1. 94°C – 120 s 2. 94°C – 30s 3. 58°C – 45s 4. 72°C – 60s Repeat 2-4 29x 5. 72°C – 120s 6. 4°C – pause	1 band, 100bp
Cre	F: GCTTCTGTCCGTTTGCCG R: ACTGTGTCCAGACCAGGC	1. 94°C – 60 s 2. 94°C – 30s	1 band, 600bp
MTB	F: ACCGTACTCGTCAATTCCAAGGG R: TGCCGCCATTATTACGACAAGC	3. 56°C – 30s 4. 72°C – 60s	1 band, 500bp
ESR1	F: GCCTTTGCAGTTGCTCATCC R: TTGTAGACATGCTCCATGCC	Repeat 2-4 34x 5. 72°C – 5 min 6. 4°C – pause	WT: 1 band, 126bp; HET: 2 bands, 126bp & 160bp; HOMO: 1 band, 160bp

4.2.2. DNA extraction and excision PCR

Mammary glands were harvested and the DNA was extracted with phenol-chloroform. 500uL of phenol-chloroform was added to Eppendorf tube and centrifuge at room temperature at 13000 RPM for 5 minutes. Then, the supernatant aqueous phase was transferred to a new tube and 500uL of chloroform was added, followed by centrifuging at 13000 RPM for 5 minutes. 100% EtOH was added to the samples and centrifuged at 4°C for 10 minutes. The supernatant

was aspirated and the pellet was submerged with 70% EtOH and centrifuged at 4°C for 10 minutes at 13000 RPM. After that, the supernatant was aspirated and the tubes were allowed to air dry. Once dry, 200uL of TE buffer was added to suspend the pellet.

After DNA extraction, 2uL of DNA was added to 24uL PCR mix containing 10x EasyTaq buffer (Trans), 5mM dNTPs, 10uM primers, and 0.5units Taq DNA polymerase. And the mix was run through PCR programs, followed by being run on 2% agarose gel with EtBr and imaged by UV light.

Table 2: Excision PCR primer sequences, programs, and band size

Transgene	Primer sequence (5' to 3')	PCR program	Band size
Excision ER	F: TGTCTAGGCTTCAGAGAGCC R: ATCTCCAGGAGCAGGTCGG	1. 95°C – 2 min 2. 95°C – 30s 3. 59°C – 25s 4. 72°C – 70s Repeat 2-4 30x 5. 72°C – 2 min 6. 4°C – pause	1 band, 638bp

4.3. RNA Analysis

4.3.1. RNA extraction

RNA was extracted from the flash frozen mammary gland or tumor tissues with the RNA extraction kit (Favorgen) according to the manufacturer's instructions. NanoDrop Spectrophotometer ND-1000 has been used for RNA concentration measurement and quality control.

4.3.2. Quantitative Reverse Transcriptase PCR (qRT-PCR)

Transgen Biotech kit (AT341) was used to generate cDNA from purified RNA samples. Roche LC480 SYBR Green RT-PCR kit (Roche) was used for qRT-PCR. The samples were loaded in triplicates and run with a LightCycler (Roche). The resulting crossing point values

were normalized to beta-actin to generate the relative transcript level using formula: $2^{-(\text{average } \beta\text{-Actin crossing point} - \text{average target X crossing point})}$. The primers are listed in table 4-3.

Table 3: Primers used in qRT-PCR

Gene	Primer sequence	Tm
FOXA1	F: ATGAGAGCAACGACTGGAACA R: TCATGGAGTTCATAGAGCCCA	60°C
Cre	F: CGGGCTGCCACGACCAAGTGACAG R: GTTATAAGCAATCCCCAGAAATGCCAG	60°C
Beta-actin	F: TCCATCATGAAGTGTGACGT R: GAGCAATGATCTTCAT	60°C

4.4. Cell Culture

4.4.1. Cell lines and maintenance

WT NIC and Stat3^{flx/flx}/NIC cell lines were generated in the Muller lab. All Cells were cultured in DMEM media (Wisent) supplemented with 10% fetal bovine serum (FBS, Wisent), 5ul/mL human insulin, 1ug/mL hydrocortisone, 5ng/mL epidermal growth factor (EGF), 35ug/mL BPE, 50ug/mL gentamycin, 1% penicillin-streptomycin and 1% amphotericin. Cells were incubated in at 37°C in 5% CO₂ incubators. Fresh media were given to the cells every three days after PBS wash. When confluent, cells were incubated with trypsin (Wisent) (2mL for 10cm plates, and 1mL for 6cm plates) at 37°C for 5 minutes to allow cell detachment. The trypsin reaction was stopped with 4mL of 5% FBS DMEM. Then, cells were collected and centrifuged at 800RPM for 3 minutes, followed by aspiration of supernatant and resuspension in fresh media. Eventually, 1/6 of the cells were seeded on the new plate.

4.4.2. 3D mammary gland-derived organoids

Mammary gland pairs 2,3, and 4 were harvested from mice following necropsy, followed by fine chopping with scissors. The chopped tissues were added to digestion media (DMEM/F12 with 1% penicillin-streptomycin and 1% amphotericin, and incubated with rotation at 37°C for 1 to 2 hours. After that, epithelial cells were pelleted by centrifugation at 1000RPM for 5 minutes, and washed 5 times with PBS with 5% FBS. The pellets were treated with Trypsin for 13 to 20 minutes to ensure the breaking of clumps into single cells. Then the trypsin was neutralized with calf serum and the supernatant was passed through a 45uM strainer. After centrifuging, the single cells were re-suspended with EpiCult-B Mouse Medium Kit (STEMCELL Technologies) and seeded on 20uL Geltrex (Gibco).

4.4.3. *In vitro* migration and invasion assay

Boyden chambers (8um pore, BD Falcon) and 24-well plate (BD Falcon) were used in migration and invasion assay. The lower chamber was given 1 mL of DMEM media (Wisent) with 10% FBS. In the invasion assay, the upper chamber was coated with 5% Matrigel (VWR) diluted in DMEM, and incubated for 30 minutes in the 37°C incubator. The cells were trypsinized, counted, and resuspended to a concentration of 120,000 cells/500uL in DMEM without FBS. 120,000 cells in 500uL DMEM were plated in the upper chamber and incubated for 16 hours in the 37°C incubator with 5% CO₂. In the migration and invasion assay with drug treatment, the drug or DMSO was added in the upper chamber and mixed well.

After incubation, the Boyden chambers were fixed with 10% neutral-buffered formalin for 20 minutes, followed by 3 washes with water and stained with 0.1% Crystal Violet solution (Sigma) for 20 minutes. The Boyden chambers were washed 3 times in the 24-well plate, and the cells in the upper chamber were manually removed with Q-tips, leaving only the cells that has

migrated to the underside of the chambers. The chambers were dried overnight, and imaged using AxioZoom 16 microscope equipped with digital camera (Carl Zeiss, Inc). Experiments were performed in duplicates.

4.4.4. shRNA knockdown stable cell lines

Three shRNA that has been used for Lgals3 knockdown, including TRCN0000054863, TRCN0000054864, and TRCN0000054865, and the non-mammalian target luciferase (shControl) in a pLKO.1 vector, were obtained from McGill platform for cellular perturbation (Core facility at McGill University). Virus were packaged with 0.5ug pMD2.G, 4.5ug psPAX2, and 5ug Lenti-vector. Virus media was collected after virus proliferation for 48 hours in the 293FT cell line in the DMEM media with 30% FBS. NIC cell lines were transfected by growing in the virus-containing media, and were selected with puromycin.

4.4.5. *In vitro* proliferation assay

5000 cells were plated on the 96-well plate in triplicates in regular media, and allowed to grow for 24 hours. After that, the regular media was replaced by fresh media with DMSO or drug, and the plate was put in the Incucyte machine. Incucyte machine took pictures of each well every 6 hours and calculated the cell confluency for a total of 72 hours.

4.5. Protein Analysis

4.5.1. Protein extraction and immunoblotting

Cells were washed with cold PBS, followed by RIPA buffer (10 mM Tris pH 8.0, 1 mM EDTA, 0.5 mM EGTA, 1% Triton X-100, 0.1% sodium deoxycholate, 0.1% SDS, 140 mM NaCl, freshly added 1ug/mL aprotinin, 1ug/mL leupeptin, and 1mM sodium orthovanadate), incubation for 10 minutes. The cells were then scraped and centrifuged at 13000 RPM at 4°C for 10 minutes. The

supernatant was collected. As for mammary glands, frozen tissues were crushed to powder in liquid nitrogen using a mortar and pestle. They were then lysed for 30 minutes on a rotator in the 4°C fridge using the same RIPA buffer. Lysates were centrifuged at 13000RPM for 10 minutes at 4°C. The supernatant was collected.

Bradford assay (BioRad) was used to quantify the protein concentration of the cell and mammary gland lysates. Protein lysates were normalized to equal concentration (2ug/uL for cells and 4ug/uL for mammary glands) using additional RIPA buffer and 6X SDS-PAGE loading buffer (375 mM Tris pH 6.8, 10% SDS, 60% glycerol, 0.6 mM DTT, 0.06% bromophenol blue). Lysates were boiled at 95°C for 10 minutes and stored at -20°C for future use. Lysates were run on polyacrylamide gels of various concentrations (6-20%), and then transferred to PDVF membranes. After blocking in Licor blocking buffer for one hour, membranes were incubated overnight at 4°C in primary antibody solutions. The next day, membranes were washed with TBST (137 mM NaCl, 2.7 mM KCl, 19 mM Tris base, 0.1% Tween20) for 3 times and 5 minutes for each wash. The membranes were then incubated with fluorescently-labelled secondary antibodies for 1 hour at room temperature, followed by 3X 5 minutes TBST washes, and then scanned. Results were analyzed using ImageStudioLite Software.

4.5.2. Fluorescent immunohistochemistry

Paraffin-embedded tissue sections were deparaffinized and dehydrated with Xylene and ethanol incubation. Antigen retrieval was then performed in 10mM sodium Citrate buffer (pH 6, Vector Lab, Cat# H-3300) using a pressure cooker for 10 minutes. After cooling down with running water for 10 minutes, the slides were incubated with 3% H₂O₂, and blocked with power blocking buffer (Biogenex, Cat# HK083-50K) for 5 minutes. Slides were then incubated with primary antibody diluted in 2% BSA-TBST for 30 minutes at room temperature, followed by

three quick washes with TBST. Then, slides were incubated with Immpress HRP Polymer conjugated secondary antibody (Vector Labs) for 30 minutes at room temperature, followed by another three quick washes with TBST. After the washes, the slides were incubated in Opal working solution (AKOYA Biosciences) for 10 minutes at room temperature and then placed in antigen retrieval buffer and subjected to pressure cooker for 10 minutes. The protocol was repeated for other primary antibodies (maximum 4 antibodies). After the last round of primary antibody, polymer and Opal incubation, the slides were incubated with DAPI (4', 6-diamidino-2-phenylindole) (0.5ng/mL in water) for 10 minutes at room temperature, washed with water, and mounted with Immu-Mount mounting media (ThermoFisher Scientific). AxioScan was used to scan the slides and staining was quantified with HALO (Indica Lab).

4.5.3. Immunofluorescence

Cells or organoids were grown on glass coverslips in 24-well NUNC plates. They were fixed with 2% PFA solutions for 20 minutes, washed with PBS and permeabilized with 0,2% Triton X-100 in PBS. Cells were then blocked with 2% BSA in IF buffer (PBS, 0.2% Triton X-100, 0.05% Tween-20) for 30 minutes in room temperature. Following blocking, the cells or organoids were incubated in diluted primary antibody in the blocking solution for 45 minutes and washed with TBST for 3X 5 minutes. Then, the cells or organoids were incubated in secondary antibodies, and washed with TBST for 3X 5 minutes. They were counterstained with DAPI same as above for 10 minutes and mounted with Immu-Mount mounting media (ThermoFisher Scientific). Immunostained samples were imaged using a Zeiss LSM800 confocal microscope and analyzed with ZEN software.

4.5.4. List of antibodies for immunoblotting, immunohistofluorescence, immunofluorescence

Table 4: List of antibodies

Antibody	Company	Catalogue	Application	Figures
Gal-3	Cell Signaling	89572	WB, IHF, IF	5b, 5c, 5d, 6, 9, 15
Beta-actin	Sigma	A5441	WB	3, 5b, 9
Stat3	Cell Signaling	9139S	WB	3, 5b
Phosphorylated-Stat3	Cell Signaling	9145L	IHF	2, 5d, 15
HER2	DAKO	A0485	IHF	15
Phosphorylated-FAK	Cell Signaling	3284	WB	3, 9
Vinculin	EMD Millipore	MAB3574	WB	3, 9
Phosphorylated-paxillin	Cell Signaling	69363	WB	3, 9
Paxillin	EMD Millipore	05-417	WB	3, 9
FOXA1	abcam	Ab170933	IHF	22a, 22b, 24
Cre	Cell Signaling	12830	IHF	24
Ki67	Cell Signaling	12202S	IHF	13, 24
Cleaved caspase 3	Cell Signaling	9661	IHF	2, 13
ErbB2	Cell Signaling	2541	WB	5b
E-Cadherin	BD Biosciences	610182	IF	22a, 22b

4.6. Statistics

All statistical and graphical analysis were generated using Prism software (GraphPad, San Diego, CA). Statistical significance was measured using the two-tailed unpaired Student's t-test.

Chapter 5: References

- Agrawal, S., Reemtsma, K., Bagiella, E., Oluwole, S. F., & Braunstein, N. S. (2004). Role of TAP-1 and/or TAP-2 antigen presentation defects in tumorigenicity of mouse melanoma. *Cell Immunol*, 228(2), 130-137. <https://doi.org/10.1016/j.cellimm.2004.04.006>
- Ahmed, H., & AlSadek, D. M. (2015). Galectin-3 as a Potential Target to Prevent Cancer Metastasis. *Clin Med Insights Oncol*, 9, 113-121. <https://doi.org/10.4137/cmo.S29462>
- Albayrak, G., Konac, E., Ugras Dikmen, A., & Bilen, C. Y. (2018). FOXA1 knock-out via CRISPR/Cas9 altered Casp-9, Bax, CCND1, CDK4, and fibronectin expressions in LNCaP cells. *Exp Biol Med (Maywood)*, 243(12), 990-994. <https://doi.org/10.1177/1535370218791797>
- Anzai, E., Hirata, K., Shibazaki, M., Yamada, C., Morii, M., Honda, T., Yamaguchi, N., & Yamaguchi, N. (2017). FOXA1 Induces E-Cadherin Expression at the Protein Level via Suppression of Slug in Epithelial Breast Cancer Cells. *Biol Pharm Bull*, 40(9), 1483-1489. <https://doi.org/10.1248/bpb.b17-00307>
- Aromatase inhibitors versus tamoxifen in premenopausal women with oestrogen receptor-positive early-stage breast cancer treated with ovarian suppression: a patient-level meta-analysis of 7030 women from four randomised trials. (2022). *Lancet Oncol*, 23(3), 382-392. [https://doi.org/10.1016/s1470-2045\(21\)00758-0](https://doi.org/10.1016/s1470-2045(21)00758-0)
- Attalla, S. S., Boucher, J., Proud, H., Taifour, T., Zuo, D., Sanguin-Gendreau, V., Ling, C., Johnson, G., Li, V., Luo, R. B., Kuasne, H., Papavasiliou, V., Walsh, L. A., Barok, M., Joensuu, H., Park, M., Roux, P. P., & Muller, W. J. (2023). HER2Delta16 Engages ENPP1 to Promote an Immune-Cold Microenvironment in Breast Cancer. *Cancer Immunol Res*, 11(9), 1184-1202. <https://doi.org/10.1158/2326-6066.CIR-22-0140>
- Ayoub, N. M., Al-Shami, K. M., & Yaghan, R. J. (2019). Immunotherapy for HER2-positive breast cancer: recent advances and combination therapeutic approaches. *Breast Cancer (Dove Med Press)*, 11, 53-69. <https://doi.org/10.2147/bctt.S175360>
- Azorsa, D. O., Cunliffe, H. E., & Meltzer, P. S. (2001). Association of steroid receptor coactivator AIB1 with estrogen receptor-alpha in breast cancer cells. *Breast Cancer Res Treat*, 70(2), 89-101. <https://doi.org/10.1023/a:1012972808558>
- Banerjee, K., & Resat, H. (2016). Constitutive activation of STAT3 in breast cancer cells: A review. *Int J Cancer*, 138(11), 2570-2578. <https://doi.org/10.1002/ijc.29923>
- Barnes, P. J. (2009). *Asthma and COPD : basic mechanisms and clinical management* (2nd ed.). Elsevier/Academic Press. <http://www.clinicalkey.com/dura/browse/bookChapter/3-s2.0-B9780123740014X00016>
<http://www.clinicalkey.com.au/dura/browse/bookChapter/3-s2.0-B9780123740014X00016>
<http://site.ebrary.com/id/10391569>
<https://search.ebscohost.com/login.aspx?direct=true&scope=site&db=nlebk&db=nlabk&AN=248944>
<https://archive.org/details/asthmacopdbasicm0ed2unse>
<http://www.myilibrary.com?id=261819>
<https://openlibrary.org/books/OL25540868M>
<https://www.sciencedirect.com/science/book/9780123740014>
<http://www.mdconsult.com/public/book/view?title=Barnes:+Asthma+and+COPD>
<http://0-www.sciencedirect.com.portail.scd.univ-tours.fr/science/book/9780123740014>

<https://frodon.univ-paris5.fr/fork?https://www.sciencedirect.com/science/book/9780120790289>
<http://www.bium.univ-paris5.fr/distant?http://www.sciencedirect.com/science/book/9780123740014>
<https://www.sciencedirect.com/portail.scd.univ-tours.fr/science/book/9780123740014>
<https://www.sciencedirect.com.ezproxy.aub.edu.lb/science/book/9780123740014>
<http://perpetual10.elsevier.com.s3.amazonaws.com/UAL01/index.html#978-0-12-374001-4>
<http://www.vlebooks.com/vleweb/product/openreader?id=none&isbn=9780080920603>
<https://www.clinicalkey.com.au/dura/browse/bookChapter/3-s2.0-B9780123740014X00016>
<https://www.clinicalkey.com/dura/browse/bookChapter/3-s2.0-B9780123740014X00016>
<http://VH7QX3XE2P.search.serialssolutions.com/?V=1.0&L=VH7QX3XE2P&S=JCs&C=TC0000355208&T=marc&tab=BOOKS>

- Baselga, J., Norton, L., Albanell, J., Kim, Y.-M., & Mendelsohn, J. (1998). Recombinant humanized anti-HER2 antibody (Herceptin™) enhances the antitumor activity of paclitaxel and doxorubicin against HER2/neu overexpressing human breast cancer xenografts. *Cancer research*, 58(13), 2825-2831.
- Behr, R., Brestelli, J., Fulmer, J. T., Miyawaki, N., Kleyman, T. R., & Kaestner, K. H. (2004). Mild nephrogenic diabetes insipidus caused by Foxa1 deficiency. *J Biol Chem*, 279(40), 41936-41941. <https://doi.org/10.1074/jbc.M403354200>
- Beikman, S., Gordon, P., Ferrari, S., Siegel, M., Zalewski, M. A., & Rosenzweig, M. Q. (2013). Understanding the implications of the breast cancer pathology report: a case study. *Journal of the advanced practitioner in oncology*, 4(3), 176.
- Bernardo, G. M., Lozada, K. L., Miedler, J. D., Harburg, G., Hewitt, S. C., Mosley, J. D., Godwin, A. K., Korach, K. S., Visvader, J. E., Kaestner, K. H., Abdul-Karim, F. W., Montano, M. M., & Keri, R. A. (2010). FOXA1 is an essential determinant of ERalpha expression and mammary ductal morphogenesis. *Development*, 137(12), 2045-2054. <https://doi.org/10.1242/dev.043299>
- Biswas, S. K., Banerjee, S., Baker, G. W., Kuo, C. Y., & Chowdhury, I. (2022). The Mammary Gland: Basic Structure and Molecular Signaling during Development. *Int J Mol Sci*, 23(7). <https://doi.org/10.3390/ijms23073883>
- Blanco-Aparicio, C., Pérez-Gallego, L., Pequeño, B., Leal, J. F., Renner, O., & Carnero, A. (2007). Mice expressing myrAKT1 in the mammary gland develop carcinogen-induced ER-positive mammary tumors that mimic human breast cancer. *Carcinogenesis*, 28(3), 584-594. <https://doi.org/10.1093/carcin/bgl190>
- Boutas, I., Potiris, A., Brenner, W., Lebrecht, A., Hasenburg, A., Kalantaridou, S., & Schmidt, M. (2019). The expression of galectin-3 in breast cancer and its association with chemoresistance: a systematic review of the literature. *Arch Gynecol Obstet*, 300(5), 1113-1120. <https://doi.org/10.1007/s00404-019-05292-9>
- Buerger, H., Simon, R., Schafer, K. L., Diallo, R., Littmann, R., Poremba, C., van Diest, P. J., Dockhorn-Dworniczak, B., & Bocker, W. (2000). Genetic relation of lobular carcinoma in situ, ductal carcinoma in situ, and associated invasive carcinoma of the breast. *Mol Pathol*, 53(3), 118-121. <https://doi.org/10.1136/mp.53.3.118>
- Cano, A., & Hermenegildo, C. (2000). The endometrial effects of SERMs. *Hum Reprod Update*, 6(3), 244-254. <https://doi.org/10.1093/humupd/6.3.244>
- Carroll, J. S., Liu, X. S., Brodsky, A. S., Li, W., Meyer, C. A., Szary, A. J., Eeckhoute, J., Shao, W., Hestermann, E. V., Geistlinger, T. R., Fox, E. A., Silver, P. A., & Brown, M. (2005). Chromosome-wide mapping of estrogen receptor binding reveals long-range regulation

- requiring the forkhead protein FoxA1. *Cell*, 122(1), 33-43.
<https://doi.org/10.1016/j.cell.2005.05.008>
- Chan, S. R., Vermi, W., Luo, J., Lucini, L., Rickert, C., Fowler, A. M., Lonardi, S., Arthur, C., Young, L. J., Levy, D. E., Welch, M. J., Cardiff, R. D., & Schreiber, R. D. (2012). STAT1-deficient mice spontaneously develop estrogen receptor α -positive luminal mammary carcinomas. *Breast Cancer Res*, 14(1), R16. <https://doi.org/10.1186/bcr3100>
- Chen, Y., Xu, J., Pan, W., Xu, X., Ma, X., Chu, Y., Wang, L., Pang, S., Li, Y., Zou, B., Zhou, G., & Gu, J. (2022). Galectin-3 enhances trastuzumab resistance by regulating cancer malignancy and stemness in HER2-positive breast cancer cells. *Thorac Cancer*, 13(13), 1961-1973. <https://doi.org/10.1111/1759-7714.14474>
- Chikarmane, S. A., Tirumani, S. H., Howard, S. A., Jagannathan, J. P., & DiPiro, P. J. (2015). Metastatic patterns of breast cancer subtypes: what radiologists should know in the era of personalized cancer medicine. *Clin Radiol*, 70(1), 1-10.
<https://doi.org/10.1016/j.crad.2014.08.015>
- Costa, R. H., Grayson, D. R., & Darnell, J. E., Jr. (1989). Multiple hepatocyte-enriched nuclear factors function in the regulation of transthyretin and alpha 1-antitrypsin genes. *Mol Cell Biol*, 9(4), 1415-1425. <https://doi.org/10.1128/mcb.9.4.1415-1425.1989>
- Dabydeen, S. A., & Furth, P. A. (2014a). Genetically engineered ER α -positive breast cancer mouse models. *Endocr Relat Cancer*, 21(3), R195-208. <https://doi.org/10.1530/ERC-13-0512>
- Dabydeen, S. A., & Furth, P. A. (2014b). Genetically engineered ER α -positive breast cancer mouse models. *Endocr Relat Cancer*, 21(3), R195-208. <https://doi.org/10.1530/erc-13-0512>
- Das, A. T., Tenenbaum, L., & Berkhout, B. (2016). Tet-On Systems For Doxycycline-inducible Gene Expression. *Curr Gene Ther*, 16(3), 156-167.
<https://doi.org/10.2174/1566523216666160524144041>
- Davies, C., Pan, H., Godwin, J., Gray, R., Arriagada, R., Raina, V., Abraham, M., Medeiros Alencar, V. H., Badran, A., Bonfill, X., Bradbury, J., Clarke, M., Collins, R., Davis, S. R., Delmestri, A., Forbes, J. F., Haddad, P., Hou, M. F., Inbar, M., . . . Peto, R. (2013). Long-term effects of continuing adjuvant tamoxifen to 10 years versus stopping at 5 years after diagnosis of oestrogen receptor-positive breast cancer: ATLAS, a randomised trial. *Lancet*, 381(9869), 805-816. [https://doi.org/10.1016/s0140-6736\(12\)61963-1](https://doi.org/10.1016/s0140-6736(12)61963-1)
- De Potter, C. R., & Quatacker, J. (1993). The p185erbB2 protein is localized on cell organelles involved in cell motility. *Clin Exp Metastasis*, 11(6), 453-461.
<https://doi.org/10.1007/bf00054936>
- Dean, L., & Kane, M. (2012). Trastuzumab Therapy and ERBB2 Genotype. In V. M. Pratt, S. A. Scott, M. Pirmohamed, B. Esquivel, B. L. Kattman, & A. J. Malheiro (Eds.), *Medical Genetics Summaries*. National Center for Biotechnology Information (US).
- Di Gregoli, K., Somerville, M., Bianco, R., Thomas, A. C., Frankow, A., Newby, A. C., George, S. J., Jackson, C. L., & Johnson, J. L. (2020). Galectin-3 Identifies a Subset of Macrophages With a Potential Beneficial Role in Atherosclerosis. *Arterioscler Thromb Vasc Biol*, 40(6), 1491-1509. <https://doi.org/10.1161/atvbaha.120.314252>
- Díaz-Alvarez, L., & Ortega, E. (2017). The Many Roles of Galectin-3, a Multifaceted Molecule, in Innate Immune Responses against Pathogens. *Mediators Inflamm*, 2017, 9247574.
<https://doi.org/10.1155/2017/9247574>

- Dustin, D., Gu, G., & Fuqua, S. A. W. (2019). ESR1 mutations in breast cancer. *Cancer*, *125*(21), 3714-3728. <https://doi.org/10.1002/cncr.32345>
- Dwivedi, S., Purohit, P., Misra, R., Lingeswaran, M., Vishnoi, J. R., Pareek, P., Misra, S., & Sharma, P. (2019). Single Cell Omics of Breast Cancer: An Update on Characterization and Diagnosis. *Indian J Clin Biochem*, *34*(1), 3-18. <https://doi.org/10.1007/s12291-019-0811-0>
- Eeckhoutte, J., Carroll, J. S., Geistlinger, T. R., Torres-Arzayus, M. I., & Brown, M. (2006). A cell-type-specific transcriptional network required for estrogen regulation of cyclin D1 and cell cycle progression in breast cancer. *Genes Dev*, *20*(18), 2513-2526. <https://doi.org/10.1101/gad.1446006>
- Fortuna-Costa, A., Gomes, A. M., Kozlowski, E. O., Stelling, M. P., & Pavão, M. S. (2014). Extracellular galectin-3 in tumor progression and metastasis. *Front Oncol*, *4*, 138. <https://doi.org/10.3389/fonc.2014.00138>
- Frech, M. S., Halama, E. D., Tilli, M. T., Singh, B., Gunther, E. J., Chodosh, L. A., Flaws, J. A., & Furth, P. A. (2005). Deregulated estrogen receptor alpha expression in mammary epithelial cells of transgenic mice results in the development of ductal carcinoma in situ. *Cancer Res*, *65*(3), 681-685.
- Friedrichs, J., Manninen, A., Muller, D. J., & Helenius, J. (2008). Galectin-3 regulates integrin alpha2beta1-mediated adhesion to collagen-I and -IV. *J Biol Chem*, *283*(47), 32264-32272. <https://doi.org/10.1074/jbc.M803634200>
- Fuentes, N., & Silveyra, P. (2019). Estrogen receptor signaling mechanisms. *Adv Protein Chem Struct Biol*, *116*, 135-170. <https://doi.org/10.1016/bs.apcsb.2019.01.001>
- Funasaka, T., Raz, A., & Nangia-Makker, P. (2014). Galectin-3 in angiogenesis and metastasis. *Glycobiology*, *24*(10), 886-891. <https://doi.org/10.1093/glycob/cwu086>
- Gajria, D., & Chandarlapaty, S. (2011). HER2-amplified breast cancer: mechanisms of trastuzumab resistance and novel targeted therapies. *Expert Rev Anticancer Ther*, *11*(2), 263-275. <https://doi.org/10.1586/era.10.226>
- Gancberg, D., Di Leo, A., Cardoso, F., Rouas, G., Pedrocchi, M., Paesmans, M., Verhest, A., Bernard-Marty, C., Piccart, M. J., & Larsimont, D. (2002). Comparison of HER-2 status between primary breast cancer and corresponding distant metastatic sites. *Ann Oncol*, *13*(7), 1036-1043. <https://doi.org/10.1093/annonc/mdf252>
- Gieniec, K. A., & Davis, F. M. (2022). Mammary basal cells: Stars of the show. *Biochim Biophys Acta Mol Cell Res*, *1869*(1), 119159. <https://doi.org/10.1016/j.bbamcr.2021.119159>
- Gil Del Alcazar, C. R., Huh, S. J., Ekram, M. B., Trinh, A., Liu, L. L., Beca, F., Zi, X., Kwak, M., Bergholtz, H., Su, Y., Ding, L., Russnes, H. G., Richardson, A. L., Babski, K., Min Hui Kim, E., McDonnell, C. H., 3rd, Wagner, J., Rowberry, R., Freeman, G. J., . . . Polyak, K. (2017). Immune Escape in Breast Cancer During In Situ to Invasive Carcinoma Transition. *Cancer Discov*, *7*(10), 1098-1115. <https://doi.org/10.1158/2159-8290.CD-17-0222>
- Gnerlich, J. L., Deshpande, A. D., Jeffe, D. B., Seelam, S., Kimbuende, E., & Margenthaler, J. A. (2011). Poorer survival outcomes for male breast cancer compared with female breast cancer may be attributable to in-stage migration. *Ann Surg Oncol*, *18*(7), 1837-1844. <https://doi.org/10.1245/s10434-010-1468-3>

- Guanizo, A. C., Fernando, C. D., Garama, D. J., & Gough, D. J. (2018). STAT3: a multifaceted oncoprotein. *Growth Factors*, 36(1-2), 1-14. <https://doi.org/10.1080/08977194.2018.1473393>
- Gunther, E. J., Belka, G. K., Wertheim, G. B., Wang, J., Hartman, J. L., Boxer, R. B., & Chodosh, L. A. (2002). A novel doxycycline-inducible system for the transgenic analysis of mammary gland biology. *Faseb j*, 16(3), 283-292. <https://doi.org/10.1096/fj.01-0551com>
- Gutierrez, C., & Schiff, R. (2011). HER2: biology, detection, and clinical implications. *Arch Pathol Lab Med*, 135(1), 55-62. <https://doi.org/10.5858/2010-0454-rar.1>
- Guy, C. T., Cardiff, R. D., & Muller, W. J. (1996). Activated neu induces rapid tumor progression. *J Biol Chem*, 271(13), 7673-7678. <https://doi.org/10.1074/jbc.271.13.7673>
- Guy, C. T., Webster, M. A., Schaller, M., Parsons, T. J., Cardiff, R. D., & Muller, W. J. (1992). Expression of the neu protooncogene in the mammary epithelium of transgenic mice induces metastatic disease. *Proc Natl Acad Sci U S A*, 89(22), 10578-10582. <https://doi.org/10.1073/pnas.89.22.10578>
- Hanahan, D., & Weinberg, R. A. (2000). The hallmarks of cancer. *Cell*, 100(1), 57-70. [https://doi.org/10.1016/s0092-8674\(00\)81683-9](https://doi.org/10.1016/s0092-8674(00)81683-9)
- Hara, A., Niwa, M., Noguchi, K., Kanayama, T., Niwa, A., Matsuo, M., Hatano, Y., & Tomita, H. (2020). Galectin-3 as a Next-Generation Biomarker for Detecting Early Stage of Various Diseases. *Biomolecules*, 10(3). <https://doi.org/10.3390/biom10030389>
- Harazono, Y., Kho, D. H., Balan, V., Nakajima, K., Zhang, T., Hogan, V., & Raz, A. (2014). Galectin-3 leads to attenuation of apoptosis through Bax heterodimerization in human thyroid carcinoma cells. *Oncotarget*, 5(20), 9992-10001. <https://doi.org/10.18632/oncotarget.2486>
- Hazan-Halevy, I., Harris, D., Liu, Z., Liu, J., Li, P., Chen, X., Shanker, S., Ferrajoli, A., Keating, M. J., & Estrov, Z. (2010). STAT3 is constitutively phosphorylated on serine 727 residues, binds DNA, and activates transcription in CLL cells. *Blood*, 115(14), 2852-2863. <https://doi.org/10.1182/blood-2009-10-230060>
- Hennighausen, L., Wall, R. J., Tillmann, U., Li, M., & Furth, P. A. (1995). Conditional gene expression in secretory tissues and skin of transgenic mice using the MMTV-LTR and the tetracycline responsive system. *J Cell Biochem*, 59(4), 463-472. <https://doi.org/10.1002/jcb.240590407>
- Hernando, C., Ortega-Morillo, B., Tapia, M., Moragón, S., Martínez, M. T., Eroles, P., Garrido-Cano, I., Adam-Artigues, A., Lluch, A., Bermejo, B., & Cejalvo, J. M. (2021). Oral Selective Estrogen Receptor Degraders (SERDs) as a Novel Breast Cancer Therapy: Present and Future from a Clinical Perspective. *Int J Mol Sci*, 22(15). <https://doi.org/10.3390/ijms22157812>
- Hou, Y., Li, X., Li, Q., Xu, J., Yang, H., Xue, M., Niu, G., Zhuo, S., Mu, K., Wu, G., Li, X., Wang, H., Zhu, J., & Zhuang, T. (2018). STAT1 facilitates oestrogen receptor α transcription and stimulates breast cancer cell proliferation. *J Cell Mol Med*, 22(12), 6077-6086. <https://doi.org/10.1111/jcmm.13882>
- Hurtado, A., Holmes, K. A., Ross-Innes, C. S., Schmidt, D., & Carroll, J. S. (2011). FOXA1 is a key determinant of estrogen receptor function and endocrine response. *Nat Genet*, 43(1), 27-33. <https://doi.org/10.1038/ng.730>

- Iqbal, N., & Iqbal, N. (2014). Human Epidermal Growth Factor Receptor 2 (HER2) in Cancers: Overexpression and Therapeutic Implications. *Mol Biol Int*, 2014, 852748. <https://doi.org/10.1155/2014/852748>
- Janiszewska, M., Primi, M. C., & Izard, T. (2020). Cell adhesion in cancer: Beyond the migration of single cells. *J Biol Chem*, 295(8), 2495-2505. <https://doi.org/10.1074/jbc.REV119.007759>
- Jeon, S. B., Yoon, H. J., Chang, C. Y., Koh, H. S., Jeon, S. H., & Park, E. J. (2010). Galectin-3 exerts cytokine-like regulatory actions through the JAK-STAT pathway. *J Immunol*, 185(11), 7037-7046. <https://doi.org/10.4049/jimmunol.1000154>
- Jin, L., Han, B., Siegel, E., Cui, Y., Giuliano, A., & Cui, X. (2018). Breast cancer lung metastasis: Molecular biology and therapeutic implications. *Cancer Biol Ther*, 19(10), 858-868. <https://doi.org/10.1080/15384047.2018.1456599>
- Jones, L. (2018). *Modeling the role of Stat3 in transgenic mouse models of breast cancer* [McGill University Libraries]. WorldCat.org. [Montreal]. <http://central.bac-lac.gc.ca/redirect?app=damspub&id=21f90c8e-af11-48bb-a0f6-26e5c4448c48>
http://digitool.Library.McGill.CA/R/?func=dbin-jump-full&object_id=154646
<https://escholarship.mcgill.ca/downloads/sf2687618.pdf>
<https://escholarship.mcgill.ca/concern/theses/ns0648258>
- Jones, L. M., Broz, M. L., Ranger, J. J., Ozcelik, J., Ahn, R., Zuo, D., Ursini-Siegel, J., Hallett, M. T., Krummel, M., & Muller, W. J. (2016). STAT3 Establishes an Immunosuppressive Microenvironment during the Early Stages of Breast Carcinogenesis to Promote Tumor Growth and Metastasis. *Cancer Res*, 76(6), 1416-1428. <https://doi.org/10.1158/0008-5472.Can-15-2770>
- Kaestner, K. H., Katz, J., Liu, Y., Drucker, D. J., & Schütz, G. (1999). Inactivation of the winged helix transcription factor HNF3alpha affects glucose homeostasis and islet glucagon gene expression in vivo. *Genes Dev*, 13(4), 495-504. <https://doi.org/10.1101/gad.13.4.495>
- Kataoka, Y., Ohshio, Y., Teramoto, K., Igarashi, T., Asai, T., & Hanaoka, J. (2019). Hypoxia-induced galectin-3 enhances RhoA function to activate the motility of tumor cells in non-small cell lung cancer. *Oncol Rep*, 41(2), 853-862. <https://doi.org/10.3892/or.2018.6915>
- Kim, H., Kim, M., Im, S. K., & Fang, S. (2018). Mouse Cre-LoxP system: general principles to determine tissue-specific roles of target genes. *Lab Anim Res*, 34(4), 147-159. <https://doi.org/10.5625/lar.2018.34.4.147>
- Konduri, S., Singh, M., Bobustuc, G., Rovin, R., & Kassam, A. (2020). Epidemiology of male breast cancer. *Breast*, 54, 8-14. <https://doi.org/10.1016/j.breast.2020.08.010>
- Konecny, G. E., Pegram, M. D., Venkatesan, N., Finn, R., Yang, G., Rahmeh, M., Untch, M., Rusnak, D. W., Spehar, G., & Mullin, R. J. (2006). Activity of the dual kinase inhibitor lapatinib (GW572016) against HER-2-overexpressing and trastuzumab-treated breast cancer cells. *Cancer research*, 66(3), 1630-1639.
- Kramer, N., Walzl, A., Unger, C., Rosner, M., Krupitza, G., Hengstschlager, M., & Dolznig, H. (2013). In vitro cell migration and invasion assays. *Mutat Res*, 752(1), 10-24. <https://doi.org/10.1016/j.mrrev.2012.08.001>
- Kumar, M. J., Ponvijay, K. S., Nandhini, R., Nagarajan, R. S., Jose, J., Srinivas, G., Nagarajan, P., Venkatesan, R., Kumar, K., & Singh, S. (2007). A mouse model for luminal epithelial like ER positive subtype of human breast cancer. *BMC Cancer*, 7, 180. <https://doi.org/10.1186/1471-2407-7-180>

- Kuntz, M. A., & Shapiro, D. J. (1997). Dimerizing the estrogen receptor DNA binding domain enhances binding to estrogen response elements. *J Biol Chem*, 272(44), 27949-27956. <https://doi.org/10.1074/jbc.272.44.27949>
- Laganière, J., Deblois, G., Lefebvre, C., Bataille, A. R., Robert, F., & Giguère, V. (2005). From the Cover: Location analysis of estrogen receptor alpha target promoters reveals that FOXA1 defines a domain of the estrogen response. *Proc Natl Acad Sci U S A*, 102(33), 11651-11656. <https://doi.org/10.1073/pnas.0505575102>
- Lai, E., Prezioso, V. R., Tao, W. F., Chen, W. S., & Darnell, J. E., Jr. (1991). Hepatocyte nuclear factor 3 alpha belongs to a gene family in mammals that is homologous to the Drosophila homeotic gene fork head. *Genes Dev*, 5(3), 416-427. <https://doi.org/10.1101/gad.5.3.416>
- Lawson, A. A., & Rentea, R. M. (2024). Oophorectomy. In *StatPearls*. StatPearls Publishing Copyright © 2024, StatPearls Publishing LLC.
- Lei, C.-X., Zhang, W., Zhou, J.-P., & Liu, Y.-K. (2009). Interactions between galectin-3 and integrin β 3 in regulating endometrial cell proliferation and adhesion. *Human Reproduction*, 24(11), 2879-2889. <https://doi.org/10.1093/humrep/dep250>
- Li, Z. D., Yu, X., Mei, Z., Zeng, T., Chen, L., Xu, X. L., Li, H., Huang, T., & Cai, Y. D. (2022). Identifying luminal and basal mammary cell specific genes and their expression patterns during pregnancy. *PLoS One*, 17(4), e0267211. <https://doi.org/10.1371/journal.pone.0267211>
- Liu, Y., Zhao, Y., Skerry, B., Wang, X., Colin-Cassin, C., Radisky, D. C., Kaestner, K. H., & Li, Z. (2016). Foxa1 is essential for mammary duct formation. *Genesis*, 54(5), 277-285. <https://doi.org/10.1002/dvg.22929>
- López-Colomé, A. M., Lee-Rivera, I., Benavides-Hidalgo, R., & López, E. (2017). Paxillin: a crossroad in pathological cell migration. *Journal of Hematology & Oncology*, 10(1), 50. <https://doi.org/10.1186/s13045-017-0418-y>
- Lu, S., Lu, T., Zhang, J., Gan, L., Wu, X., Han, D., Zhang, K., Xu, C., Liu, S., Qin, W., Yang, F., & Wen, W. (2023). CD248 promotes migration and metastasis of osteosarcoma through ITGB1-mediated FAK-paxillin pathway activation. *BMC Cancer*, 23(1), 290. <https://doi.org/10.1186/s12885-023-10731-7>
- Lumachi, F., Brunello, A., Maruzzo, M., Basso, U., & Basso, S. M. (2013). Treatment of estrogen receptor-positive breast cancer. *Curr Med Chem*, 20(5), 596-604. <https://doi.org/10.2174/092986713804999303>
- Lumachi, F., Santeufemia, D. A., & Basso, S. M. (2015). Current medical treatment of estrogen receptor-positive breast cancer. *World J Biol Chem*, 6(3), 231-239. <https://doi.org/10.4331/wjbc.v6.i3.231>
- Lusson, S. (2023). *Exploring the role of AIB1 and FOXA1 in mammary tumorigenesis using transgenic mouse models* [McGill University Libraries]. WorldCat.org. [Montreal]. <https://escholarship.mcgill.ca/concern/theses/6h440z905>
- Malhotra, G. K., Zhao, X., Band, H., & Band, V. (2010). Histological, molecular and functional subtypes of breast cancers. *Cancer Biol Ther*, 10(10), 955-960. <https://doi.org/10.4161/cbt.10.10.13879>
- Marei, H. E., Cenciarelli, C., & Hasan, A. (2022). Potential of antibody–drug conjugates (ADCs) for cancer therapy. *Cancer Cell International*, 22(1), 255. <https://doi.org/10.1186/s12935-022-02679-8>

- Margadant, C., van den Bout, I., van Boxtel, A. L., Thijssen, V. L., & Sonnenberg, A. (2012). Epigenetic regulation of galectin-3 expression by $\beta 1$ integrins promotes cell adhesion and migration. *J Biol Chem*, 287(53), 44684-44693. <https://doi.org/10.1074/jbc.M112.426445>
- Massague, J., & Obenauf, A. C. (2016). Metastatic colonization by circulating tumour cells. *Nature*, 529(7586), 298-306. <https://doi.org/10.1038/nature17038>
- Melo, F. H., Butera, D., Junqueira Mde, S., Hsu, D. K., da Silva, A. M., Liu, F. T., Santos, M. F., & Chammas, R. (2011). The promigratory activity of the matricellular protein galectin-3 depends on the activation of PI-3 kinase. *PLoS One*, 6(12), e29313. <https://doi.org/10.1371/journal.pone.0029313>
- Meng, F., Joshi, B., & Nabi, I. R. (2015). Galectin-3 Overrides PTRF/Cavin-1 Reduction of PC3 Prostate Cancer Cell Migration. *PLoS One*, 10(5), e0126056. <https://doi.org/10.1371/journal.pone.0126056>
- Metovic, J., Borella, F., D'Alonzo, M., Biglia, N., Mangherini, L., Tampieri, C., Bertero, L., Cassoni, P., & Castellano, I. (2022). FOXA1 in Breast Cancer: A Luminal Marker with Promising Prognostic and Predictive Impact. *Cancers (Basel)*, 14(19). <https://doi.org/10.3390/cancers14194699>
- Miermont, A. M., Cabrera, M. C., Frech, S. M., Nakles, R. E., Diaz-Cruz, E. S., Shiffert, M. T., & Furth, P. A. (2012). Association of Over-Expressed Estrogen Receptor Alpha with Development of Tamoxifen Resistant Hyperplasia and Adenocarcinomas in Genetically Engineered Mice. *Anat Physiol, Suppl 12*. <https://doi.org/10.4172/2161-0940.s12-001>
- Mitchell, T. J., & John, S. (2005). Signal transducer and activator of transcription (STAT) signalling and T-cell lymphomas. *Immunology*, 114(3), 301-312. <https://doi.org/10.1111/j.1365-2567.2005.02091.x>
- Mitra, S. K., Hanson, D. A., & Schlaepfer, D. D. (2005). Focal adhesion kinase: in command and control of cell motility. *Nature Reviews Molecular Cell Biology*, 6(1), 56-68. <https://doi.org/10.1038/nrm1549>
- Miziak, P., Baran, M., Błaszczak, E., Przybyszewska-Podstawka, A., Kałafut, J., Smok-Kalwat, J., Dmoszyńska-Graniczka, M., Kielbus, M., & Stepulak, A. (2023). Estrogen Receptor Signaling in Breast Cancer. *Cancers (Basel)*, 15(19). <https://doi.org/10.3390/cancers15194689>
- Mohibi, S., Mirza, S., Band, H., & Band, V. (2011). Mouse models of estrogen receptor-positive breast cancer. *J Carcinog*, 10, 35. <https://doi.org/10.4103/1477-3163.91116>
- Mortlock, R. D., Georgia, S. K., & Finley, S. D. (2021). Dynamic Regulation of JAK-STAT Signaling Through the Prolactin Receptor Predicted by Computational Modeling. *Cell Mol Bioeng*, 14(1), 15-30. <https://doi.org/10.1007/s12195-020-00647-8>
- Mousson, A., Legrand, M., Steffan, T., Vauchelles, R., Carl, P., Gies, J. P., Lehmann, M., Zuber, G., De Mey, J., Dujardin, D., Sick, E., & Rondé, P. (2021). Inhibiting FAK-Paxillin Interaction Reduces Migration and Invadopodia-Mediated Matrix Degradation in Metastatic Melanoma Cells. *Cancers (Basel)*, 13(8). <https://doi.org/10.3390/cancers13081871>
- Muller, W. J., Sinn, E., Pattengale, P. K., Wallace, R., & Leder, P. (1988). Single-step induction of mammary adenocarcinoma in transgenic mice bearing the activated c-neu oncogene. *Cell*, 54(1), 105-115. [https://doi.org/10.1016/0092-8674\(88\)90184-5](https://doi.org/10.1016/0092-8674(88)90184-5)
- Myatt, S. S., & Lam, E. W. F. (2007). The emerging roles of forkhead box (Fox) proteins in cancer. *Nature Reviews Cancer*, 7(11), 847-859. <https://doi.org/10.1038/nrc2223>

- Myers, D. J., & Walls, A. L. (2024). Atypical Breast Hyperplasia. In *StatPearls*.
<https://www.ncbi.nlm.nih.gov/pubmed/29261937>
- Nagini, S. (2014). Neem Limonoids as Anticancer Agents: Modulation of Cancer Hallmarks and Oncogenic Signaling. *Enzymes*, 36, 131-147. <https://doi.org/10.1016/b978-0-12-802215-3.00007-0>
- Nahta, R., Yuan, L. X., Du, Y., & Esteva, F. J. (2007). Lapatinib induces apoptosis in trastuzumab-resistant breast cancer cells: effects on insulin-like growth factor I signaling. *Molecular cancer therapeutics*, 6(2), 667-674.
- Nakles, R. E., Kallakury, B. V., & Furth, P. A. (2013). The PPAR γ agonist efatutazone increases the spectrum of well-differentiated mammary cancer subtypes initiated by loss of full-length BRCA1 in association with TP53 haploinsufficiency. *Am J Pathol*, 182(6), 1976-1985. <https://doi.org/10.1016/j.ajpath.2013.02.006>
- Nardin, S., Mora, E., Varughese, F. M., D'Avanzo, F., Vachanaram, A. R., Rossi, V., Saggia, C., Rubinelli, S., & Gennari, A. (2020). Breast Cancer Survivorship, Quality of Life, and Late Toxicities. *Front Oncol*, 10, 864. <https://doi.org/10.3389/fonc.2020.00864>
- Neophytou, C. M., Panagi, M., Stylianopoulos, T., & Papageorgis, P. (2021). The Role of Tumor Microenvironment in Cancer Metastasis: Molecular Mechanisms and Therapeutic Opportunities. *Cancers (Basel)*, 13(9). <https://doi.org/10.3390/cancers13092053>
- Nuciforo, P., Radosevic-Robin, N., Ng, T., & Scaltriti, M. (2015). Quantification of HER family receptors in breast cancer. *Breast Cancer Res*, 17, 53. <https://doi.org/10.1186/s13058-015-0561-8>
- Orrantia-Borunda, E., Anchondo-Nunez, P., Acuna-Aguilar, L. E., Gomez-Valles, F. O., & Ramirez-Valdespino, C. A. (2022). Subtypes of Breast Cancer. In H. N. Mayrovitz (Ed.), *Breast Cancer*. <https://doi.org/10.36255/exon-publications-breast-cancer-subtypes>
- Paterni, I., Granchi, C., Katzenellenbogen, J. A., & Minutolo, F. (2014). Estrogen receptors alpha (ER α) and beta (ER β): subtype-selective ligands and clinical potential. *Steroids*, 90, 13-29. <https://doi.org/10.1016/j.steroids.2014.06.012>
- Paul, M. K., & Mukhopadhyay, A. K. (2004). Tyrosine kinase - Role and significance in Cancer. *Int J Med Sci*, 1(2), 101-115. <https://doi.org/10.7150/ijms.1.101>
- Pavithran, H., & Kumavath, R. (2021). Emerging role of pioneer transcription factors in targeted ER α positive breast cancer. *Explor Target Antitumor Ther*, 2(1), 26-35. <https://doi.org/10.37349/etat.2021.00031>
- Peckys, D. B., Hirsch, D., Gaiser, T., & de Jonge, N. (2019). Visualisation of HER2 homodimers in single cells from HER2 overexpressing primary formalin fixed paraffin embedded tumour tissue. *Mol Med*, 25(1), 42. <https://doi.org/10.1186/s10020-019-0108-z>
- Pereira, J. X., Dos Santos, S. N., Pereira, T. C., Cabanel, M., Chammas, R., de Oliveira, F. L., Bernardes, E. S., & El-Cheikh, M. C. (2019). Galectin-3 Regulates the Expression of Tumor Glycosaminoglycans and Increases the Metastatic Potential of Breast Cancer. *J Oncol*, 2019, 9827147. <https://doi.org/10.1155/2019/9827147>
- Pérez-González, A., Bévant, K., & Blanpain, C. (2023). Cancer cell plasticity during tumor progression, metastasis and response to therapy. *Nature Cancer*, 4(8), 1063-1082. <https://doi.org/10.1038/s43018-023-00595-y>
- Peters, C., & Brown, S. (2015). Antibody–drug conjugates as novel anti-cancer chemotherapeutics. *Bioscience reports*, 35(4), e00225.
- Qu, D. C., Neu, D., Khawaja, Z. Q., Wang, R., Bartels, C. F., Lovrenert, K., Chan, E. R., Hill-Baskin, A. E., Scacheri, P. C., & Berger, N. A. (2023). Epigenetic effects of high-fat diet

- on intestinal tumorigenesis in C57BL/6J-Apc (Min/+) mice. *J Transl Genet Genom*, 7(1), 3-16. <https://doi.org/10.20517/jtgg.2022.16>
- Rakha, E. A., Reis-Filho, J. S., Baehner, F., Dabbs, D. J., Decker, T., Eusebi, V., Fox, S. B., Ichihara, S., Jacquemier, J., Lakhani, S. R., Palacios, J., Richardson, A. L., Schnitt, S. J., Schmitt, F. C., Tan, P.-H., Tse, G. M., Badve, S., & Ellis, I. O. (2010). Breast cancer prognostic classification in the molecular era: the role of histological grade. *Breast Cancer Research*, 12(4), 207. <https://doi.org/10.1186/bcr2607>
- Ranger, J. J., Levy, D. E., Shahalizadeh, S., Hallett, M., & Muller, W. J. (2009). Identification of a Stat3-dependent transcription regulatory network involved in metastatic progression. *Cancer Res*, 69(17), 6823-6830. <https://doi.org/10.1158/0008-5472.CAN-09-1684>
- Rao, T., Ranger, J. J., Smith, H. W., Lam, S. H., Chodosh, L., & Muller, W. J. (2014). Inducible and coupled expression of the polyomavirus middle T antigen and Cre recombinase in transgenic mice: an in vivo model for synthetic viability in mammary tumour progression. *Breast Cancer Res*, 16(1), R11. <https://doi.org/10.1186/bcr3603>
- Raz, A., & Geiger, B. (1982). Altered organization of cell-substrate contacts and membrane-associated cytoskeleton in tumor cell variants exhibiting different metastatic capabilities. *Cancer Res*, 42(12), 5183-5190.
- Rivenbark, A. G., O'Connor, S. M., & Coleman, W. B. (2013). Molecular and cellular heterogeneity in breast cancer: challenges for personalized medicine. *Am J Pathol*, 183(4), 1113-1124. <https://doi.org/10.1016/j.ajpath.2013.08.002>
- Robinson, J. L., & Carroll, J. S. (2012). FoxA1 is a key mediator of hormonal response in breast and prostate cancer. *Front Endocrinol (Lausanne)*, 3, 68. <https://doi.org/10.3389/fendo.2012.00068>
- Rüdiger, M. (1998). Vinculin and alpha-catenin: shared and unique functions in adherens junctions. *Bioessays*, 20(9), 733-740. [https://doi.org/10.1002/\(sici\)1521-1878\(199809\)20:9<733::Aid-bies6>3.0.Co;2-h](https://doi.org/10.1002/(sici)1521-1878(199809)20:9<733::Aid-bies6>3.0.Co;2-h)
- Sakamoto, K., Schmidt, J. W., & Wagner, K. U. (2015). Mouse models of breast cancer. *Methods Mol Biol*, 1267, 47-71. https://doi.org/10.1007/978-1-4939-2297-0_3
- Sauer, B. (1998). Inducible gene targeting in mice using the Cre/lox system. *Methods*, 14(4), 381-392. <https://doi.org/10.1006/meth.1998.0593>
- Seachrist, D. D., Anstine, L. J., & Keri, R. A. (2021). FOXA1: A Pioneer of Nuclear Receptor Action in Breast Cancer. *Cancers (Basel)*, 13(20). <https://doi.org/10.3390/cancers13205205>
- Sedlář, A., Trávníčková, M., Bojarová, P., Vlachová, M., Slámová, K., Křen, V., & Bačáková, L. (2021). Interaction between Galectin-3 and Integrins Mediates Cell-Matrix Adhesion in Endothelial Cells and Mesenchymal Stem Cells. *Int J Mol Sci*, 22(10). <https://doi.org/10.3390/ijms22105144>
- Sellier, H., Rébillard, A., Guette, C., Barré, B., & Coqueret, O. (2013). How should we define STAT3 as an oncogene and as a potential target for therapy? *Jakstat*, 2(3), e24716. <https://doi.org/10.4161/jkst.24716>
- Seyfried, T. N., & Huysentruyt, L. C. (2013). On the origin of cancer metastasis. *Crit Rev Oncog*, 18(1-2), 43-73. <https://doi.org/10.1615/critrevoncog.v18.i1-2.40>
- Sheikh, M. S., & Satti, S. A. (2021). The emerging CDK4/6 inhibitor for breast cancer treatment. *Mol Cell Pharmacol*, 13(3), 9-12.
- Shirakawa, K., Endo, J., Kataoka, M., Katsumata, Y., Yoshida, N., Yamamoto, T., Isobe, S., Moriyama, H., Goto, S., Kitakata, H., Hiraide, T., Fukuda, K., & Sano, M. (2018). IL

- (Interleukin)-10-STAT3-Galectin-3 Axis Is Essential for Osteopontin-Producing Reparative Macrophage Polarization After Myocardial Infarction. *Circulation*, 138(18), 2021-2035. <https://doi.org/10.1161/circulationaha.118.035047>
- Siegel, P. M., Ryan, E. D., Cardiff, R. D., & Muller, W. J. (1999). Elevated expression of activated forms of Neu/ErbB-2 and ErbB-3 are involved in the induction of mammary tumors in transgenic mice: implications for human breast cancer. *Embo j*, 18(8), 2149-2164. <https://doi.org/10.1093/emboj/18.8.2149>
- Siersbæk, R., Scabia, V., Nagarajan, S., Chernukhin, I., Papachristou, E. K., Broome, R., Johnston, S. J., Joosten, S. E. P., Green, A. R., Kumar, S., Jones, J., Omarjee, S., Alvarez-Fernandez, R., Glont, S., Aitken, S. J., Kishore, K., Cheeseman, D., Rakha, E. A., D'Santos, C., . . . Carroll, J. S. (2020). IL6/STAT3 Signaling Hijacks Estrogen Receptor α Enhancers to Drive Breast Cancer Metastasis. *Cancer Cell*, 38(3), 412-423.e419. <https://doi.org/10.1016/j.ccell.2020.06.007>
- Simond, A. M., Ling, C., Moore, M. J., Condotta, S. A., Richer, M. J., & Muller, W. J. (2020). Point-activated ESR1(Y541S) has a dramatic effect on the development of sexually dimorphic organs. *Genes Dev*, 34(19-20), 1304-1309. <https://doi.org/10.1101/gad.339424.120>
- Slebe, F., Rojo, F., Vinaixa, M., García-Rocha, M., Testoni, G., Guiu, M., Planet, E., Samino, S., Arenas, E. J., Beltran, A., Rovira, A., Lluch, A., Salvatella, X., Yanes, O., Albanell, J., Guinovart, J. J., & Gomis, R. R. (2016). FoxA and LIPG endothelial lipase control the uptake of extracellular lipids for breast cancer growth. *Nat Commun*, 7, 11199. <https://doi.org/10.1038/ncomms11199>
- Society, C. C. (2023a). *Breast cancer statistics* Retrieved February 3rd from <https://cancer.ca/en/cancer-information/cancer-types/breast/statistics>
- Society, C. C. (2023b). *Survival statistics for breast cancer*. Retrieved February 3rd from <https://cancer.ca/en/cancer-information/cancer-types/breast/prognosis-and-survival/survival-statistics>
- Song, M., Pan, Q., Yang, J., He, J., Zeng, J., Cheng, S., Huang, Y., Zhou, Z.-Q., Zhu, Q., Yang, C., Han, Y., Tang, Y., Chen, H., Weng, D.-S., & Xia, J.-C. (2020). Galectin-3 favours tumour metastasis via the activation of β -catenin signalling in hepatocellular carcinoma. *British Journal of Cancer*, 123(10), 1521-1534. <https://doi.org/10.1038/s41416-020-1022-4>
- Song, M., Pan, Q., Yang, J., He, J., Zeng, J., Cheng, S., Huang, Y., Zhou, Z. Q., Zhu, Q., Yang, C., Han, Y., Tang, Y., Chen, H., Weng, D. S., & Xia, J. C. (2020). Galectin-3 favours tumour metastasis via the activation of beta-catenin signalling in hepatocellular carcinoma. *Br J Cancer*, 123(10), 1521-1534. <https://doi.org/10.1038/s41416-020-1022-4>
- Srivastava, J., & DiGiovanni, J. (2016). Non-canonical Stat3 signaling in cancer. *Mol Carcinog*, 55(12), 1889-1898. <https://doi.org/10.1002/mc.22438>
- Steinhaeuser, S. S., Morera, E., Budkova, Z., Schepsky, A., Wang, Q., Rolfsson, O., Riedel, A., Krueger, A., Hilmarsdottir, B., Maelandsmo, G. M., Valdimarsdottir, B., Sigurdardottir, A. K., Agnarsson, B. A., Jonasson, J. G., Ingthorsson, S., Traustadottir, G. A., Oskarsson, T., & Gudjonsson, T. (2020). ECM1 secreted by HER2-overexpressing breast cancer cells promotes formation of a vascular niche accelerating cancer cell migration and invasion. *Laboratory Investigation*, 100(7), 928-944. <https://doi.org/10.1038/s41374-020-0415-6>

- Sternberg, N., & Hamilton, D. (1981). Bacteriophage P1 site-specific recombination. I. Recombination between loxP sites. *J Mol Biol*, 150(4), 467-486. [https://doi.org/10.1016/0022-2836\(81\)90375-2](https://doi.org/10.1016/0022-2836(81)90375-2)
- Stewart, T. A., Hollingshead, P. G., & Pitts, S. L. (1988). Multiple regulatory domains in the mouse mammary tumor virus long terminal repeat revealed by analysis of fusion genes in transgenic mice. *Mol Cell Biol*, 8(1), 473-479. <https://doi.org/10.1128/mcb.8.1.473-479.1988>
- Stewart, T. A., Pattengale, P. K., & Leder, P. (1984). Spontaneous mammary adenocarcinomas in transgenic mice that carry and express MTV/myc fusion genes. *Cell*, 38(3), 627-637. [https://doi.org/10.1016/0092-8674\(84\)90257-5](https://doi.org/10.1016/0092-8674(84)90257-5)
- Stuelten, C. H., Parent, C. A., & Montell, D. J. (2018). Cell motility in cancer invasion and metastasis: insights from simple model organisms. *Nature Reviews Cancer*, 18(5), 296-312. <https://doi.org/10.1038/nrc.2018.15>
- Swain, S. M., Shastry, M., & Hamilton, E. (2023). Targeting HER2-positive breast cancer: advances and future directions. *Nature Reviews Drug Discovery*, 22(2), 101-126. <https://doi.org/10.1038/s41573-022-00579-0>
- Tammineni, P., Anugula, C., Mohammed, F., Anjaneyulu, M., Larner, A. C., & Sepuri, N. B. (2013). The import of the transcription factor STAT3 into mitochondria depends on GRIM-19, a component of the electron transport chain. *J Biol Chem*, 288(7), 4723-4732. <https://doi.org/10.1074/jbc.M112.378984>
- Tao, C.-C., Cheng, K.-M., Ma, Y.-L., Hsu, W.-L., Chen, Y.-C., Fuh, J.-L., Lee, W.-J., Chao, C.-C., & Lee, E. H. Y. (2020). Galectin-3 promotes A β oligomerization and A β toxicity in a mouse model of Alzheimer's disease. *Cell Death & Differentiation*, 27(1), 192-209. <https://doi.org/10.1038/s41418-019-0348-z>
- Tian, L., Huang, C. K., Ding, F., & Zhang, R. (2021). Galectin-3 Mediates Thrombin-Induced Vascular Smooth Muscle Cell Migration. *Front Cardiovasc Med*, 8, 686200. <https://doi.org/10.3389/fcvm.2021.686200>
- Tilli, M. T., Frech, M. S., Steed, M. E., Hruska, K. S., Johnson, M. D., Flaws, J. A., & Furth, P. A. (2003). Introduction of estrogen receptor-alpha into the tTA/TAg conditional mouse model precipitates the development of estrogen-responsive mammary adenocarcinoma. *Am J Pathol*, 163(5), 1713-1719. [https://doi.org/10.1016/s0002-9440\(10\)63529-8](https://doi.org/10.1016/s0002-9440(10)63529-8)
- Torres-Arzuayus, M. I., Font de Mora, J., Yuan, J., Vazquez, F., Bronson, R., Rue, M., Sellers, W. R., & Brown, M. (2004). High tumor incidence and activation of the PI3K/AKT pathway in transgenic mice define AIB1 as an oncogene. *Cancer Cell*, 6(3), 263-274. <https://doi.org/10.1016/j.ccr.2004.06.027>
- Tower, H., Ruppert, M., & Britt, K. (2019). The Immune Microenvironment of Breast Cancer Progression. *Cancers (Basel)*, 11(9). <https://doi.org/10.3390/cancers11091375>
- Trinh, A., Gil Del Alcazar, C. R., Shukla, S. A., Chin, K., Chang, Y. H., Thibault, G., Eng, J., Jovanovic, B., Aldaz, C. M., Park, S. Y., Jeong, J., Wu, C., Gray, J., & Polyak, K. (2021). Genomic Alterations during the In Situ to Invasive Ductal Breast Carcinoma Transition Shaped by the Immune System. *Mol Cancer Res*, 19(4), 623-635. <https://doi.org/10.1158/1541-7786.MCR-20-0949>
- Ursini-Siegel, J., Hardy, W. R., Zuo, D., Lam, S. H., Sanguin-Gendreau, V., Cardiff, R. D., Pawson, T., & Muller, W. J. (2008). ShcA signalling is essential for tumour progression in mouse models of human breast cancer. *Embo j*, 27(6), 910-920. <https://doi.org/10.1038/emboj.2008.22>

- van Seijen, M., Lips, E. H., Thompson, A. M., Nik-Zainal, S., Futreal, A., Hwang, E. S., Verschuur, E., Lane, J., Jonkers, J., Rea, D. W., Wesseling, J., & team, P. (2019). Ductal carcinoma in situ: to treat or not to treat, that is the question. *Br J Cancer*, *121*(4), 285-292. <https://doi.org/10.1038/s41416-019-0478-6>
- Vatamaniuk, M. Z., Gupta, R. K., Lantz, K. A., Doliba, N. M., Matschinsky, F. M., & Kaestner, K. H. (2006). Foxa1-deficient mice exhibit impaired insulin secretion due to uncoupled oxidative phosphorylation. *Diabetes*, *55*(10), 2730-2736. <https://doi.org/10.2337/db05-0470>
- Vishnoi, K., Viswakarma, N., Rana, A., & Rana, B. (2020). Transcription Factors in Cancer Development and Therapy. *Cancers (Basel)*, *12*(8). <https://doi.org/10.3390/cancers12082296>
- Vuong, L., Kouverianou, E., Rooney, C. M., McHugh, B. J., Howie, S. E. M., Gregory, C. D., Forbes, S. J., Henderson, N. C., Zetterberg, F. R., Nilsson, U. J., Leffler, H., Ford, P., Pedersen, A., Gravelle, L., Tantawi, S., Schambye, H., Sethi, T., & MacKinnon, A. C. (2019). An Orally Active Galectin-3 Antagonist Inhibits Lung Adenocarcinoma Growth and Augments Response to PD-L1 Blockade. *Cancer Res*, *79*(7), 1480-1492. <https://doi.org/10.1158/0008-5472.Can-18-2244>
- Wahba, H. A., & El-Hadaad, H. A. (2015). Current approaches in treatment of triple-negative breast cancer. *Cancer Biol Med*, *12*(2), 106-116. <https://doi.org/10.7497/j.issn.2095-3941.2015.0030>
- Wang, R., Zhu, Y., Liu, X., Liao, X., He, J., & Niu, L. (2019). The Clinicopathological features and survival outcomes of patients with different metastatic sites in stage IV breast cancer. *BMC Cancer*, *19*(1), 1091. <https://doi.org/10.1186/s12885-019-6311-z>
- Webb, D. J., Donais, K., Whitmore, L. A., Thomas, S. M., Turner, C. E., Parsons, J. T., & Horwitz, A. F. (2004). FAK–Src signalling through paxillin, ERK and MLCK regulates adhesion disassembly. *Nature Cell Biology*, *6*(2), 154-161. <https://doi.org/10.1038/ncb1094>
- Weigel, D., & Jäckle, H. (1990). The fork head domain: a novel DNA binding motif of eukaryotic transcription factors? *Cell*, *63*(3), 455-456. [https://doi.org/10.1016/0092-8674\(90\)90439-1](https://doi.org/10.1016/0092-8674(90)90439-1)
- Weigel, D., Jürgens, G., Küttner, F., Seifert, E., & Jäckle, H. (1989). The homeotic gene fork head encodes a nuclear protein and is expressed in the terminal regions of the Drosophila embryo. *Cell*, *57*(4), 645-658. [https://doi.org/10.1016/0092-8674\(89\)90133-5](https://doi.org/10.1016/0092-8674(89)90133-5)
- Weigelt, B., Geyer, F. C., & Reis-Filho, J. S. (2010). Histological types of breast cancer: how special are they? *Mol Oncol*, *4*(3), 192-208. <https://doi.org/10.1016/j.molonc.2010.04.004>
- Welch, D. R., & Hurst, D. R. (2019). Defining the Hallmarks of Metastasis. *Cancer Res*, *79*(12), 3011-3027. <https://doi.org/10.1158/0008-5472.Can-19-0458>
- Yang, E. H., Rode, J., Howlader, M. A., Eckermann, M., Santos, J. T., Hernandez Armada, D., Zheng, R., Zou, C., & Cairo, C. W. (2017). Galectin-3 alters the lateral mobility and clustering of β 1-integrin receptors. *PLoS One*, *12*(10), e0184378. <https://doi.org/10.1371/journal.pone.0184378>
- Yang, F., Zhang, F., Ji, X., Jiang, X., Xue, M., Yu, H., Hu, X., & Bao, Z. (2020). Secretory galectin-3 induced by glucocorticoid stress triggers stemness exhaustion of hepatic progenitor cells. *J Biol Chem*, *295*(49), 16852-16862. <https://doi.org/10.1074/jbc.RA120.012974>

- Yang, J., Ju, J., Guo, L., Ji, B., Shi, S., Yang, Z., Gao, S., Yuan, X., Tian, G., Liang, Y., & Yuan, P. (2022). Prediction of HER2-positive breast cancer recurrence and metastasis risk from histopathological images and clinical information via multimodal deep learning. *Comput Struct Biotechnol J*, 20, 333-342. <https://doi.org/10.1016/j.csbj.2021.12.028>
- Yuan, T., Wang, Y., Pao, L., Anderson, S. M., & Gu, H. (2011). Lactation defect in a widely used MMTV-Cre transgenic line of mice. *PLoS One*, 6(4), e19233. <https://doi.org/10.1371/journal.pone.0019233>
- Yue, J., Zhang, Y., Liang, W. G., Gou, X., Lee, P., Liu, H., Lyu, W., Tang, W. J., Chen, S. Y., Yang, F., Liang, H., & Wu, X. (2016). In vivo epidermal migration requires focal adhesion targeting of ACF7. *Nat Commun*, 7, 11692. <https://doi.org/10.1038/ncomms11692>
- Zacksenhaus, E., Liu, J. C., Jiang, Z., Yao, Y., Xia, L., Shrestha, M., & Ben-David, Y. (2017). Transcription Factors in Breast Cancer-Lessons From Recent Genomic Analyses and Therapeutic Implications. *Adv Protein Chem Struct Biol*, 107, 223-273. <https://doi.org/10.1016/bs.apcsb.2016.10.003>
- Zeng, P., Sun, S., Li, R., Xiao, Z. X., & Chen, H. (2019). HER2 Upregulates ATF4 to Promote Cell Migration via Activation of ZEB1 and Downregulation of E-Cadherin. *Int J Mol Sci*, 20(9). <https://doi.org/10.3390/ijms20092223>
- Zhang, M. H., Man, H. T., Zhao, X. D., Dong, N., & Ma, S. L. (2014). Estrogen receptor-positive breast cancer molecular signatures and therapeutic potentials (Review). *Biomed Rep*, 2(1), 41-52. <https://doi.org/10.3892/br.2013.187>
- Zhou, F. H., Downton, T., Freeland, A., Hurwitz, J., Caldon, C. E., & Lim, E. (2023). CDK4/6 inhibitor resistance in estrogen receptor positive breast cancer, a 2023 perspective. *Front Cell Dev Biol*, 11, 1148792. <https://doi.org/10.3389/fcell.2023.1148792>
- Zou, S., Tong, Q., Liu, B., Huang, W., Tian, Y., & Fu, X. (2020). Targeting STAT3 in Cancer Immunotherapy. *Mol Cancer*, 19(1), 145. <https://doi.org/10.1186/s12943-020-01258-7>
- Zwijsen, R. M., Wientjens, E., Klompaker, R., van der Sman, J., Bernards, R., & Michalides, R. J. (1997). CDK-independent activation of estrogen receptor by cyclin D1. *Cell*, 88(3), 405-415. [https://doi.org/10.1016/s0092-8674\(00\)81879-6](https://doi.org/10.1016/s0092-8674(00)81879-6)